Université d'Ottawa • University of Ottawa

Design and Analysis of Congestion Control for High-Speed Networks

Author: Hongyi Zhang

A Thesis Submitted to

the School of Graduate Studies and Research

in Partial Fulfillment of

the Requirement for the Degree of

Doctor of Philosophy

School of Information Technology and Engineering

University of Ottawa

Ottawa, Ontario, Canada

0-612-67226-3

Abstract

In this thesis, we first use the fluid flow modeling technique to build an end-to-end model and a hop-by-hop model for the high-speed networks respectively. We then use the control theory to design distributed rate-based traffic controllers to flow-regulate the best-effort service (e.g., ABR) traffic and guaranteed service traffic through a high-speed switch. The controllers are distributed among the source nodes and have a very simple structure. Their local controller at each source node is open-loop stable and only requires the knowledge of the queue length at the bottleneck switch. We say that the network is open-loop stable if the feedback loop breaks. Based on the simulation results obtained from OPNET and MATLAB, we finally show that the controllers are fair and can stabilize the network with long variable delays. Our controllers overcome the oscillation problem which exists in most of current existing rate-based controllers.

Acknowledgments

During the past six years of my studying Ph.D. program, I have received a lot of assistance from many people. First of all, I like to thank Professor Oliver Yang for his academic supervision that allows me to continue my study, and complete my research.

I would also like to thank Prof. H. Mouftah for his advice, and many members in our computer communication network group, led by Professor Oliver Yang, by providing me many helpful suggestions, in particular Mr. Kevin Huynh for providing his simulation results on ABR traffic.

Finally thanks to my wife, Min Yang, and my son, Boyang, for their encouragement, patience and understanding – especially when I worked late in the evenings.

My Ph.D. research in congestion control in high-speed networks has been financially supported by NSERC and TRIO (through Prof. Mouftah).

Contents

List of Figures

List of Tables

Chapter 1

Introduction

Traffic and congestion control is a major issue in ATM networks. One basic problem in the design of efficient traffic and congestion control schemes is related to the wide variety of services with different traffic characteristics and multiple qualities of services (QoS) offered by ATM networks. The traffic management specification TM4.0 [1] specifies five classes of services: constant bit rate (CBR), real time variable bit rate (rt-VBR), non-real-time variable bit rate (nrt-VBR), available bit rate (ABR), and unspecified bit rate (UBR).

CBR is used by connections that request a constant amount of bandwidth which must be continuously available during the connection lifetime; an example is the circuit emulation. rt-VBR is intended for real-time applications which require tightly constrained delay and delay variation; an example is the application of voice and video. nrt-VBR is intended for non-real-time applications which have bursty traffic characteristics; an example is the data traffic. UBR is intended for non-real-time applications; an example is the traditional computer communication applications like file transfer and email. ABR is intended for applications that can take advantage of bandwidth elasticity; an example is the TCP/IP traffic. Among of them, the ABR and UBR services have been specifically designed for efficient handling of data traffic.

One of the challenges in designing ATM traffic control is to support multimedia traffic consisting of a variety of traffic classes with a different quality of service requirement, while attempting to make maximum use of network resources. According to the ATM service categories and QoS requirements, two basic classes of services can be defined: reserved traffic with guaranteed service (e.g. CBR, rt-VBR and nrt-VBR), and best-effort service traffic with no explicit guaranteed service (e.g. UBR) or with guaranteed minimum bandwidth (e.g. ABR) [27].

In order to ensure the required quality of service for all types of traffic, it requires that the offered traffic be adequately monitored and controlled, since if traffic from several bursty sources are directed to a single ATM switch, statistical multiplexing of ATM cells with no mechanism to control the source rate will lead to severe cell loss. This loss will be aggravated if the incoming cell rates exceed the switch's bandwidth and the burst size are large.

Currently, two classes of congestion control strategies have been discussed for high-speed ATM networks: open-loop control, and closed-loop control. The strategy of open-loop control is preventive in nature; it is aimed at keeping the operation of a network at a certain point of power such that congestion can be avoided [2]. This kind of control mechanism can support real-time and delay-sensitive communication services such as CBR service and VBR service, by which audio and motion video can be intergrated into the network. Although the open-loop control also supports the best-effort service traffic class, it cannot predict its bandwidth requirement, because sources are expected to specify only their peak rates at connection time. Since bandwidth requirements for the best-effort service traffic can vary over time, an explicit guarantee of service cannot be provided. This means that open-loop control is not efficient for best-effort service traffic.

In order to support best-effort traffic to maximize the utilization of the network resources, ABR service is designed to implement a closed-loop feedback mechanism to allow an end system to adapt its sending rate to catch the rest of bandwidth left over by guaranteed service traffic, and to prevent congestion in the network, thus offering the most effective solution to bandwidth sharing among all competing users. Two kinds of feedback schemes have been proposed: credit-based and rate-based.

The credit-based scheme is based on a per-link, per-VC window flow control mechanism [29]. Each link consists of a sender node (either a source end system or a switch) and a receiver node (either a switch or a destination end system). Each node maintains a separate queue for each VC. The receiver monitors the queue lengths of each VC and determines the number of cells the sender can transmit on that VC. This number is called a "credit". The sender can transmit only as many cells as allowed by the credit. This scheme can prevent cell loss which is important for best-effort service traffic; however, it requires that each virtual connection must obtain buffer reservations for its cell transmission on each link, which results in considerable hardware complexity, and complicated queue management for every connection.

The rate-based scheme, on the other hand, regulates the source rate from an end system. It is simpler than the credit-based control schemes. The original proposal for a rate-based approach consists of end-to-end control using a single-bit feedback from the network [2]. In these schemes, the intermediate switches monitor their queue lengths and, if congested, set the explicit forward congestion indication (EFCI) bit in the cell header to the destination. The destinations monitor EFCI bits; if set, the destinations generate an resource management (RM) cell back to the sources. The sources then use an additive increase and multiplicative decrease algorithm (see [2]) to adjust their transmission rates. The RM cells are sent only to decrease the rate, but no

RM cells are required to increase rate.

The rate-based approach for the ABR service has evolved for nine years since 1991 and has been enhanced greatly [2]. We will give more discussion on how the rate-based approaches are used to control ABR traffic and what problems they have in the following sections.

1.1 Literature Review

Due to the highly bursty nature of traffic and long propagation delays in the ATM networks, congestion control for ABR service poses more challenging problems than other services, and it has recently been attractive to a lot of researchers in this areas. In this section, we discuss in more details of other works that are related to our research work.

1.1.1 Network Modeling

First, we are interested in identifying what modeling techniques have been used for the design of ABR traffic control and the performance evaluation. Since the exact analysis of flow networks is often intractable, fluid approximations [44] are used to simplify the complexity of systems. These are first-order approximation of queuing network whose discrete cell flows are approximated by continuous fluid-like flows. Continuous approximations can be expected to perform well whenever individual changes in the state of the network are "infinitesimally" small relative to the absolute value of the state [6]. This explains why they are widely used in the short-range analysis of overloaded queuing system or long-range stability analysis in general.

Under the basic assumptions that all sources share a common buffer in a queue served according to the FIFO discipline, a variety of first-order fluid models have been used to analyze the ABR traffic; some of them allow integration of both ABR service traffic and non ABR service traffic. These models can be classified into:

- stochastic continuous time-delayed fluid model [8], [9] and [45],
- deterministic continuous time-delayed fluid model [44], [45] and [21],
- deterministic discrete time-delayed fluid model with periodic sampling [10], [12] and [13], and
- deterministic discrete time-delayed fluid model with aperiodic sampling [5].

A Brownian model of traffic was employed in [8] to study the effects of randoms introduced by guaranteed traffic (e.g. CBR and VBR). In this model, ABR traffic is described as fluids (processes with continuous sample paths) which flow into a common shared queue after propagation delays, and guaranteed traffic (e.g., CBR and VBR) is described as continuous Wiener process. Then the interaction between the resulting queue process and time-delayed ABR traffic as well as guaranteed traffic can be described by a stochastic continuous time-delayed fluid model. This model has been effective in analyzing the asymptotic properties such as long-run utilization of bandwidth, data loss and queue length, as the switch's service rate goes to infinity. However, this model is not appropriate to study the network's stability and transient behavior due to the complex behavior of guaranteed traffic.

A pointwise stationary fluid flow model is proposed in [9] and [45] to approximate the mean behavior of a queue with specified arrival and service distribution. If traffic distribution can be specified, the queuing behavior can be described by a single nonlinear first-order differential equation. Clearly, this model is not suitable for control purpose because the distribution of the guaranteed service traffic can not be specified.

Although the stochastic modeling technique is a good choice for performance evaluation, it has been found that this technique has difficulty in analyzing dynamic behavior of a system and in designing a traffic control for ABR traffic which is regulated based on the system's dynamic states (see [10], [11] and [12]). An alternate way to study and to describe a high speed network that integrates both guaranteed traffic and best-effort traffic is to use the deterministic fluid model.

When a queue system is in a heavy-traffic condition (the queue sizes are large compared to unity and the waiting times are large compared to average service times), the arrival processes and unfinished work, both discontinuous and stochastic, can be approximated by continuous and deterministic processes [44]. In [21] and [45], it is shown that under the heavy-traffic condition, the queue length of a congested node can be approximated by a first-order nonlinear differential equation. In [11], a continuous-time fluid model was first used to describe the high-speed networks with long propagation delays. This model describes the queue length of a congested node with one single VC carrying ABR service traffic. Due to the simplicity, the model proposed in [11] has now become a base model for studying and verifying the performance for the rate-based control algorithms such as EFCI and ER [5]. In this model, the propagation between the source and destination is constant, which implies that no queuing delay is considered.

Since the feedback flow is intrinsically discrete in the high speed networks compared to the data flow (e.g., single/binary bit type of feedback [2] and explicit type of feedback) [4], the deterministic discrete-time fluid model is employed to analyze the feedback controlled network's behavior. In general, a discrete-time fluid model can be obtained by discretizing its corresponding continuous-time fluid model. The sampling rate is an important factor in the process of discretization. It is well known that the sampling rate should be significantly faster than the dynamics to be regulated in order to avoid sever performance degradation.

In [10] and [12], a discrete-time fluid model is obtained by discretizing a continuous-time fluid model with a single VC at the rate of the round-trip delay. This discrete-time model describes the buffer occupancy occupied by a VC in an interval of the round-trip delay. This model is very crude since a lot of information would be lost if the round-trip delay is long. Also the controller designed on this model may produce poor performance since the source responses very slowly to the change of the buffer occupancy caused by guaranteed traffic. In [13], a discrete-time fluid model is obtained by discretizing a continuous-time fluid model with multiple VCs, where each VC may have a different propagation delay. It is assumed that the propagation delays are multiples of the sampling time. Since the sampling rate used in [13] is faster than that used in [12], it is demonstrated that better performance can be obtained by using this model. In [22], a discrete-time fluid model is also obtained by discretizing a continuous-time fluid model with multiple VCs. While this model describes a switch's bandwidth behavior instead of buffer occupancy, similar results are obtained as in [13].

1.1.2 Rate-Based Control

Many approaches to this category of congestion control for ABR traffic in ATM networks have been developed in the past decade. Typical examples of rate-based congestion control are the single/binary-bit type schemes which include the forward explicit congestion notification (FECN) approach and the backward explicit congestion notification (BECN) approach [2]. In these schemes, a periodic-sampling feedback control is used (see [18] and [19]). Due to long propagation delays, rapid change of source rate may cause network congestion. It has been accepted that at fixed intervals (i.e., a periodic sampling interval), source rate is proportionally increased or proportionally decreased to the current cell rate according to network state information stored in a congestion bit carried by the piggyback packet. These control strategies are well-known and very effective in conventional packet-switched networks. However, since the propagation delay is long compared to the transmission time of a data unit in high-speed networks, the network state information received by the local controller of a virtual connection may be outdated. Thus the simple proportional increase and decrease scheme may cause the local controllers and the whole network to operate at an unstable point. This yields the notorious oscillation problem that greatly degrades the network performance. Also this type of scheme has two other major problems. One problem is the open-loop unstable problem, which occurs when RM cells are lost due to heavy congestion in the reverse path, the sources keep on increasing their rate in the forward path [3]. Another is the beat-down problem which occurs when a VC is going through more congested links, its data cells will be marked more often than those VCs going through fewer congested nodes. Consequently, such a VC will have a lower allowed transmission rate than others [5]. This undesirable effect on VCs is also referred to as the VC starvation problem.

In order to alleviate the problems in the single/binary bit congestion control approaches, an explicit rate (ER) scheme was developed in [4] and [5]. In this scheme, a distributed algorithm is carried out in the source nodes, destination nodes and intermediate switches respectively. In the source nodes, forward RM cells are inserted in the data stream at a certain frequency of $\frac{1}{M}$ (i.e., 1 RM cell every $M-1$ data cells). The source rate is regulated according to returned RM cells. In the switches, RM cells may be modified according to congestion detection, and to calculation on explicit rate and fair share. In the destination nodes, modified RM cells are looped back to the source according to some specified procedures. When a source receives the RM cells, it will regulate its transmission rate based on the explicit rate specified in the RM cells. It is shown by simulation that properly designed explicit rate schemes can significantly outperform single/binary-bit type schemes in terms of much reduced buffer size requirement with much less queuing oscillation and fairness. This advantage is achieved 1) by direct control of the ABR traffic based on the measured available switch's bandwidth, 2) by restriction of sources to transmit a fixed number of cells during two RM cells (i.e., an aperiodic-sampling feedback is used), and 3) by using per-VC accounting or per-VC queuing technique [19].

The per-VC accounting technique is to use a table indexed by each ABR VC connection to maintain the accounting information. The information maintained in the table is then applied to selectively marked VCs so that the switch can dynamically monitor the number of active VCs and the cell rate of each VC. Thus, reasonably fair allocations of bandwidth for each VC is possible with this technique. The per-VC queuing technique is to isolate the interaction among the VCs by having a separate queue for each of VCs. Thus, a complete fair share can be achieved from this technique.

The major advantage of most proposed single/binary-bit type and explicit-type rate-based control schemes is their simplicity in implementation. Neither dynamic traffic model is established nor round-trip delays and impact of guaranteed traffic are considered. Also the performance of these schemes can only been obtained by simulation. A new control approach based on control-theoretic concepts was first proposed in [10] to stabilize the network without oscillatory behavior. The advantage of using control theory is that a systematic analysis on the network dynamic behavior is made possible.

In [10], a network with one single source node was considered. It was shown that the round trip delay is measurable via the time stamp technique. Then the network was described by a second order discrete time fluid model by choosing the sampling time equal to the round trip delay. Due to the simplicity of this model, a simple control algorithm was also found to maintain the network's stability. However, this approach may not be applicable to a network with multiple source nodes since multiple round trip delays are involved.

The control schemes which can stabilize a network with multiple source nodes were proposed in [13] and [14]. In the approach of [13], the main controller is placed in the bottleneck switch and has to calculate the feasible admission rates for each virtual connection before sending these rates to each source node to throttle its traffic. Since the bottleneck switch may occur anywhere in the network, this kind of control structure is complicated and may not be easily implemented. In the approach of [14], a nonlinear control algorithm is proposed to stablize the network with long propagation delays.

When both VBR traffic and ABR traffic are explicitly taken into account in the system model, simulation [22] shows that the high frequency in VBR traffic may severely deteriorate the system's stability, especially in the transport of bursty VBR traffic. One approach to alleviate the oscillation problem due to the bursty nature of VBR traffic is to use a filter to eliminate high frequency of the VBR traffic. In [22], a linear discrete-time model is established to capture the switch bandwidth unused by the low frequency component of filtered VBR traffic. All high frequency traffic is absorbed and smoothed out via limited buffering. An optimal controller is then designed to stablize the switch's bandwidth behavior, while the queuing behavior is still unstable, which implies this approach does not solve the problems caused by long propagation delays.

Another approach to alleviate the oscillation problem due to the long end-to-end loop delays is to use the hop-by-hop control algorithms. Recently, hop-by-hop rate-based control algorithms [32], [33] and [36] have been proposed to reduce the control delay and hence the reaction time of a network to the congestion at a switching node. This is achievable due to the assumption that hop-by-hop propagation delays are usually much less than the end-to-end propagation delay. Therefore a long end-to-end loop can be segmented to a group of hop-by-hop loops between the so called virtual source and virtual destination. In [33], the feedback information sent from the downstream switch is used by the upstream switch to determine the target sending rate for a single connection. The basic idea is that switches can make control decision to avoid congestion by predicting the behavior of its downstream switching node at a specific time in the future. It is shown that, with this hop-by-hop flow control algorithm used, the whole network is stable and has a better transient behavior comparing with the end-to-end rate-based control algorithms. However, this control algorithm can only be applied to the network with a symmetric property, i.e., all neighboring switching nodes have the same distance.

In summary, the rate-based control has been widely recognized as an efficient feedback mechanism to control ABR traffic in the ATM networks. However, the few control algorithms that have been proposed to implement this feedback mechanism, have some of the following weaknesses in general:

- the controllers are open-loop unstable in the sense that the network is unstable if the closed loop breaks,
- the network is closed-loop unstable (except [10], [13]),
- queuing delays are ignored,
- the impact of the guaranteed traffic is not considered (except [22]), and
- the robustness analysis is not available, for example, how the controller responses to the change of delay and traffic load.

1.2 Motivations and Objectives

The basic problem in the design of traffic control in the communication networks consists in finding efficient traffic control algorithms. In a slightly loaded network subject to a stationary load, the problem is simple and mature through conventional approaches, since each switch can choose a route that best serves its own interests and determine how much traffic can pass through at any given time (e.g., using the window flow control). However, when the offered traffic increases the problem become significantly complex since the competition for limited network resources gives rise to various nonlinear phenomena that can result in deadlocks or overall network congestion. Also, the procedures that satisfied the QoS of individual users in the slightly loaded network may provide a poor service for all users within the network when traffic is heavy.

The current rate-based approach specified in TM 4.0 [1] is now widely recognized as an efficient control mechanism for ABR traffic. However, since this approach is based on intuitive observation and is in lack of systematical analysis, it still has many problems such as the expected efficiency. Therefore in this thesis, we shall try to apply control theory to analyze ABR traffic behavior and to design robust rate-based ABR traffic controllers.

Also in this thesis, we shall use the fluid-flow model described in the chapter 2 to design a traffic controller that is geographically distributed over the source nodes. Two types of control schemes are considered:

1) deterministic, continuous-time control, and

2) deterministic, discrete-time control with periodic sampling.

The major objective in this thesis is to design two types of feedback traffic control: (1) a proportional feedback traffic control, and (2) a proportional and integral feedback traffic control.

Not only can these controllers stabilize the network, but they also have the following properties:

1. it is robust in the sense that the system's stability is not sensitive to the change of the number of active VCs, and the variation of propagation delays, queuing delays and other processing delays,

2. it is fair to each virtual connection in the sense that each source always tries to catch up its own allocated transmission rate without interference from other source nodes, and

3. it has a high utilization in the sense that the source can always transmit at the maximum allowed rate.

1.3 Approaches and Methodology

Due to the limitations of conventional approaches, we shall concentrate on the modeling and optimization of dynamic traffic flows. The basic model of dynamic traffic flows is the fluid-flow model which can be either described by a nonlinear differential equation in the continuous time domain, or a nonlinear difference equation in the discrete time domain. Therefore, the traffic control algorithm can also be designed either in continuous time domain or in the discrete time domain. Since the traffic in the ATM networks is discrete in nature, the final traffic control algorithm should also be represented in discrete.

There are three basic approaches to design a discrete time traffic controller based on the fluid flow model to achieve the required performance. One is a simulation design. In this approach, a hueristic controller is first provided by observation and experience, and then refined by simulation. Since this approach only requires a quite rough description of the system model

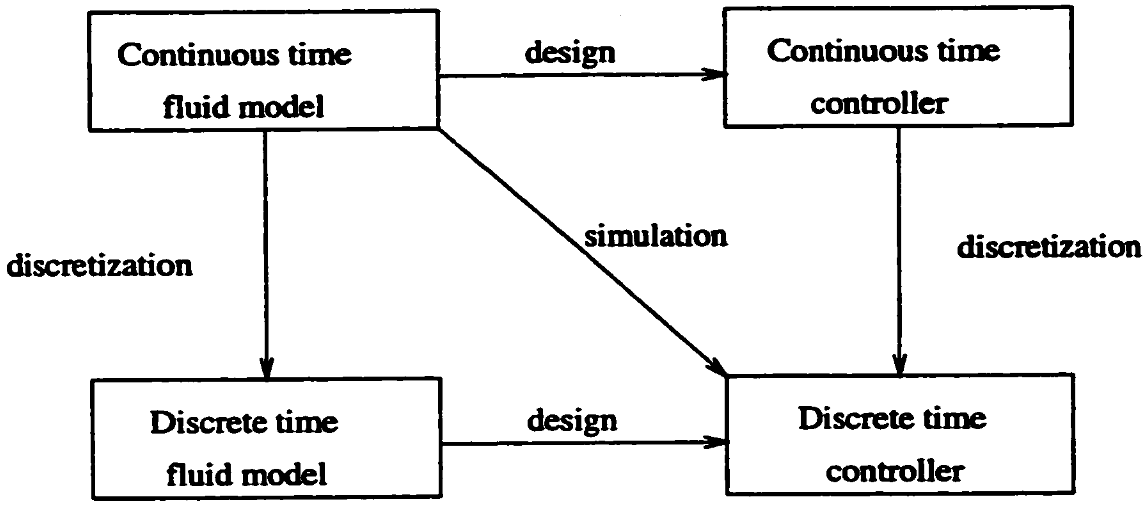

Fig. 1. Design methodology

and often provides not only simple but efficient control, it is widely used in control design for communication systems. The single/binary bit type controllers and the explicit type controllers are the examples of this approach.

The second approach is to design a continuous time controller as the first step, then to discretize it to arrive at the final discrete time controller. The advantages of this way are that analog design is natural and well-known and that one could normally expect recovery of the performance as the sampling rate increases.

The third approach is to discretize the model first and then to perform a discrete time design to obtain the controller. The advantage of this way is that the effect of sampling is out of the design phase since its rate is selected *a priori*. The last two approaches strongly depend on the sampling rate which is required to be significantly faster than the dynamics to be regulated.

In this thesis, we will explore the above mentioned approaches to design flow controllers in high-speed networks. We will search for the controllers in the forms of *continuous-time* and *discrete-time*. Since the long propagation delay is a major source that destabilizes the network and degrades the performance of controlling ABR traffic, the Lyapunov method and the typical z-transform method will be used to analyze the network's stability when the designed controllers are applied.

In order to evaluate the performance of our traffic control algorithms, we use the MATLAB tool [54] to carry out the simulation for the traffic controllers based on the discrete-time fluid flow model, and the OPNET tool [55] to carry out the simulation for the traffic controllers based on the continuous-time fluid flow model. It should be pointed out that we are not going to compare our simulation results with the results from other types of ABR control algorithms listed in [1], [2] and [5], because our Master student Kevin Huynh has demonstrated by OPNET that all these control algorithms are not stable and have the undesirable oscillation behavior [48].

1.4 Contributions

Our main contributions are as follows.

1. We identify two types of fluid models that capture the integration of guaranteed service traffic and best-effort service traffic. These two models can be applied to describe either an end-to-end system or a hop-by-hop system in high-speed networks. To the best of our knowledge, there is no prior work on applying the fluid model to the hop-by-hop networks.

2. We formalize a few desirable properties for ABR traffic control which deal with stability, fairness, robustness, utilization and bounded buffering.

3. We design the following static/dynamic feedback control algorithms which satisfy the properties in section 1.2. These control algorithms include:

- a proportional continuous-time controller which can be applied to the network with random but bounded delays,
- a proportional and integral continuous-time controller which can be applied to the network with random but bounded delays, and requires lower buffer size,
- a proportional discrete-time controller which is robust and can response fast to the load change, and
- a hop-by-hop proportional discrete-time controller which further reduces the response time to the load change and requires the lower buffer size and less overhead in the feedback loop.

4. We demonstrate through simulations that our designed control algorithms can achieve the adaptability and the required performance, which is stable, fair, robust and responsive. All these control algorithms are distributed and stable with a very simple control structure compared with the existing control algorithms.

1.5 Organization

This thesis is organized as follows. Section 1 introduces the background and development of ABR traffic management in ATM switching networks, including the traffic classification and ABR traffic control defined in the ATM forum and other literatures. We discuss how the existing control algorithms (e.g., BECN and ER) work for ABR traffic and their weaknesses and limitations. Also in this section, we discuss the our objectives on the design of the congestion controller.

In Section 2, two types of fluid flow models are proposed in the continuous time and discrete time domain respectively to describe the queue dynamics of a high-speed network. These models can be applied to either an end-to-end or a hop-by-hop control. It can be shown later that the switch's queuing behavior driven by our controllers based on the fluid model are very accurate according to the simulation results obtained from the OPNET simulation tool.

In Section 3, through an analysis using the Lyapunov approach in the continuous time model, two types of end-to-end continuous time controllers are discussed. One is the proportional controller and the other is the proportional and integral controller. Both are designed to stabilize a network with variable but bounded round-trip delays in the switching nodes. Simulations on these two types of controllers are provided and performed on the OPNET simulation tool.

In Section 4 and 5, through an analysis using the z-transform approach in the discrete time model, a class of discrete time controllers are proposed for either end-to-end or hop-by-hop ABR traffic control. These controllers are robust and provide fairness and high performance. Simulation results are also provided for each type of controller but are obtained from the MATLAB tool.

Finally in Section 6, a brief conclusion is given to summerize our results in the ABR traffic control.

1.6 Published Papers

The following is a list of our published papers related to this research:

[1] H. Zhang, O. Yang and H. Mouftah, "Adaptive rate-based congestion control in ATM switching networks," *Computer Syst. Sci. & Eng.*, vol 6, pp. 361-367, 1996.

[2] H. Zhang, O. Yang and H. Mouftah, "A control for the stabilization of end-to-end congestion: single source case," in *Proc. of the 4th International Conference on Telecommunication Systems*, pp. 340-346, 1996.

[3] H. Zhang, O. Yang and H. Mouftah, "A control policy for the stabilization of end-to-end congestion: multiple sources case," in *Proc. of the 34th Annual Allerton Conf. on Communication, Control, and Computing*, pp. 1-9, 1996.

[4] H. Zhang, O. Yang and H. Mouftah, "Design of robust congestion controllers for ATM networks," in *Proc. IEEE INFOCOM'97*, pp. 302-309, 1997.

[5] H. Zhang, O. Yang and H. Mouftah, "Discrete-time model of a hop-by-hop controller," presented in *Annual Conf. OR and Info. Tech. Management*, May 27, 1997.

[6] H. Zhang, O. Yang and H. Mouftah, "The hop-by-hop flow controller for high-speed networks: a single VC case," in *Proc. IEEE GLOBECOM'97*, pp. 785-789, 1997.

[7] H. Zhang, O. Yang and H. Mouftah, "A hop-by-hop flow controller for a virtual path," *Computer Networks and ISDN Systems*, vol. 32, pp. 99-119, 2000.

[8] H. Zhang, O. Yang and H. Mouftah, "The distributed robust traffic controller for ATM networks," *Int. J. of Commun. Syst*, Vol. 14, 2001.

[9] H. Zhang, O. Yang and H. Mouftah, "Design of congestion control in high-speed networks with variable delay," in *Proc. of ICC 2000*, New Orleans, June 2000

1.6.1 Notations:

Unless otherwise specified, the following notations will pertain to the remainder of the thesis.

A. Notations Used in Continuous and Discrete Time Models

$d(n)$	the number of cells flowing to the switch from uncontrolled traffic in $[nT, (n+1)T)$	§2.1.2
e_i	an on/off function	§2.1.1
$q_i(t)$	the ith source rate at time t	§2.1.2
$x(n)$	buffer occupancy at time $t = nT$	§2.1.2
$x(t)$	buffer occupancy at time t	§2.1.1
x_0	buffer threshold	§2.1.1
$\hat{x}$	difference between x and x_0	§2.1.1
$u_i(n)$	local control function for source i at time $t = nT$	§2.1.2
$w(t)$	uncontrolled source rate at time t	§2.1.1
C_n	Banach space of continuous time functions	§3.1
K	buffer size	§2.1.1
M	the number of active virtual connections to be controlled	§4.2.2
N	the maximum number of virtual connections to be controlled	§2.1.1
$\bar{N}$	the number of output buffers in a switching node	
R^n	n-dimensional linear space	§3.1
$S_K()$	saturation function	§2.1.1
T	sampling time	§2.1.2
$V(t, x)$	Lyponov function	§3.1
$X(z)$	the z-transform of $x(n)$	§4.2.3
$\lambda_i(n)$	the number of cells to be transmitted by the ith source in $[nT, (n+1)T)$	§2.1.2
α	stability factor	§4.1.2
μ	the number of cells emitted from the switch in the interval of T	§2.1.2
μ_i^{max}	the maximum transmission rate assigned to the ith source	§2.1.1
μ_i^{min}	the minimum transmission rate assigned to the ith source	§4.0
ν	service data rate of the switch	§2.1.2
$\nu_A(n)$	service rate available to the controlled traffic at time $t = nT$	§2.1.2
$\nu_A(t)$	service rate available to the controlled traffic at time t	§2.1.1
τ	uniform delay normalized with respect to T	§2.1.2
τ_i	total delay for the ith VC	§2.1.2
τ_{1i}	normalized feedforward delay from the ith source to the switch	§2.1.2

τ_{2i}	normalized feedback delay from the switch to the ith source	§2.1.2
τ'_{1i}	path delay from the ith source to the switch	§2.1.1
τ'_{2i}	path delay from the switch to the ith source	§2.1.1
$\mathcal{N}_{\mathcal{T}_i}$	a set of integers corresponding to active VCs over $\mathcal{T}_i$	§4.0
$\mathcal{T}_i$	an interval $[t_i, t_{i+1})$, where the number of VCs is changed at the point t_i	§4.0

B. Notations Used in Hop-by-Hop Models

$d_i(n)$	the number of uncontrolled packets flowing to VP switch i in $[nT, (n+1)T)$	§2.3.2
$d'_i(n)$	the number of uncontrolled packets leaving VP switch i in $[nT, (n+1)T)$	§2.3.2
$j\|i$	the external node j that is linked to VP switch i	§2.3.2
$q_{i,i+1}(t)$	the controlled transmission rate from VP switch i to VP switch $(i+1)$	§2.3.2
$q_{ji}(t)$	the controlled transmission rate from external node $j\|i$ to VP switch i	§2.3.2
$u_i(n)$	local control function for VP switch i	§2.3.2
$u_{ji}(n)$	local control function for external node $j\|i$	§2.3.2
$w_i(t)$	uncontrolled traffic rate to VP switch i	§2.3.2
$w'_i(t)$	uncontrolled traffic rate out of VP switch i	§2.3.2
$x_i(n)$	buffer occupancy of VP switch i at time $t = nT$	§2.3.2
$x_i(t)$	buffer occupancy of VP switch i at time t	§2.3.2
H	the number of intermediate VP switches along a VP connection	§2.3.2
I	the last congested switch along the VP	§5.2.1
K_i	buffer size of VP switch i	§2.3.2
L_i	the number of active external VCs going to VP switch i	§2.3.2
M_i	the number of active VCs carried by the link between VP switch $(i-1)$ and VP switch i	§5.2.1
N_i	the maximum number of VCs allowed to enter VP switch i	§5.2.1
α_i	stability factor of loop i	§5.1.1
ϵ_i	a parameter to adjust the feedback gain	§5.2.1
Γ_i	the maximum number of packets emitted out of VP switch i	§5.2.2
Γ_i^*	the maximum number of packets emitted from VP switch i to VP switch $(i+1)$ in the interval of T	§5.2.2
$\lambda_i(n)$	the number of packets to be transmitted from VP switch i to VP switch $(i+1)$ in $[nT, (n+1)T)$	§2.3.2

$\mu_i(n)$	the number of packets emitted from VP switch i in the interval of T	§2.3.2
μ_{ji}	the maximum number of packets emitted from the external VC j to VP switch i	§2.3.2
μ_i^*	the maximum number of packets allowed to transmit from VP $(i-1)$ switch to VP switch i	§5.1
$\nu_i(t)$	allowed service data rate of VP switch i	§2.3.2
ν_i	maximum service data rate of VP switch i	§2.3.2
ν_i^*	the maximum link transmission rate from VP switch i to VP switch $(i+1)$	§2.3.2
ν_{ji}	the maximum link transmission rate from the external VC j to VP switch i	§2.3.2
τ_i	the ith one-hop loop delay between VP switch $(i-1)$ and VP switch i	§2.3.2
τ_{max}^i	an integer greater than τ_i and τ_j^i, $j = 1, 2, \cdots, L_i$	§2.3.2
$\hat{\tau}_i$	a design parameter satisfying $\hat{\tau}_i + \tau_i = \tau_{max}^i$	§5.2.2
$\tau_{i-1,i}$	normalized feedforward delay from VP switch $(i-1)$ to VP switch i	§2.3.2
$\tau_{i,i-1}$	normalized feedback delay from VP switch i to VP switch $(i-1)$	§2.3.2
$\tau_{i-1,i}'$	link delay from VP switch $(i-1)$ to the VP switch i	§2.3.2
$\tau_{i,i-1}'$	link delay from VP switch i to VP switch $(i-1)$	§2.3.2
τ_j^i	the ith one-hop loop delay between VP switch i and its external node $j\|i$	§2.3.2
$\hat{\tau}_j^i$	a design parameter satisfying $\hat{\tau}_j^i + \tau_j^i = \tau_{max}^i$	§5.2.2
τ_{ji}	normalized feedforward delay from the external node $j\|i$ to VP switch i	§2.3.2
τ_{ij}	normalized feedback delay from VP switch i to the external node $j\|i$	§2.3.2
τ_{ji}'	link delay from external node $j\|i$ to VP switch i	§2.3.2
τ_{ij}'	link delay from VP switch i to external node $j\|i$	§2.3.2

Chapter 2

Network Modeling and Assumptions

We first want to present in this section the network operations which provide the common descriptions and assumptions of the network we are going to investigate. We then use the fluid flow modeling technique to build the network models based on our assumptions.

2.1 Network Operations and Modeling

A data communication network is typically composed of a number of geographically distributed source/destination nodes (see Fig. 2). Cells generated at a source node are delivered to their destination through a sequence of intermediate nodes. Figure 3 shows an example of an intermediate node which is an $\overline{N} \times \overline{N}$ output buffered ATM switch that can route cells from a set of incoming links to a set of outgoing links.

It is assumed that the source can transmit a RM (Resource Management) cell at every sampling time T. This cell goes through all the intermediate switching nodes to its destination, and then it is sent back by the destination node to the originating source. The RM cell carries three values: the buffer occupancy in a switching node, a time stamp and the number of active controlled VCs M in the switch. The buffer occupancy is used for the rate-based controller to allocate bandwidth for the source. Initially, the value of the buffer occupancy is zero, and this value will be replaced if a switching node has a larger value of buffer occupancy.

To model the traffic flowing through an intermediate node would therefore depend on the number of source-destination pairs that are routed through the node, and the rates at which the sources introduce cells into the network.

Our proposed traffic controllers are geographically distributed over the source nodes. Each source node has its own local controller. Based on the feedback information on the buffer occupancy in the bottleneck switch, the local controller calculates the maximum rate at which a source can transmit data to the network. Two types of control schemes are considered:

1) deterministic, continuous-time control, and

2) deterministic, discrete-time control with periodic sampling.

Unlike the control scheme in [13], our control schemes don't need to place a main controller in the bottleneck switch to accomplish the calculation of traffic rates for all sources. Also unlike the single/binary bit type control schemes discussed in [2] and the explicit type control schemes discussed in [5], the local controllers in our control scheme are open-loop stable which is an important consideration for system stability, e.g., when VC links are broken.

There are two types of fluid models for the implementation of ABR traffic controllers:

1. end-to-end model, which is suitable for homogeneous environment, e.g., single network administration, and for small size of network,

2. hop-by-hop model, which describes the traffic flow between two neighboring switches and provides the most tight structure to achieve the most effective control.

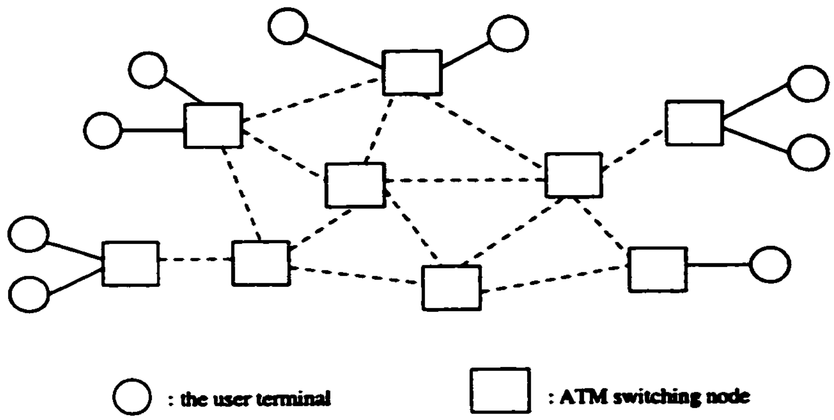

Fig. 2. The topology of an ATM network

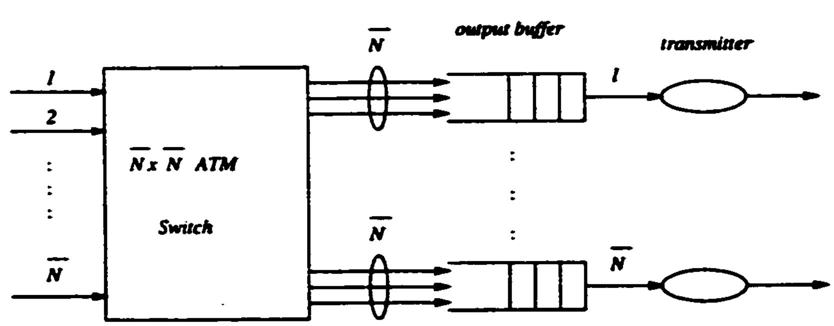

Fig. 3. an example of an ATM switch with output buffer

In the thesis, the end-to-end network modeling and hop-by-hop network modeling are considered. All of our proposed traffic controllers are designed based on the fluid model. It will demonstrate that the queuing dynamics controlled by the proposed controllers based on the fluid model are very accurate to the simulation results obtained from the OPNET simulation tool [55].

2.2 End-to-End Fluid Modeling

Figure 4 represents the model to be considered here, which captures the essential dynamic behavior of an ATM network depicted in Figures 2 and 3.

In Figure 4, the switching node accumulates multiple virtual connections (VC). This switching node may be any one of the intermediate switching nodes whenever it has the largest value of buffer occupancy. The number of controlled VCs which go through the switching node is assumed to be equal to the number of active source nodes to be controlled, and this number may vary with time t. The maximum number of virtual connections allowed through the node is assumed to be N. The switching node has a finite buffer space K to store the incoming cells, and its output link has a varying data rate $\nu_A(t)$.

2.2.1 Continuous Time Model

Assume that there are L intermediate switching nodes between a pair of source and destination. Let $x_l(t)$ be the buffer occupancy in switching node l, and τ_j^l be the delay between node l and node j, where the source is node 0, the destination is node $L+1$. Then when the the RM

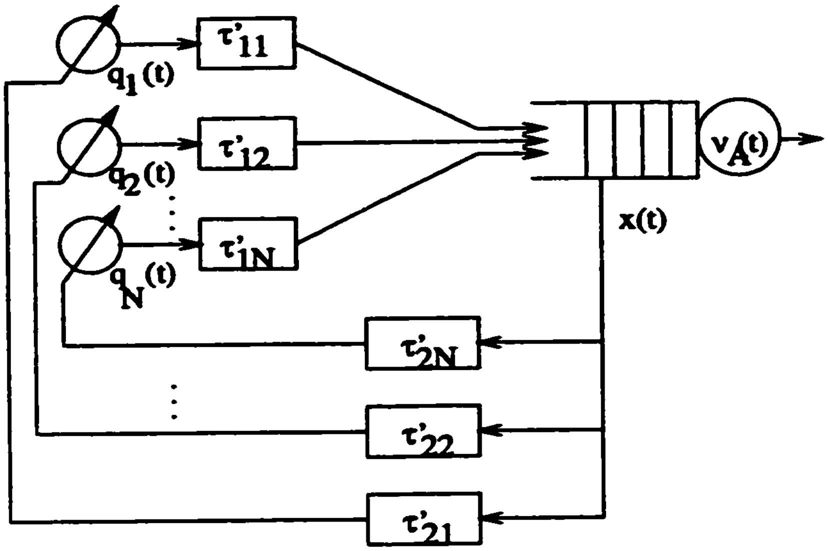

Fig. 4. Analytical model for an ATM switching network

cell arrives at the destination node, it contains the following value:

$$x(t) = \max\{x_l(t - \tau_l^{L+1});\ l = 1, 2, \cdots, L\} .$$

The time stamp records the time when the RM cell finds a switch which has the buffer occupancy $x(t)$.

There are two kinds of delays for VC's: τ'_{1i} is the path delay from the ith source node to the switching node and τ'_{2i} is the path delay from the switching node to the ith source node. There are two kinds of traffic: 1) uncontrolled traffic (e.g., guaranteed service traffic), which is not throttled at the source node as long as it conforms to specifications, and 2) controlled traffic (e.g., best-effort service traffic), which can only be transmitted when there is no congestion in the network. The congestion can be measured by the difference between buffer occupancy and specified buffer threshold. Let ν be the switch's service bandwidth and $w(t)$ be the total uncontrolled traffic rate, then the service rate available to the controlled traffic is given by

$$\nu_A(t) = \nu - w(t) . \tag{2.1}$$

Also let $q_i(t)$ be the controlled traffic rate from the ith source. $q_i(t)$ will be regulated based on buffer occupancy $x(t)$ which is sent to the controlled source nodes every T seconds. Finally we assume that the service to the controlled traffic is FCFS and the cell length is constant.

According to the modeling assumptions, the buffer occupancy of a switching node can be described by a non-linear, time-variant, and integral equation with path delays (see [13] and [19])

$$x(t) = Sat_K\{\int_0^t \left[\sum_{i=1}^{N} e_i(s-\tau'_{1i})q_i(s-\tau'_{1i}) - \nu_A(s)\right] ds\} \tag{2.2}$$

where K is the buffer size, $x(t)$ is the buffer occupancy, and

$$Sat_K\{x\} = \begin{cases} K & x > K \\ x & 0 \le x \le K \\ 0 & x < 0 \end{cases}$$

$$e_i = \begin{cases} 1 & \text{the } i\text{th source node is active} \\ 0 & \text{otherwise.} \end{cases}$$

In the system described by (2.2), the ith active source node can only measure the buffer occupancy $x(t)$ after a path delay τ'_{2i}. It implies that if the feedback control is employed, the system has to include input functions involving the round trip delays $\tau'_i := \tau'_{1i} + \tau'_{2i}$, $i = 1, 2, \cdots, N$. Let $u_i(t) = q_i(t + \tau'_{2i})$, then equation (2.2) can be rewritten as

$$x(t) = Sat_K\{\int_0^t \left[\sum_{i=1}^{N} e_i(t-\tau'_{1i})u_i(s-\tau'_i) - \nu_A(s)\right] ds\} \ . \tag{2.3}$$

In comparison with conventional fluid models for a switch network, the most important features added to our models are that 1) both best-effort service traffic and guaranteed service traffic are integrated into the switch's fluid model, and 2) the number of active VCs can be changed over time as the factors e_i are time-variant. We shall formulate in the following a controller for the buffer occupancy due to these unpredictable traffic streams.

2.2.2 Discrete Time Model with Periodic Sampling

In this model, we assume that the switching node sends information to the source nodes every T seconds, and that path delay factors τ'_{1i}/T can be decomposed as $\tau_{1i} + \gamma_i/T$, where τ_{1i} is an integral multiple of T and is called the feedforward delay from the source node to the bottleneck node, and $0 \leq \gamma_i < T$, $i = 1, 2, \cdots, N$. Then the change of buffer occupancy of the switching node in Fig. 4 is given by the following discrete-time expression (see [13]):

$$x(n+1) = Sat_K\{x(n) + \sum_{i=1}^{N} e_i(n - \tau_{1i} - \frac{\gamma_i}{T})\lambda_i(n - \tau_{1i} - \frac{\gamma_i}{T}) - \mu_A(n)\} \tag{2.4}$$

where $\lambda_i(n) = \int_{nT}^{(n+1)T} u_i(t)dt$ denote the numbers of cells flowing into the network from the ith VC during the the nth interval of T, and $\mu_A(n) = T\nu_A(nT)$ denotes the number of controlled cells emitted from the switching node during the the nth interval of T.

Remark 2.2.1 *Although the equation (2.2) cannot be directly discretized into Equ. (2.4), we can obtain Equ. (2.4) by discretizing Equ. (2.2) without saturation first, and then by adding saturation to the discretized equation.*

Let $\mu = T\nu$ and let $d(n) = \int_{nT}^{(n+1)T} w(t)dt$ denote the numbers of cells flowing into the switch from the uncontrolled traffic during the the nth interval of T. Then the service bandwidth available to the controlled traffic is expressed by

$$\mu_A(n) = \mu - d(n) \ . \tag{2.5}$$

In the following, we consider the case where the path delay τ'_{1i} is a multiple of T, i.e., $\gamma_i = 0$, $i = 1, 2, \cdots, N$. This is reasonable because we can always add a small delay to the path delay by holding the cells at source nodes. The buffer equation given in (2.4) can then be rewritten as

$$x(n+1) = Sat_K\{x(n) + \sum_{i=1}^{N} e_i(n - \tau_{1i})\lambda_i(n - \tau_{1i}) - \mu_A(n)\} \tag{2.6}$$

We similarly assume that the path delay τ'_{2i} is a multiple of T, i.e., $\tau'_{2i} = \tau_{2i}T$, $i = 1, 2, \cdots, N$. The integer τ_{2i} is then called the feedback delay from the bottleneck node to the source node. Define

$$u_i(n) = \lambda_i(n + \tau_{2i}) - \mu_i^{max}$$

where μ_i^{max} is the maximum number of cells the ith source node is allowed to transmit the data into the network in an interval T.

Let $\hat{\mu}_A(n) = \mu_A(n) - \sum_{i=1}^{N} e_i(n - \tau_{1i})\mu_i^{max}$. We then have from (2.4),

$$x(n+1) = Sat_K\{x(n) + \sum_{i=1}^{N} e_i(n - \tau_{1i})u_i(n - \tau_i) - \hat{\mu}_A(n)\} \ , \tag{2.7}$$

where $\tau_i := \tau_{1i} + \tau_{2i}$ is called the total delay for the ith VC.

2.3 Hop-by-Hop Fluid Modelling

Using the concept the virtual source and virtual destination [36], we can segment an end-to-end controlled network to a hop-by-hop controlled network.

2.3.1 Continuous Time Model

We only model a single virtual path (see Figure 5) that goes through a sequence of intermediate VP switching nodes to a destination node. All traffic from the source nodes which join to any VP switching node in the virtual path will go along this virtual path to the same destination. It is not required that uncontrolled traffic goes through this virtual path to the end. Each VP

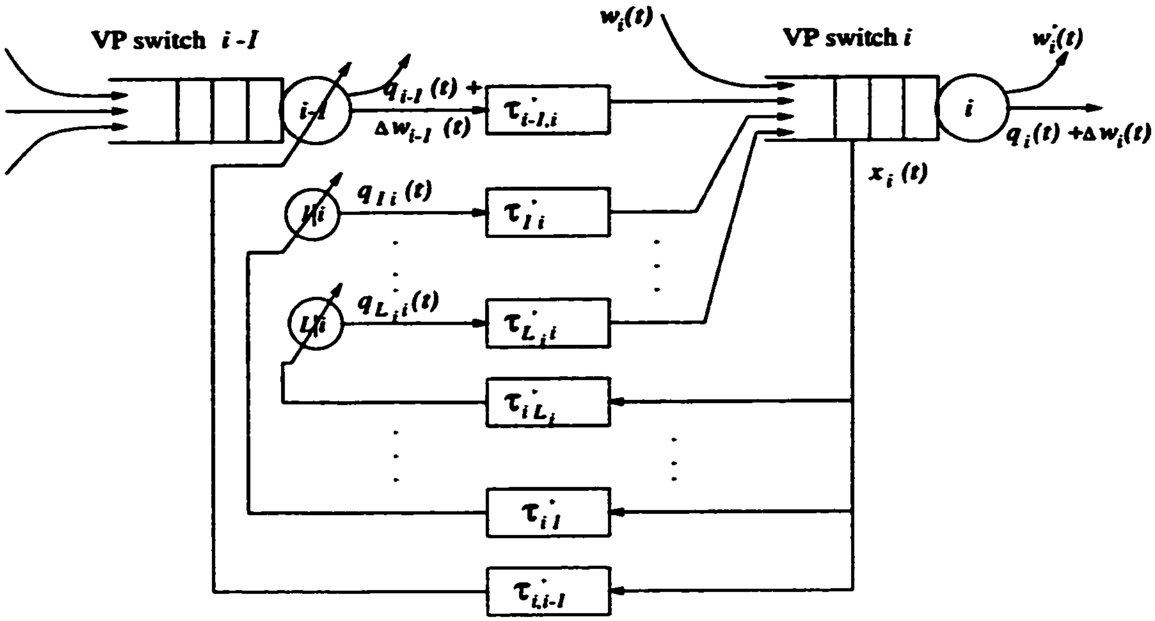

Fig. 5. System model

switching node has a finite buffer space K_i to store the incoming packets and a service capacity of ν_i, where ν_i is constant. There are two kinds of propagation delays between two VP switching nodes: $\tau'_{i-1,i}$ is the link delay from VP switch $(i-1)$ to VP switch i, and $\tau'_{i,i-1}$ is the link delay from VP switch i to VP switch $(i-1)$.

Besides VP links between the VP switches, each VP switch also accepts controlled traffic from external nodes(e.g., the other intermediate VP switches or terminals). There are two kinds of propagation delays between external source nodes and a VP switching node: τ'_{ji}, $j = 1, 2, \cdots, L_i$, is the link delay from the external node $j|i$ to VP switch i, and τ'_{ij}, $j = 1, 2, \cdots, L_i$, is the link delay from VP switch i to the external node $j|i$.

For each VP switch i, let $x_i(t)$ be the buffer occupancy. Let $w_i(t)$ be the rate of incoming uncontrolled traffic, $w_i'(t)$ be the rate of outgoing uncontrolled traffic to switches other than VP switch $(i+1)$, and $\Delta w_i(t)$ be the rate of outgoing uncontrolled traffic to VP switch $(i+1)$.

Let $q_i(t)$ be the rate of outgoing controlled traffic. The value of $q_{i-1}(t)$ is regulated based on buffer occupancy $x_i(t)$, which is send back to VP switch $(i-1)$ every T seconds. Furthermore, we assume that the service is FCFS, and the uncontrolled traffic $w_i(t)$ and $\Delta w_i(t)$ have higher service priority.

Let ν_i denote the node capacity of VP switch i, which is the maximal allowed rate at which the switch can serve the traffic. Let ν_i^* denote the link capacity of VP switch i, which is the maximum link rate at which VP switch i can transmit traffic to VP switch $(i+1)$. It is clear that $\nu_i^* \leq \nu_i$ since only a portion of total service rate may be allocated to serve the uncontrolled traffic. Two types of congestion may occur in a VP switch.

1) Node congestion:

$$Sat_{\nu_i^*}\{q_i(t) + \Delta w_i(t)\} + w_i'(t) > \nu_i, \quad i = 1, 2, \cdots, H, \tag{2.8}$$

This implies that the capacity of switch i is exhausted by the egress traffic $q_i + \Delta w_i$ to the down-stream VP switch $(i+1)$, and the egress traffic w_i'.

2) Link congestion:

$$q_i(t) + \Delta w_i(t) > \nu_i^*, \quad i = 1, 2, \cdots, H, \tag{2.9}$$

where H is the number of VP switches in a virtual path. In this case, the capacity of the link to the down-stream VP switch $(i+1)$ is exhausted.

A VP switch is called node-congested if node congestion (type 1) occurs only. A VP switch is called link-congested if link congestion (type 2) occurs only. A VP switch is called congestion free if it is not node-congested nor link-congested. Note that a VP switch may be both node-and link- congested, in which case, we simply refer to it as a congested switch.

The following definitions are needed when we discuss the network's steady state behavior. A VP switch is called *persistently node-congested* if it is node-congested as $t \to \infty$. A VP switch is called *persistently link-congested* if it is link-congested as $t \to \infty$.

Now consider that if there are some VP switches which are link-congested, we assume that VP switch I is the last one which is link-congested along the virtual path. Then, according to the modeling assumptions, the dynamics of the ith VP switch in a virtual path can be described by a non-linear, time-invariant and delay-input integral equations:

$$x_i(t) = Sat_{K_i}\{\int_0^t \left[q_{i-1}(s-\tau'_{i-1,i}) + \sum_{j=1}^{L_i} q_{ji}(s-\tau'_{ji}) + w_i(s) + \Delta w_{i-1}(s-\tau'_{i-1,i}) - \nu_i(s)\right] ds\},$$

$$\nu_i(t) = \begin{cases} Sat_{\nu_i}\{Sat_{\nu_i^*}\{q_i(t)+\Delta w_i(t)\} + w'_i(t)\}, & i = 1,2,\cdots,I-1, \\ Sat_{\nu_I}\{\nu_I^* + w'_I(t)\}, & i = I \end{cases} \tag{2.10}$$

where $q_0(t) = 0$, and $\nu_i(t)$ is traffic flow leaving VP switch i,

$$Sat_{K_i}\{x_i\} = \begin{cases} K_i & x_i > K_i \\ x_i & 0 \le x_i \le K_i \\ 0 & x_i < 0 \end{cases} .$$

2.3.2 Discrete Time Model with Periodic Sampling

Assume that the VP switching node sends information to the upstream nodes every T seconds. Also assume that the link delay factors $\tau'_{i-1,i}/T$ can be decomposed as $\tau_{i-1,i} + \gamma_i/T$, where $0 \leq \gamma_i < T$, $i = 1, 2, \cdots, I$, and that the link delay factor τ'_{ji}/T can be decomposed as $\tau_{ji} + \gamma_{ji}/T$, $j = 1, 2, \cdots L_i$. Then the change of buffer occupancy of the switch node can be discretized in the form

$$
\begin{aligned}
x_i(n+1) &= Sat_{K_i}\{x_i(n) + \lambda_{i-1}(n - \tau_{i-1,i} + \frac{\gamma_i}{T}) + \sum_{j=1}^{L_i} \lambda_{ji}(n - \tau_{ji} - \frac{\gamma_{ji}}{T}) \\
&\quad + d_i(n) + \Delta d_{i-1}(n - \tau_{ji} - \frac{\gamma_{ji}}{T}) - \mu_i(n)\},
\end{aligned}
\tag{2.11}
$$

$$
\mu_i(n) = \begin{cases} Sat_{\Gamma_i}\{Sat_{\Gamma_i^*}\{\lambda_i(n) + \Delta d_i(n)\} + d'_i(n)\}, & i = 1, 2, \cdots, I-1, \\ Sat_{\Gamma_I}\{\Gamma_I^* + d'_I(n)\}, & i = I \end{cases}
$$

where, during the the nth interval of T, $\lambda_{i-1}(n) = \int_{nT}^{(n+1)T} q_{i-1}(t)dt$ denotes the number of controlled packets transmitted from VP switch $(i-1)$ to VP switch i, where $\lambda_0(n) = 0$, $\lambda_{ji}(n) = \int_{nT}^{(n+1)T} q_{ji}(t)dt$ denotes the number of controlled packets transmitted from external node $j|i$ to VP switch i, $d_i(n) = \int_{nT}^{(n+1)T} w_i(t)dt$ denotes the number of uncontrolled packets flowing into VP switch i, $d'_i(n) = \int_{nT}^{(n+1)T} w'_i(t)dt$ and $\Delta d_i(n) = \int_{nT}^{(n+1)T} \Delta w_i(t)dt$ denote the numbers of uncontrolled packets leaving VP switch i, and $\mu_i(n) = \int_{nT}^{(n+1)T} \nu_i(t)dt$ denotes the number of packets emitted from VP switch i. Γ_i and Γ_i^* are the upper bounds for the node capacity and the link capacity respectively.

For the link between VP switch $(i-1)$ to VP switch i, we consider the case where the link delay is the multiple of T, i.e., $\gamma_i = 0$. Otherwise, we can always add a small delay to the link delay such that it is the multiple of T. Then $\tau_{i-1,i}$ is called the feedforward delay normalized with T. Let $\tau_i = \tau_{i-1,i} + \tau_{i,i-1}$, where $\tau_{i,i-1}$, called the feedback delay normalized with T, is also assumed to be integer. Let $u_{i-1}(n) = \lambda_{i-1}(n + \tau_{i,i-1}) - \mu_{i-1}$, where $\mu_{i-1} := \sum_{k=1}^{M_i} \mu_k^i$ is the maximum number of controlled packets allowed for VP $(i-1)$ switch to transmit the data into VP switch

i, and μ_k^i is the maximum number of controlled packets allowed for the kth VC carried in VP switch $(i-1)$, in the interval of T.

For the external links to VP switch i, let $\tau_j^i = \tau_{ji} + \tau_{ij}$, and τ_{ij} is the normalized feedback delay from VP switch i to the external node $j|i$, $j = 1, 2, \cdots L_i$, and let $u_{ji} = \lambda_{ji}(n + \tau_{ij}) - \mu_{ji}$, where μ_{ji} is the maximum number of controlled packets allowed for the external VC j to transmit the data into the VP switch i in the interval of T. We then have

$$
\begin{aligned}
x_i(n+1) &= Sat_{K_i}\{x_i(n) + u_{i-1}(n-\tau_i) + \sum_{j=1}^{L_i} u_{ji}(n-\tau_j^i) + d_i(n) + \Delta d_{i-1}(n-\tau_i) - \hat{\mu}_i(n)\}, \\
\mu_i(n) &= \begin{cases} Sat_{\Gamma_i}\{Sat_{\Gamma_i^*}\{\lambda_i(n) + \Delta d_i(n)\} + d_i'(n)\}, & i = 1, 2, \cdots, I-1 \\ Sat_{\Gamma_I}\{\Gamma_I^* + d_I'(n)\}, & i = I \end{cases}
\end{aligned}
\tag{2.12}
$$

where $u_0(n) = 0$, and $\hat{\mu}_i(n) = \mu_i(n) - \mu_{i-1} - \sum_{j=1}^{L_i} \mu_{ji}$.

2.4 Concluding Remarks

In this chapter, the fluid flow modeling technique is used to build the mathematical model for the high-speed networks. The model, defined either in the continuous-time domain or in the discrete-time domain, describes the queuing behavior associated with traffic rates in the source nodes, intermediate switching nodes and destination nodes. The propagation delays play an important role in the model and will be a major concern on the design of traffic control in the following sections.

In the following chapters, we will apply the network models to develop our traffic controllers. In order to investigate the stability of the networks provided in this chapter, it has been shown in [10] and [13] that it is sufficient to study the locally asymptotical stability properties of the system by removing the saturation nonlinearities posed on the network models and the controller. The reason is that

1. a rigorous proof of stability of the system using Liapunov's second approach [46] may be possible, but the gain from the analysis is slight, and

2. these nonlinearities will not be activated for small deviations around network's operating point.

Thus in the following chapters, we only study the system's stability of linear-time networks with linear-time traffic controllers applied. Our simulation experiments, however, are conducted with finite buffer size K. As one shall see, the results of our simulations in turn support and confirm the feasibility of this important assumption.

Chapter 3

End-to-End Continuous-Time Control

In this chapter, we use the Lyapunov theory to design continuous-time controllers to control ABR service traffic based on the continuous-time fluid model described by Equ. (2.3). In section 3.1, a preliminary lemma is introduced to provide the sufficient conditions that a differential equation with a bounded delay is asymptotically stable. This result will then be used in section 3.2 and 3.3 for our development on the congestion control of the high-speed network with variable long delays.

3.1 Preliminaries

Let R^n denote an n-dimensional linear vector space over the reals with Euclid norm $||\cdot||$. Let $C_n = C([0,r], R^n)$ be the Banach space of continuous functions mapping the interval $[0,r]$ into R^n with the topology of uniform convergence. For given $f \in C_n$, define $||f(t,\theta)||_r := \sup_{0\leq\theta\leq r} ||f(t-\theta)||$. Let $R = (-\infty, \infty)$, $R^+ = [0, \infty)$. The following result is important to our following development.

Consider a time-delayed differential equation:

$$\begin{aligned} \dot{x}(t) &= f(t, x(t-\theta)), \quad t \geq t_0 \textit{ and } \theta \in [0, r] \\ x(t_0 - \theta) &= \psi(\theta), \qquad \theta \in [0, r] \, . \end{aligned} \tag{3.1}$$

where $\psi(\theta) \in R^n$ is a given function of θ.

Lemma 3.1.1 *([31] and [47]) Suppose $u, v, w : R^+ \rightarrow R^+$ are continuous, strictly monotonous increasing functions, $u(s)$, $v(s)$, and $w(s)$ are positive for $s > 0$, and $u(0) = v(0) = 0$. If there is continuous function $V : R \times R^n \rightarrow R^+$ such that*

1.

$$u(||x||) \leq V(t, x) \leq v(||x||), \quad t \in R, x \in R^n \tag{3.2}$$

2. for any $t_0 \in R$,

$$\dot{V}(t, x) \leq -w(||x(t)||) \tag{3.3}$$

if there is a continuous nondecreasing function $p(s) > s$ for $s > 0$ (see [47]),

$$V(t-\theta, x(t-\theta)) < p(V(t, x(t))), \quad \theta \in [0, r], t \geq t_0 \tag{3.4}$$

or if there exists a constant $\alpha > 1$ (see [31]),

$$||x(t, \theta)||_r < \alpha ||x(t)||, \quad t \geq t_0 \, , \tag{3.5}$$

then the zero solution of (3.1) is uniformly asymptotically stable. If $u(s) \rightarrow \infty$ as $s \rightarrow \infty$, then the zeros solution of (3.1) is also uniformly asymptotically stable in the large.

3.2 Proportional Feedback Control

Now we can use the result in the previous section to study a congestion controller that can stablize the network with bounded variable propagation, queuing or processing delays.

Let $\hat{x}(t) = x(t) - x_0$, where x(t) is the buffer occupancy at time t, and x_0 is the buffer threshold that indicates the congestion level. Without consideration of the saturation imposed on the buffer occupancy equation (2.3), the dynamics of the buffer occupancy can be described by a linear continuous-time differential fluid model:

$$\dot{\hat{x}}(t) = \sum_{i=1}^{N} e_i(t - \tau'_{1i})u_i(t - \tau'_i) + w(t) - \nu \tag{3.6}$$

where τ'_i is the round trip delay between the source i and its destination. When this delay includes the queuing delay, it would be the function of time t, i.e.,

$$\tau'_i := \tau'_i(t) \ .$$

Since we use RM cells to measure the propagation delays encountered between source nodes and destination node, and the RM cells has the highest priority of service, we then assume that τ'_i is bounded by a positive constant h_i. This implies that

$$0 \le \tau'_i(t) \le h_i, \qquad t \ge 0. \tag{3.7}$$

Consequently, it is reasonable to assume that the propagation delays are approximately measurable and bounded. In order to shorten the length of equations, we shall use τ'_i to denote $\tau'_i(t)$ in the following development.

3.2.1 Controller Design and Stability Analysis

Without consideration of saturation on (3.6), we obtain

$$\dot{\hat{x}}(t) = \sum_{i=1}^{N} e_i(t - \tau'_{1i})u_i(t - \tau'_i) + w(t) - \nu \ . \tag{3.8}$$

Define a proportional continuous-time controller:

$$u_i(t) = \mu_i^{max} - k_i\hat{x}(t), \quad i = 1, 2, \cdots, N, \tag{3.9}$$

where μ_i^{max} is the peak cell rate allowed at source i, and k_i is constant. Therefore the transmission rate at source i is given by

$$q_i(t) = \mu_i^{max} - k_i[x(t - \tau_{2i}^{'}) - x_0], \quad i = 1, 2, \cdots, N. \tag{3.10}$$

Substituting (3.9) into the system (3.6) results in the following closed-loop system

$$\dot{x}(t) = -\sum_{i=1}^{N} k_i e_i(t - \tau_{1i}^{'})\hat{x}(t - \tau_i^{'}) + \sum_{i=1}^{N} e_i(t - \tau_{1i}^{'})\mu_i^{max} + w(t) - \nu \ . \tag{3.11}$$

By a straightforward calculation, we have

$$\begin{aligned} \dot{x}(t) &= -\sum_{i=1}^{N} k_i e_i(t - \tau_{1i}^{'})\hat{x}(t) + \sum_{i=1}^{N} k_i e_i(t - \tau_{1i}^{'}) \int_{t-\tau_i^{'}}^{t} \dot{\hat{x}}(s)ds + \sum_{i=1}^{N} e_i(t - \tau_{1i}^{'})\mu_i^{max} + w(t) - \nu \\ &= -\sum_{i=1}^{N} k_i e_i(t - \tau_{1i}^{'})\hat{x}(t) + \sum_{i=1}^{N} k_i e_i(t - \tau_{1i}^{'}) \int_{t-\tau_i^{'}}^{t} \Bigg[-\sum_{j=1}^{N} k_j e_j(s - \tau_{1j}^{'})\hat{x}(s - \tau_j^{'}) \\ &\quad \sum_{j=1}^{N} e_j(s - \tau_{1j}^{'})\mu_j^{max} + w(s) - \nu\Bigg] ds + \sum_{i=1}^{N} e_i(t - \tau_{1i}^{'})\mu_i^{max} + w(t) - \nu \ . \end{aligned} \tag{3.12}$$

Let

$$\hat{w}(t) := \sum_{i=1}^{N} k_i e_i(t - \tau_{1i}^{'}) \int_{t-\tau_i^{'}}^{t} [\sum_{j=1}^{N} e_j(s - \tau_{1j}^{'})\mu_j^{max} + w(s) - \nu]ds + \sum_{i=1}^{N} e_i(t - \tau_{1i}^{'})\mu_i^{max} + w(t) - \nu.$$

Then Eq. (3.12) becomes

$$\dot{x}(t) = -\sum_{i=1}^{N} k_i e_i(t - \tau_{1i}^{'})\hat{x}(t) - \sum_{i=1}^{N} k_i e_i(t - \tau_{1i}^{'}) \left[\sum_{j=1}^{N} k_j \int_{t-\tau_i^{'}}^{t} e_j(s - \tau_{1j}^{'})\hat{x}(s - \tau_j^{'})\right] ds + \hat{w}(t). \tag{3.13}$$

When we consider the asymptotical stability of the system (3.13), we can remove the exterior disturbance term $\hat{w}(t)$ from the system (3.13). Thus we have the following result:

Theorem 3.2.1 *The closed-loop system (3.13) with $\hat{w}(t) = 0$ is uniformly asymptotically stable in the large if*

$$\begin{aligned} &k_i > 0, \quad i = 1, 2, \cdots, N, \\ &\sum_{j=1}^{N} k_j < \frac{1}{h_{max}}, \end{aligned} \tag{3.14}$$

where $h_{max} := max\{h_i,\ i = 1, 2, \cdots, N\}$.

Proof. Define a quadratic Lyapunov function:

$$V(\hat{x}) = \frac{1}{2}\hat{x}^2(t). \tag{3.15}$$

By the time derivative of $V(\hat{x}(t))$ along the trajectories of (3.12), we have

$$\begin{aligned} \dot{V}(\hat{x}(t)) &= \hat{x}(t)\dot{\hat{x}}(t) \\ &= -\hat{x}(t)\{\sum_{i=1}^{N} k_i e_i(t - \tau_{1i}^{'})\hat{x}(t) + \sum_{i=1}^{N} k_i e_i(t - \tau_{1i}^{'}) \int_{t-\tau_i^{'}}^{t} \left[\sum_{j=1}^{N} k_j e_j(s - \tau_{1j}^{'})\hat{x}(s - \tau_j^{'})\right] ds\} \\ &= -\left[\sum_{i=1}^{N} k_i e_i(t - \tau_{1i}^{'})\right] \hat{x}^2(t) + \hat{x}(t) \sum_{i=1}^{N} k_i e_i(t - \tau_{1i}^{'}) \int_{t-\tau_i^{'}}^{t} \left[\sum_{j=1}^{N} k_j e_j(s - \tau_{1j}^{'})\hat{x}(s - \tau_j^{'})\right] ds. \end{aligned}$$

From (3.7), we have

$$\begin{aligned} &|\hat{x}(t) \sum_{i=1}^{N} k_i e_i(t - \tau_{1i}^{'}) \int_{t-\tau_i^{'}}^{t} \left[\sum_{j=1}^{N} k_j e_j(s - \tau_{1j}^{'})\hat{x}(s - \tau_j^{'})\right] ds| \\ &\leq \sum_{i=1}^{N} |k_i| e_i(t - \tau_{1i}^{'}) \sum_{j=1}^{N} |k_j| \tau_i^{'} ||e_j(t, \theta)||_{\tau_i^{'}+\tau_j^{'}} ||\hat{x}(t, \theta)||_{\tau_i^{'}+\tau_j^{'}} |\hat{x}(t)| \\ &\leq \sum_{i=1}^{N} h_i |k_i| e_i(t - \tau_{1i}^{'}) \sum_{j=1}^{N} |k_j| ||e_j(t, \theta)||_{\tau_i^{'}+\tau_j^{'}} ||\hat{x}(t, \theta)||_{\tau_i^{'}+\tau_j^{'}} |\hat{x}(t)|. \end{aligned}$$

Let $\tau_{max} := \max\{\tau_i^{'} + \tau_j^{'},\ i, j = 1, 2, \cdots, N\}$. Suppose that there exists a positive constant α such that $||\hat{x}(t, \theta)||_{\tau_{max}} < \alpha|\hat{x}(t)|$. Then we have

$$\begin{aligned} \dot{V}(\hat{x}(t)) &\leq -\left[\sum_{i=1}^{N} k_i e_i(t - \tau_{1i}^{'})\right] \hat{x}^2(t) + \sum_{i=1}^{N} h_i |k_i| e_i(t - \tau_{1i}^{'})| \sum_{j=1}^{N} |k_j| ||e_j(t, \theta)||_{\tau_{max}} ||\hat{x}(t, \theta)||_{\tau_{max}} |\hat{x}(t)| \\ &\leq -\left[\sum_{i=1}^{N} k_i e_i(t - \tau_{1i}^{'})\right] \hat{x}^2(t) + \alpha \sum_{i,j=1}^{N} h_i |k_i k_j| e_i(t - \tau_{1i}^{'})\hat{x}^2(t) \\ &:= -\beta \hat{x}^2(t) \end{aligned}$$

where

$$\beta = \sum_{i=1}^{N} \left[k_i - \alpha h_i \sum_{j=1}^{N} |k_i k_j| \right] e_i(t - \tau'_{1i}).$$

If the condition (3.14) holds, then there exists a sufficient small number ϵ such that

$$k_i - (1+\epsilon) h_i \sum_{j=1}^{N} k_i k_j > 0, \quad i = 1, 2, \cdots, N.$$

Let $\alpha = 1 + \epsilon$. Then $\alpha > 1$, and $\beta > 0$ for all t. Thus it follows Lemma 3.1.1 that the closed-loop system is uniformly asymptotically stable in the large. ¶

Remark 3.2.1 *(Fairness) By choosing*

$$k_1 = k_2 = \cdots = k_N = k,$$

where

$$k < \frac{1}{N h_{max}},$$

then the fairness is achieved in the sense that each source has the same feedback gain.

Also by choosing

$$k_i = \frac{\mu_i^{max}(1-\alpha)}{\hat{x}},$$

where α is a constant which should be selected such that the conditions 3.2.1 are satisfied, we then have

$$u_1(t) = u_2(t) = \cdots = u_N(t).$$

Thus, the fairness is achieved in the sense that each source shares the same bandwidth available in the switching node.

Now consider the steady behavior of the network (3.8) controlled by (3.9). Let x_s, u_{is}, q_{is} and w_s be the steady state values corresponding to $x(t)$, $u_i(t)$, $q_i(t)$ and $w(t)$ respectively as

$t \to \infty$. We then have

$$-\sum_{i=1}^{N} k_i e_{is}[x_s - x_0] + \sum_{i=1}^{N} e_{is}\mu_i^{max} + w_s - \nu = 0.$$

So,

$$x_s = x_0 + \frac{\sum_{i=1}^{N} e_{is}\mu_i^{max} + w_s - \nu}{\sum_{i=1}^{N} k_i e_{is}} \tag{3.16}$$

If we have $\sum_{i=1}^{N} e_{is}\mu_i^{max} + w_s = \nu$, then we obtain zero deviation of queue length from its threshold x_0, i.e.,

$$x_s = x_0.$$

3.2.2 Implementation of the Proportional Controller

Since the controller (3.10) only depends on the difference between queue length $x(t)$ and the threshold x_0 in the congested node, this controller can be distributely implemented in the source nodes.

The resource management (RM) cells are used to carry the differential value between the queue length measured in the switch and the buffer threshold x_0 defined in the switch. The RM cells are generated in sources with zero queue length every M_r data cells. Then RM cells go through all the switches in the connection to the destination. The value of queue length in the RM cells is updated if the real differential value of queue length with its threshold in the switch is larger than that value in the RM cells. The destination will broadcast the RM cells to the sources after it receives every M_r data cells. Finally when the source receives the feedback RM cells, it uses to the control algorithm given by (3.10) to adjust the data transmission rate.

Also in order to smooth the fluctuation in the queue, a filter is used in each source:

$$\dot{\bar{x}}(t) + \alpha\bar{x}(t) = x(t),$$

where $\alpha > 0$ is a positive constant, and $\bar{x}(t)$ is the output of the filter, which is used as the measured queue length in the controller (3.10).

3.2.3 Simulation on the Proportional Controller

We use the OPNET tool to perform the simulation on the model described by (5.1) with the proportional controller given in (3.10). Since our traffic controller aims to regulate the source rates over time, we are particularly interested in analyzing both the transient and steady behaviors of the network. Transient behaviors such as the duration of response time, the maximum transient queue length, and the deviation of the queue length from the threshold are usually the main interests in performance analysis.

First we focus on the traffic control of a switch with a single source node. This will show us how the source responds to the congestion in the switch and regulates its transmission rate and how it can catch up the bandwidth unused in the switch. We then perform the simulation on the control of a switch with multiple sources. We can see how the source nodes independently regulate their rates according to the queue length information sent back from the destination and fairly share the bandwidth in the switch.

A. **Single Source Node**

For the simulation on the traffic control of single source depicted in Fig. 6, it is assumed that the service rate of the switch is $200Kbps$, the minimum transmission rate μ^{min} of the source is $20Kbps$, and the maximum transmission rate μ^{max} of the source is $200Kbps$. Also it is assumed that the uncontrolled source generates the traffic data with a constant transmission

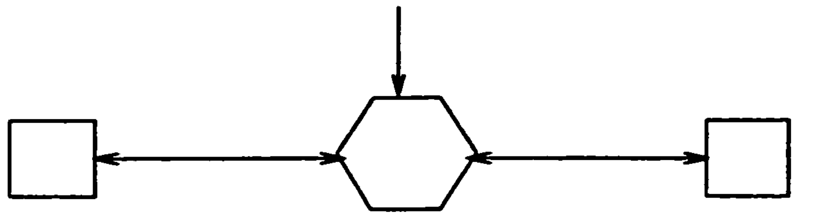

Fig. 6. A network with single source node

rate of $100Kbps$. The threshold x_0 for the queue in the switch is 150 cells.

Case 1. $\tau_1' = \tau_2' = 0.01sec$ and $k = 10$.

In this case, the static round-trip delay is 0.02 sec. If the bound of the round-trip delay $h_{max} = 0.08sec$, it follows from Theorem 3.2.1 that the network is asymptotically stable, if the feedback gain is $k < \dfrac{1}{h_{max}} = 12.5$. Figure 8 shows that the source rate and queue length is stable and have no oscillation when using $k = 10$.

It can be seen from Figure 8 that the steady value of queue length is about 173 cells which is similar to the value from Equation (3.16):

$$\begin{aligned} x_s &= x_0 + \frac{\mu^{max} + w_s - \nu}{k} \\ &= 150 + \frac{(200Kbps + 100Kbps - 200Kbps)/424}{10} \\ &= 173.58(cells). \end{aligned}$$

Also from Figure 8, we can observe that when the uncontrolled traffic flows into the switch at $t = 0.5$ sec, the queue length accumulates linearly. As the queue length reaches the threshold $x_0 = 150$ cells, it takes 0.01 second delay for the source to make response. The source controller reduces the transmission rate quickly till the queue length reaches a new level $x_s = 173.58$ cells. This responsive transient time is about 0.2 second.

Case 2. $\tau_1' = \tau_2^1 = 0.08sec$ and $k = 10$.

In this case, the static round-trip delay is 0.16 sec. Since $k > \frac{1}{0.16}$, it follows from Theorem 3.2.1 that the network may not be asymptotically stable. It is shown in Figure 9 that the source rate and queue length are both unstable with oscillation.

B. <u>**Multiple Source Nodes**</u>

For the simulation on the traffic control of multiple sources depicted in Fig. 7, it is assumed that the service rate of the switch is $2Gbps$, all the traffic data are routed to one destination, and the uncontrolled source generates the periodic on/off traffic with the minimum transmission rate zero and the maximum transmission rate 1 Gpbs. The threshold x_0 for the queue in the switch is 150 cells. The Table 1 gives the attributes of sources and links.

Source i	μ_i^{min} (Mbps)	μ_i^{max} (Mbps)	τ'_{1i} (msec)	τ'_{2i} (msec)
1	150	550	5	5
2	100	500	5	5
3	100	450	9	9
4	100	400	9	9
5	100	350	9	9

Table 1.The parameters for source nodes and links

According to Table 1, the maximum static round-trip delay is 0.018 second. Now we set the upper bound of round-trip delay is 0.019 second. By choosing the feedback gain $k_i = 10$, $i = 1, 2, 3, 4, 5$, we have that

$$\sum_{i=1}^{5} k_i = 50 < \frac{1}{0.019}.$$

It then follows from Theorem 3.2.1 that the network is asymptotically stable.

Figure 11 demonstrates how the sources respond to the change of the periodic uncontrolled

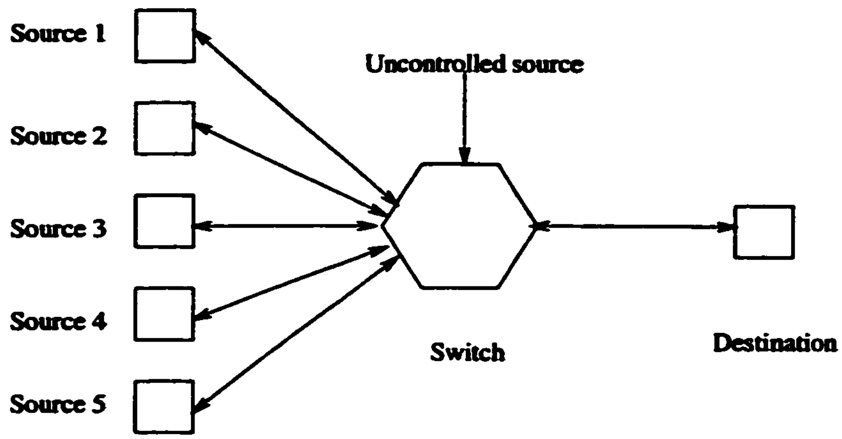

Fig. 7. A Network with Multiple Source Nodes

traffic depicted in Figure 10. The uncontrolled traffic is used to congest the switch. Figure 10 confirms that the queue length is piecewise stable.

It can be seen from Figure 11 that each local controller can respond quickly to decrease its rate when the uncontrolled traffic rate jumps up to the maximum rate, and to increase its rate when uncontrolled traffic rate jumps down to the minimum rate.

It can also be seen that the fairness is achieved because each source reduces its rate by 2.5 when the uncontrolled traffic increases to cause the switch congested, and each source increases its rate by 2.5 when the uncontrolled traffic reduce its rate.

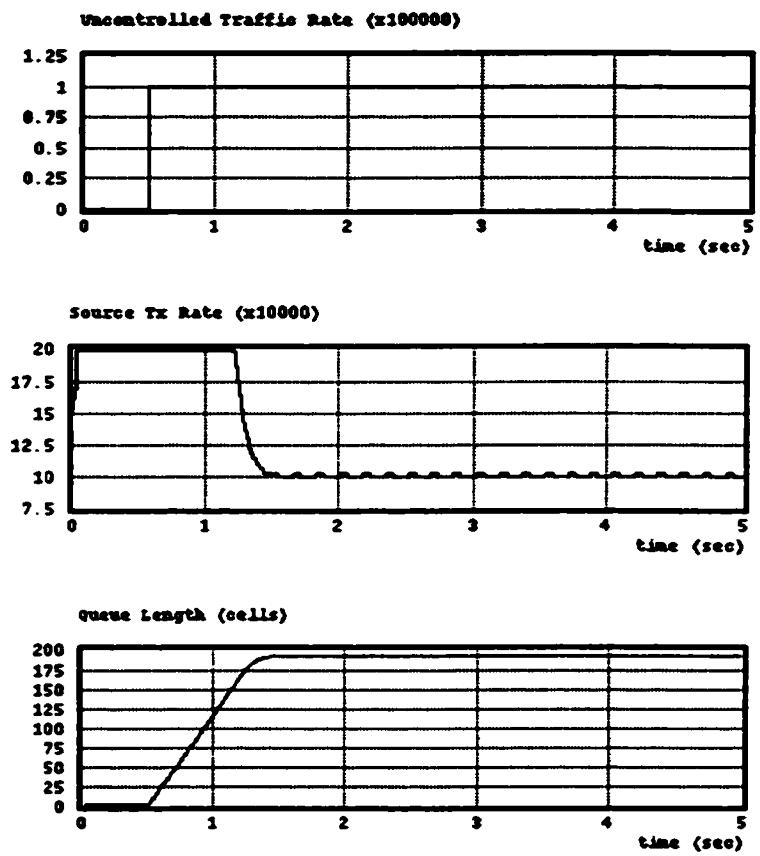

Fig. 8. Single source with τ_1', $\tau_2' = 0.01$ and $k = 10$

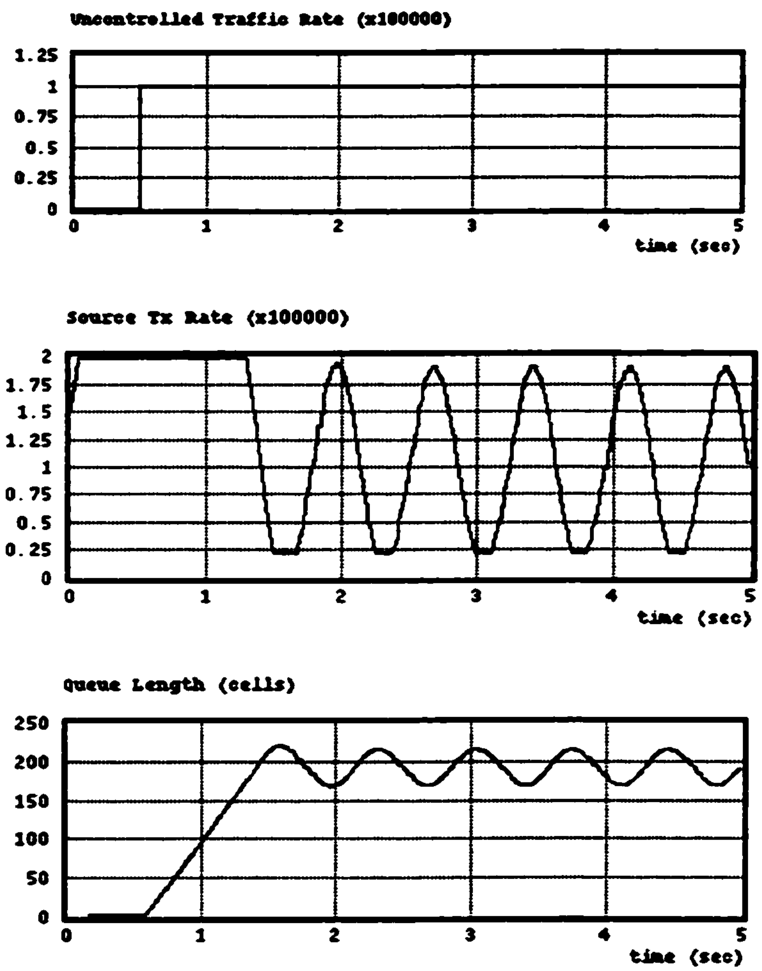

Fig. 9. Single source with τ_1', $\tau_2' = 0.08$ and $k = 10$

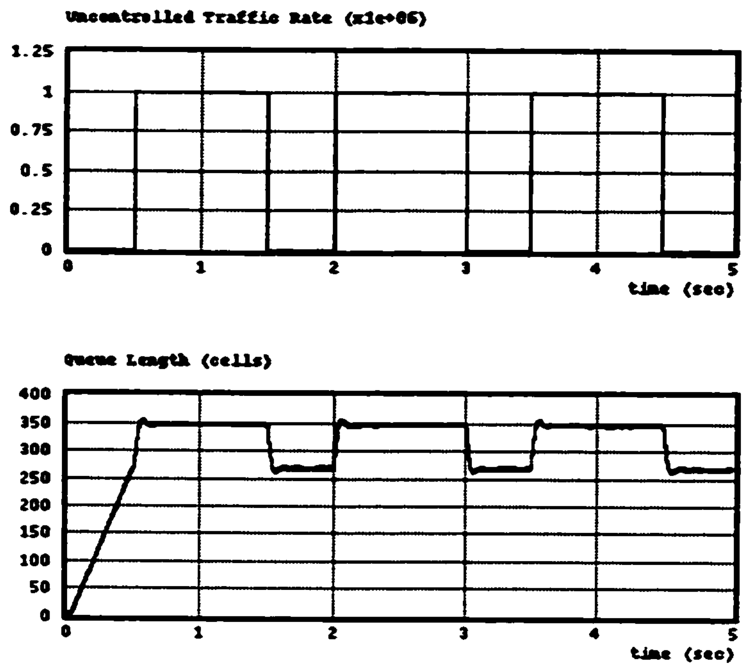

Fig. 10. Queue length in multiple sources with $k = 10$

3.3 Proportional and Integral Control

It can be observed from Eqn. 3.16 that the steady value of queue length x_s is often greater that the specified threshold value x_0. Also this deviation of queue length from its threshold increases as the uncontrolled traffic rate increases. Therefore it is desirable to design a traffic controller which can achieve zero queue deviation.

Using the same idea as presented in the previous section, we can design a proportional and integral traffic controller by adding an integral element to the pure proportional controller:

$$u_i(t) = \mu_i^{max} - \bar{k}_{Pi}\hat{x}(t) + k_{Ii}\int_0^t \hat{x}(s)ds \tag{3.17}$$

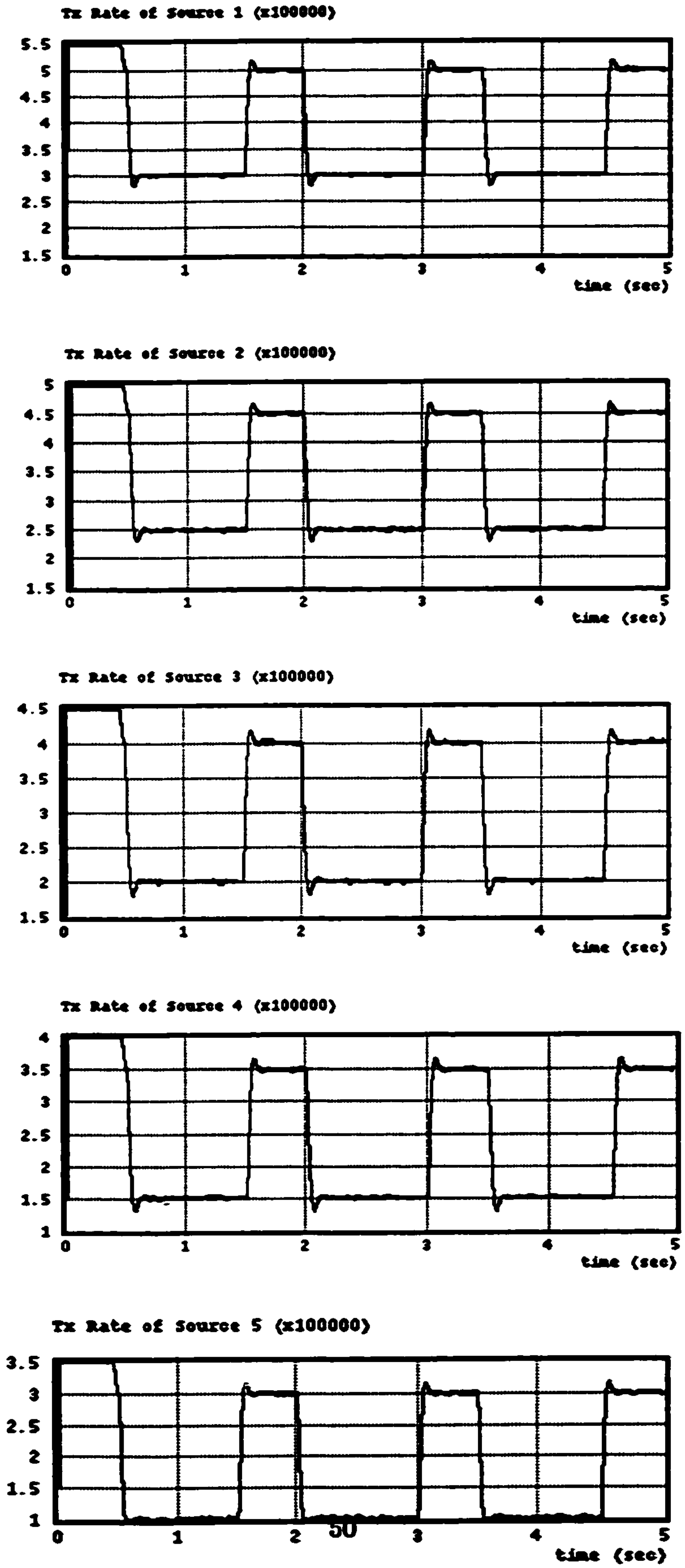

Fig. 11. Source rates in multiple sources with $k = 10$

to stabilize the network given by

$$\dot{\hat{x}}(t) = \sum_{i=1}^{N} e_i(t-\tau'_{1i})u_i(t-\tau'_i) + w(t) - \nu, \tag{3.18}$$

where k_{pi} and $\bar{k}_{Ii}$ are the parameters to be determined.

The controller (3.17) can also be described in the following form:

$$\begin{aligned} \dot{\xi}(t) &= -l_{Ii}\hat{x}(t), \\ u_i(t) &= \mu_i^{max} - k_{Pi}\hat{x}(t) - k_{Ii}\xi(t), \end{aligned} \tag{3.19}$$

where $\bar{k}_{Ii} = k_{Ii}l_{Ii}$.

Therefore, the transmission rate $q_i(t)$ at source i is determined by

$$\begin{aligned} \dot{\xi}(t) &= -l_{Ii}[x(t-\tau'_{2i}) - x_0], \\ q_i(t) &= \mu_i^{max} - k_{Pi}[x(t-\tau'_{2i}) - x_0] - k_{Ii}\xi(t). \end{aligned} \tag{3.20}$$

Let

$$\eta = \begin{bmatrix} \hat{x} \\ \xi \end{bmatrix}, \quad \Lambda_i = \begin{bmatrix} 0 & 0 \\ 0 & l_{Ii} \end{bmatrix}, \quad E_0 = \begin{bmatrix} 1 \\ 0 \end{bmatrix}, \quad K_i = -\begin{bmatrix} k_{Pi} & k_{Ii} \end{bmatrix}.$$

Then by substituting the controller (3.19) to the network given by (3.18), we have

$$\begin{aligned} \dot{\eta}(t) &= -\Lambda_0\eta(t) + \sum_{i=1}^{N} e_i(t-\tau'_{1i})E_0u_i(t-\tau'_i) + E_0(w(t)-\nu), \\ u_i(t) &= \mu_i^{max} - K_i\eta(t), \quad i = 1, 2, \cdots, N. \end{aligned} \tag{3.21}$$

Let

$$\mu^{max}(t) := \sum_{i=1}^{N} e_i(t-\tau'_i)\mu_i^{max}$$

then by a straightforward calculation, we have

$$\begin{aligned}\dot{\eta}(t) &= -\Lambda_i\eta(t) - \sum_{i=1}^{N} e_i(t-\tau_{1i}')E_0K_i\eta(t-\tau_i') + E_0(\mu^{max}(t) + w(t) - \nu) \\ &= -(\Lambda_i + \sum_{i=1}^{N} e_i(t-\tau_{1i}')E_0K_i)\eta(t) + \sum_{i=1}^{N} e_i(t-\tau_{1i}')E_0K_i \int_{t-\tau_i'}^{t} \dot{\eta}(s)ds + \\ &\quad E_0(\mu^{max}(t) + w(t) - \nu) \\ &= -(\Lambda_i + \sum_{i=1}^{N} e_i(t-\tau_{1i}')E_0K_i)\eta(t) - \sum_{i=1}^{N} e_i(t-\tau_{1i}')E_0K_i \int_{t-\tau_i'}^{t} [\Lambda_i\eta(s) + \\ &\quad \sum_{j=1}^{N} e_j(s-\tau_{1j}')E_0K_j\eta(s-\tau_j') - E_0(\mu^{max}(s) + w(s) - \nu)]ds + E_0(\mu^{max}(t) + w(t) - \nu).\end{aligned} \tag{3.22}$$

Let

$$\hat{w}(t) := \sum_{i+1}^{N} e_i(t-\tau_{1i}')E_0K_i \int_{t-\tau_i'}^{t} E_0[\mu^{max}(s) + w(s) - \nu]ds + E_0(\mu^{max}(t) + w(t) - \nu).$$

Then Eq. (3.22) becomes

$$\begin{aligned}\dot{\eta}(t) &= -(\Lambda_i + \sum_{i=1}^{N} e_i(t-\tau_{1i}')E_0K_i)\eta(t) - \sum_{i=1}^{N} e_i(t-\tau_{1i}')E_0K_i \int_{t-\tau_i'}^{t} [\Lambda_i\eta(s) + \\ &\quad \sum_{j=1}^{N} e_j(s-\tau_{1j}')E_0K_j\eta(s-\tau_j')]ds + \hat{w}(t).\end{aligned} \tag{3.23}$$

Define a quadratic Lyapunov function:

$$V(\eta) = \eta^T(t)\eta(t). \tag{3.24}$$

By the time derivative of $V(\eta(t))$ along the trajectories of (3.23) with the assumption of $\hat{w}(t) = 0$, we have

$$\begin{aligned}\dot{V}(\eta(t)) &= \eta^T(t)\dot{\eta}(t) + \dot{\eta}^T(t)\dot{\eta}(t) \\ &= -\eta^T(t)\left\{(\Lambda_i + \Lambda_i^T + \sum_{i=1}^{N} e_i(t-\tau_{1i}')(E_0K_i + K_i^TE_0^T)\right\}\eta(t) - \\ &\quad 2\left\{\eta^T(t)\sum_{i=1}^{N} e_i(t-\tau_{1i}')E_0K_i \int_{t-\tau_i'}^{t}[\Lambda_i\eta(s) - \sum_{j=1}^{N} e_j(s-\tau_{1j}')E_0K_j\eta(s-\tau_j')]ds.\right\}\end{aligned} \tag{3.25}$$

3.3.1 Case 1: Equal Feedback Gains

Now we consider the case that all the feedback gains to the sources are the same. It is then assumed that $l_{Ii} = l_I$ and $K_i = K$, $i = 1, 2, \cdots, N$, where

$$K = [k_P, k_I].$$

Let

$$m(t) = \sum_{i=1}^{N} e_i(t - \tau'_{1i}).$$

Then the equation (3.25) can be rewritten as

$$\begin{aligned} \dot{V}(\eta(t)) &= -\eta^T(t)\left\{(\Lambda_i + \Lambda_i^T + m(t)(E_0 K + K^T E_0^T)\right\}\eta(t) - \\ & 2\left\{\eta^T(t)\sum_{i=1}^{N} e_i(t-\tau'_{1i})E_0 K_i \int_{t-\tau'_i}^{t} [\Lambda_i \eta(s) - \sum_{j=1}^{N} e_j(s-\tau'_{1j})E_0 K_j \eta(s-\tau'_j)]ds\right\} \end{aligned} \quad (3.26)$$

Let

$$G := -[\Lambda_i + \Lambda_i^T + m(t)(E_0 K + K^T E_0^T)]. \quad (3.27)$$

Then the eigenvalues of G given in (3.27) is given by

$$\begin{aligned} eig(G) &= eig(-\begin{bmatrix} 2m(t)k_P & m(t)k_I \\ m(t)k_I & 2l_I \end{bmatrix}) \\ &= \{s|(s+2l_I)(s+2m(t)k_P) - m^2(t)k_I^2 = 0\} \\ &= \{s|s^2 + 2(l_I + m(t)k_P)s + 4m(t)l_I k_P - m^2(t)k_I^2 = 0\}. \end{aligned}$$

It is clear that if

$$4l_I k_P > m(t)k_I^2, \quad (3.28)$$

all of the eigenvalues of G are in the left side of the complex plane. Let s_1, s_2 be the eigenvalues of G. Then the simple calculation gives that

$$\begin{aligned} s_1 &= -l_I - m(t)k_P + \sqrt{(l_I - m(t)k_P)^2 + m^2(t)k_I^2}, \\ s_2 &= -l_I - m(t)k_P - \sqrt{(l_I - m(t)k_P)^2 + m^2(t)k_I^2}. \end{aligned} \tag{3.29}$$

Remark 3.3.1 *If we assume that $m(t)k_P > l_I$ in Equ. (3.29), we will then derive another set of parameters for the controller (3.18).*

According to the inequality equation:

$$\sqrt{a^2 + b^2} \leq |a| + |b|,$$

we have

$$s_i \leq -l_I - m(t)k_P + |l_I - m(t)k_P| + m(t)|k_I|), \quad i = 1, 2.$$

Assume that

$$k_P > 0, \quad k_I > 0 \quad and \quad m(t)k_P < l_I. \tag{3.30}$$

We further have

$$s_i \leq -2m(t)(k_P - \frac{1}{2}k_I), \quad i = 1, 2. \tag{3.31}$$

It is obvious that if (3.30) is true and $k_P > \frac{1}{2}k_I$, then all the eigenvalues of G given in (3.27) are in the left side of the complex plane.

On the other hand, it follows from (3.25) that

$$
\begin{aligned}
&||\eta^T(t)\sum_{i=1}^{N} e_i(t-\tau_{1i}^{'})E_0K\int_{t-\tau_i^{'}}^{t}[\Lambda_i\eta(s)-\sum_{j=1}^{N}e_j(s-\tau_{1j}^{'})E_0K\eta(s-\tau_j^{'})]ds|| \\
&\leq \sum_{i=1}^{N}\tau_i^{'}e_i(t-\tau_{1i}^{'})||E_0K\Lambda_i||\cdot||\eta(t,\theta)||_{\tau_i^{'}}||\eta(t)||+ \\
&\quad \sum_{i,j=1}^{N}\tau_i^{'}e_i(t-\tau_{1i}^{'})||e_j(t,\theta)||_{\tau_i^{'}+\tau_{1j}^{'}}||(E_0K)^2||\cdot||\eta(t,\theta)||_{\tau_i^{'}+\tau_j^{'}}||\eta(t)|| \\
&\leq \sum_{i=1}^{N}h_ie_i(t-\tau_{1i}^{'})||E_0K\Lambda_i||\cdot||\eta(t,\theta)||_{\tau_i^{'}}||\eta(t)||+ \\
&\quad \sum_{i,j=1}^{N}h_ie_i(t-\tau_{1i}^{'})||(E_0K)^2||\cdot||\eta(t,\theta)||_{\tau_i^{'}+\tau_j^{'}}||\eta(t)|| \\
&\leq h_{max}\sum_{i=1}^{N}e_i(t-\tau_{1i}^{'})||E_0K\Lambda_i||\cdot||\eta(t,\theta)||_{\tau_i^{'}}||\eta(t)||+ \\
&\quad h_{max}\sum_{i,j=1}^{N}e_i(t-\tau_{1i}^{'})||(E_0K)^2||\cdot||\eta(t,\theta)||_{\tau_i^{'}+\tau_j^{'}}||\eta(t)||
\end{aligned} \tag{3.32}
$$

where $h_{max} = \max\{h_i | i = 1, 2, \cdots, N\}$ and $0 \leq \tau_i^{'} \leq h_i$. Now assume that there exists a constant α such that $||\eta(t,\theta)||_{h_{max}} < \alpha||\eta(t)||$. Then we have

$$
\begin{aligned}
&||\eta^T(t)\sum_{i=1}^{N} e_i(t-\tau_{1i}^{'})E_0K\int_{t-\tau_i^{'}}^{t}[\Lambda_i\eta(s)-\sum_{j=1}^{N}e_j(s-\tau_{1j}^{'})E_0K\eta(s-\tau_j^{'})]ds|| \\
&\leq \alpha h_{max}m(t)||E_0K\Lambda_i||\cdot||\eta(t)||^2+\alpha h_{max}\sum_{i,j=1}^{N}e_i(t-\tau_{1i}^{'})||(E_0K)^2||\cdot||\eta(t)||^2 \\
&\leq \alpha h_{max}m(t)[||E_0K\Lambda_i||+N||(E_0K)^2||]||\eta(t)||^2.
\end{aligned} \tag{3.33}
$$

On noting that

$$
E_0K\Lambda_i = \begin{bmatrix} 0 & k_Il_I \\ 0 & 0 \end{bmatrix}, \qquad (E_0K)^2 = \begin{bmatrix} k_P^2 & k_Pk_I \\ 0 & 0 \end{bmatrix}
$$

we have

$$
||E_0K\Lambda_i|| \leq k_Il_I, \qquad ||(E_0K)^2|| \leq k_P\sqrt{k_P^2+k_I^2} \leq \sqrt{2}k_P^2
$$

where it is assumed that

$$
k_I \leq k_P. \tag{3.34}
$$

Then we obtain

$$
\begin{aligned}
&||\eta^T(t)\sum_{i=1}^{N} e_i(t-\tau_{1i}^{'})E_0K\int_{t-\tau_i^{'}}^{t}[\Lambda_i\eta(s)-\sum_{j=1}^{N} e_j(s-\tau_{1j}^{'})E_0K\eta(s-\tau_j^{'})]ds|| \\
&< \alpha h_{max}m(t)(k_Il_I+\sqrt{2}Nk_P^2)||\eta(t)||^2.
\end{aligned}
$$

Hence, it follows from (3.26) that

$$
\begin{aligned}
\dot{V}(\eta(t)) &\leq -2m(t)[k_P-0.5k_I]||\eta(t)||^2+2\alpha h_{max}m(t)[k_Il_I+\sqrt{2}Nk_P^2]||\eta(t)||^2 \\
&= -2m(t)[k_P-0.5k_I-\alpha h_{max}(k_Il_I+\sqrt{2}Nk_P^2)]||\eta(t)||^2 \qquad (3.35)\\
&:= -2m(t)\beta||\eta(t)||^2,
\end{aligned}
$$

where

$$\beta = k_P - 0.5k_I - \alpha h_{max}(k_Il_I+\sqrt{2}Nk_P^2).$$

Theorem 3.3.1 *The closed-loop system (3.18) with $\hat{w}(t)=0$ is uniformly asymptotically stable in the large if*

$$
\begin{aligned}
0 < k_I &< \frac{k_P}{0.5+h_{max}l_I}[1-h_{max}\sqrt{2}Nk_P], \\
k_I < k_P &< min\{\frac{l_I}{m(t)}, \ \frac{1}{\sqrt{2}Nh_{max}}\}.
\end{aligned} \qquad (3.36)
$$

Proof. If the conditions (3.36) are satisfied, it follows that

$$k_P - 0.5k_I > h_{max}(k_Il_I+\sqrt{2}Nk_P^2).$$

Then there exists a sufficient small positive constant ϵ such that

$$k_P - 0.5k_I - (1+\epsilon)h_{max}(k_Il_I+\sqrt{2}Nk_P^2) > 0.$$

Let $\alpha = 1+\epsilon$. Then $\alpha > 1$ and $\beta > 0$ for all t. It is observed from (3.36) that the conditions (3.30) and (3.34) are also satisfied. Thus it follows from Lemma 3.1.1 and equation (3.35) that the closed-loop system is uniformly asymptotically stable in the large. ¶

3.3.2 Case 2: Unequal Feedback Gains

Let

$$
\begin{aligned}
G &:= -[\Lambda_i + \Lambda_i^T + \sum_{i=1}^{N} e_i(t-\tau_{1i}^{'})(E_0 K_i + K_i^T E_0^T)] \\
&= -\begin{bmatrix} 2\sum_{i=1}^{N} e_i(t-\tau_{1i}^{'})k_{Pi} & \sum_{i=1}^{N} e_i(t-\tau_{1i}^{'})k_{Ii} \\ \sum_{i=1}^{N} e_i(t-\tau_{1i}^{'})k_{Ii} & 2l_{Ii} \end{bmatrix}.
\end{aligned}
\tag{3.37}
$$

Then the eigenvalues of G are given by

$$
\begin{aligned}
eig(G) &= \{s|(s+2l_{Ii})(s+2\sum_{i=1}^{N} e_i(t-\tau_{1i}^{'})k_{Pi}) - (\sum_{i=1}^{N} e_i(t-\tau_{1i}^{'})k_{Ii})^2 = 0\} \\
&= \{s|s^2 + 2(l_{Ii} + \sum_{i=1}^{N} e_i(t-\tau_{1i}^{'})k_{Pi})s + 4\sum_{i=1}^{N} e_i(t-\tau_{1i}^{'})k_{Pi}l_{Ii} - (\sum_{i=1}^{N} e_i(t-\tau_{1i}^{'})k_{Ii})^2 = 0\}
\end{aligned}
$$

It is clear that if

$$
4\sum_{i=1}^{N} e_i(t-\tau_{1i}^{'})k_{Pi}l_{Ii} > (\sum_{i=1}^{N} e_i(t-\tau_{1i}^{'})k_{Ii})^2, \tag{3.38}
$$

all of the eigenvalues of G are in the left side of the complex plane. Let s_1, s_2 be the eigenvalues of G. Then the simple calculation gives that

$$
\begin{aligned}
s_1 &= -l_{Ii} - \textstyle\sum_{i=1}^{N} e_i(t-\tau_{1i}^{'})k_{Pi} + \sqrt{(l_{Ii} - \sum_{i=1}^{N} e_i(t-\tau_{1i}^{'})k_{Pi})^2 + (\sum_{i=1}^{N} e_i(t-\tau_{1i}^{'})k_{Ii})^2}, \\
s_1 &= -l_{Ii} - \textstyle\sum_{i=1}^{N} e_i(t-\tau_{1i}^{'})k_{Pi} - \sqrt{(l_{Ii} - \sum_{i=1}^{N} e_i(t-\tau_{1i}^{'})k_{Pi})^2 + (\sum_{i=1}^{N} e_i(t-\tau_{1i}^{'})k_{Ii})^2}.
\end{aligned}
\tag{3.39}
$$

Therefore,

$$
s_i \le -l_{Ii} - \sum_{i=1}^{N} e_i(t-\tau_{1i}^{'})k_{Pi} + |l_{Ii} - \sum_{i=1}^{N} e_i(t-\tau_{1i}^{'})k_{Pi}| + \sum_{i=1}^{N} e_i(t-\tau_{1i}^{'})|k_{Ii}|.
$$

It is assumed that

$$
0 < \sum_{i=1}^{N} e_i(t-\tau_{1i}^{'})k_{Pi} < l_{Ii} \quad and \quad k_{Ii} \ge 0. \tag{3.40}
$$

Then

$$
\begin{aligned}
s_i \le\ & -2\sum_{i=1}^{N} e_i(t-\tau_{1i}^{'})k_{Pi} + \sum_{i=1}^{N} e_i(t-\tau_{1i}^{'})k_{Ii} \\
& -2\sum_{i=1}^{N} e_i(t-\tau_{1i}^{'})[k_{Pi} + -\frac{1}{2}k_{Ii}].
\end{aligned}
$$

This implies that if the condition (3.40 is true, and $k_{Ii} < 2k_{Pi}$, where $i = 1, 2, \cdots, N$, then all the eigenvalues of G given in (3.37) are in the left side of the complex plane.

Now consider the absolute value of the second term from the right side in (3.25). It follows

$$||\eta^T(t)\sum_{i=1}^{N} e_i(t-\tau_{1i}')E_0K_i\int_{t-\tau_i'}^{t}[\Lambda_i\eta(s)-\sum_{j=1}^{N} e_j(s-\tau_{1j}')E_0K_j\eta(s-\tau_j')]ds||$$

$$\begin{aligned}
&\leq \sum_{i=1}^{N}\tau_i' e_i(t-\tau_{1i}')||E_0K_i\Lambda_i||\cdot||\eta(t,\theta)||_{\tau_i'}||\eta(t)||+\\
&\quad\sum_{i,j=1}^{N}\tau_i' e_i(t-\tau_{1i}')||e_j(t,\theta)||_{\tau_i'+\tau_{1j}'}||E_0K_iE_0K_j||\cdot||\eta(t,\theta)||_{\tau_i'+\tau_j'}||\eta(t)||\\
&\leq \sum_{i=1}^{N}h_i e_i(t-\tau_{1i}')||E_0K_i\Lambda_i||\cdot||\eta(t,\theta)||_{\tau_i'}||\eta(t)||+\\
&\quad\sum_{i,j=1}^{N}h_i e_i(t-\tau_{1i}')||E_0K_iE_0K_j||\cdot||\eta(t,\theta)||_{\tau_i'+\tau_j'}||\eta(t)||\\
&\leq h_{max}\sum_{i=1}^{N}e_i(t-\tau_{1i}')||E_0K_0\Lambda_i||\cdot||\eta(t,\theta)||_{\tau_i'}||\eta(t)||+\\
&\quad h_{max}\sum_{i,j=1}^{N}e_i(t-\tau_{1i}')||E_0K_iE_0K_j||\cdot||\eta(t,\theta)||_{\tau_i'+\tau_j'}||\eta(t)||,
\end{aligned}$$

where $h_{max} = \max\{h_i|i = 1, 2, \cdots, N\}$ and $0 \leq \tau_i' \leq h_i$. Now assume that there exists a constant α such that $||\eta(t,\theta)||_{h_{max}} < \alpha||\eta(t)||$. Then we have

$$\begin{aligned}
&||\eta^T(t)\sum_{i=1}^{N} e_i(t-\tau_{1i}')E_0K_i\int_{t-\tau_i'}^{t}[\Lambda_i\eta(s)-\sum_{j=1}^{N} e_j(s-\tau_{1j}')E_0K_j\eta(s-\tau_j')]ds||\\
&\leq \alpha h_{max}m(t)||E_0K_i\Lambda_i||\cdot||\eta(t)||^2+\alpha h_{max}\sum_{i,j=1}^{N}e_i(t-\tau_{1i}')||E_0K_iE_0K_j||\cdot||\eta(t)||^2 \qquad (3.41)\\
&\leq \alpha h_{max}m(t)[||E_0K_i\Lambda_i||+\sum_{i,j=1}^{N}e_i(t-\tau_{1i}')||E_0K_iE_0K_j||]||\eta(t)||^2.
\end{aligned}$$

Since

$$E_0K_i\Lambda_i = \begin{bmatrix} 0 & k_{Ii}l_{Ii} \\ 0 & 0 \end{bmatrix}, \qquad E_0K_iE_0K_j = \begin{bmatrix} k_{Pi}k_{Pj} & k_{Pi}k_{Ij} \\ 0 & 0 \end{bmatrix},$$

the Euclid norms of the above matrices are given by

$$||E_0K_i\Lambda_i|| \leq k_{Ii}l_{Ii}, \qquad ||E_0K_iE_0K_j|| \leq k_{Pi}\sqrt{k_{Pj}^2+k_{Ij}^2} \leq \sqrt{2}k_{Pi}k_{Pj},$$

where it is assumed that

$$k_{Ii} \leq k_{Pi}. \tag{3.42}$$

Then we obtain

$$\begin{aligned} & ||\eta^T(t)\sum_{i=1}^{N} e_i(t-\tau'_{1i})E_0K_i\int_{t-\tau'_i}^{t}[\Lambda_i\eta(s) - \sum_{j=1}^{N} e_j(s-\tau'_{1j})E_0K_j\eta(s-\tau'_j)]ds|| \\ < \; & \alpha h_{max}\sum_{i=1}^{N} e_i(t-\tau'_{1i})(k_{Ii}l_{Ii} + \sqrt{2}k_{Pi}\sum_{j=1}^{N} k_{Pj})||\eta(t)||^2. \end{aligned}$$

Hence, it follows from (3.26) that

$$\begin{aligned} \dot{V}(\eta(t)) \;\; \leq \;\; & -2\sum_{j=1}^{N} e_i(t-\tau'_{1i})[k_{Pi} - 0.5k_{Ii}]||\eta(t)||^2 + \sum_{i=1}^{N} e_i(t-\tau'_{1i})(k_{Ii}l_{Ii} + \sqrt{2}k_{Pi}\sum_{j=1}^{N} k_{Pj})||\eta(t)||^2 \\ = \;\; & -2\sum_{j=1}^{N} e_i(t-\tau'_{1i})[k_{Pi} - 0.5k_{Ii} - \alpha h_{max}(k_{Ii}l_{Ii} + \sqrt{2}k_{Pi}\sum_{j=1}^{N} k_{Pj})]||\eta(t)||^2 \\ := \;\; & -2\beta||\eta(t)||^2, \end{aligned} \tag{3.43}$$

where

$$\beta = \sum_{j=1}^{N} e_i(t-\tau'_{1i})[k_{Pi} - 0.5k_{Ii} - \alpha h_{max}(k_{Ii}l_{Ii} + \sqrt{2}k_{Pi}\sum_{j=1}^{N} k_{Pj})].$$

Theorem 3.3.2 *The closed-loop system (3.18) with $\hat{w}(t) = 0$ is uniformly asymptotically stable in the large if for $i = 1, 2, \cdots, N$,*

$$\begin{aligned} 0 < k_{Ii} < \min\{k_{Pi}, \; \frac{k_{Pi}}{0.5 + h_{max}l_{Ii}}[1 - h_{max}\sqrt{2}\sum_{j=1}^{N} k_{Pj}]\}, \\ \sum_{i=1}^{N} k_{Pi} < \min\{l_{Ii}, \; \frac{1}{\sqrt{2}h_{max}}\}. \end{aligned} \tag{3.44}$$

Proof. It is easy to verify that the conditions (3.40) and (3.42) are both satisfied. Now if $k_{Ii} < \frac{k_{Pi}}{0.5 + h_{max}l_{Ii}}[1 - h_{max}\sqrt{2}\sum_{j=1}^{N} k_{Pj}]$, it follows that

$$k_{Pi} - 0.5k_{Ii} > h_{max}(k_{Ii}l_{Ii} + \sqrt{2}k_{Pi}\sum_{j=1}^{N} k_{Pj}).$$

Then there exists a sufficient small positive constant ϵ_i such that for $i = 1, 2, \cdots, N$,

$$k_{Pi} - 0.5k_{Ii} - (1 + \epsilon_i)h_{max}(k_{Ii}l_{Ii} + \sqrt{2}k_{Pi}\sum_{j=1}^{N} k_{Pj}) > 0$$

Let $\epsilon = min\{\epsilon_i \mid i = 1, 2, \cdots, N\}$. It then gives that

$$\sum_{i=1}^{N} e_i(t - \tau'_{1i})[k_{Pi} - 0.5k_{Ii} - (1+\epsilon)h_{max}(k_{Ii}l_{Ii} + \sqrt{2}k_{Pi}\sum_{j=1}^{N} k_{Pj})] > 0.$$

Now let $\alpha = 1+\epsilon$. Then $\alpha > 1$ and $\beta > 0$ for all t. Thus if follows from Lemma 3.1.1 and equation (3.35) that the closed-loop system is uniformly asymptotically stable in the large. ¶

3.3.3 Simulation on Proportional and Integral Control

The OPNET tool is also used to perform simulation on the proportional and integral controllers given by 3.18.

A. Single Source Node

For the simulation on the traffic control of single source depicted in Fig. 12, it is assumed that the service rate of the switch is $200Kbps$, the minimum transmission rate μ^{min} of the source is $20Kbps$, and the maximum transmission rate μ^{max} of the source is $200Kbps$. Also it is assumed that the uncontrolled source generates the traffic data with a constant transmission rate of $100Kbps$. The threshold x_0 for the queue in the switch is 150 cells.

It can be seen from Figure 13 that the buffer occupancy is linearly increased at the beginning when the uncontrolled traffic rate jumps to 100Kbs till it reaches about 340 cells. Then it drops very quickly and tends to a steady value 160 cells which is close to the threshold value $x_0 = 150$ cells. The little difference between the steady value and the threshold value is due to the discretization.

B. Multiple Source Nodes

For the simulation on the traffic control of multiple sources depicted in Fig. 14, it is assumed that the service rate of the switch is $2Gbps$, all the traffic data are routed to one destination,

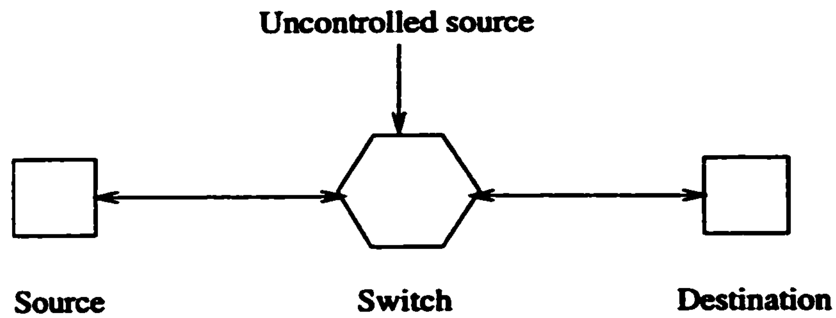

Fig. 12. A network with single source node

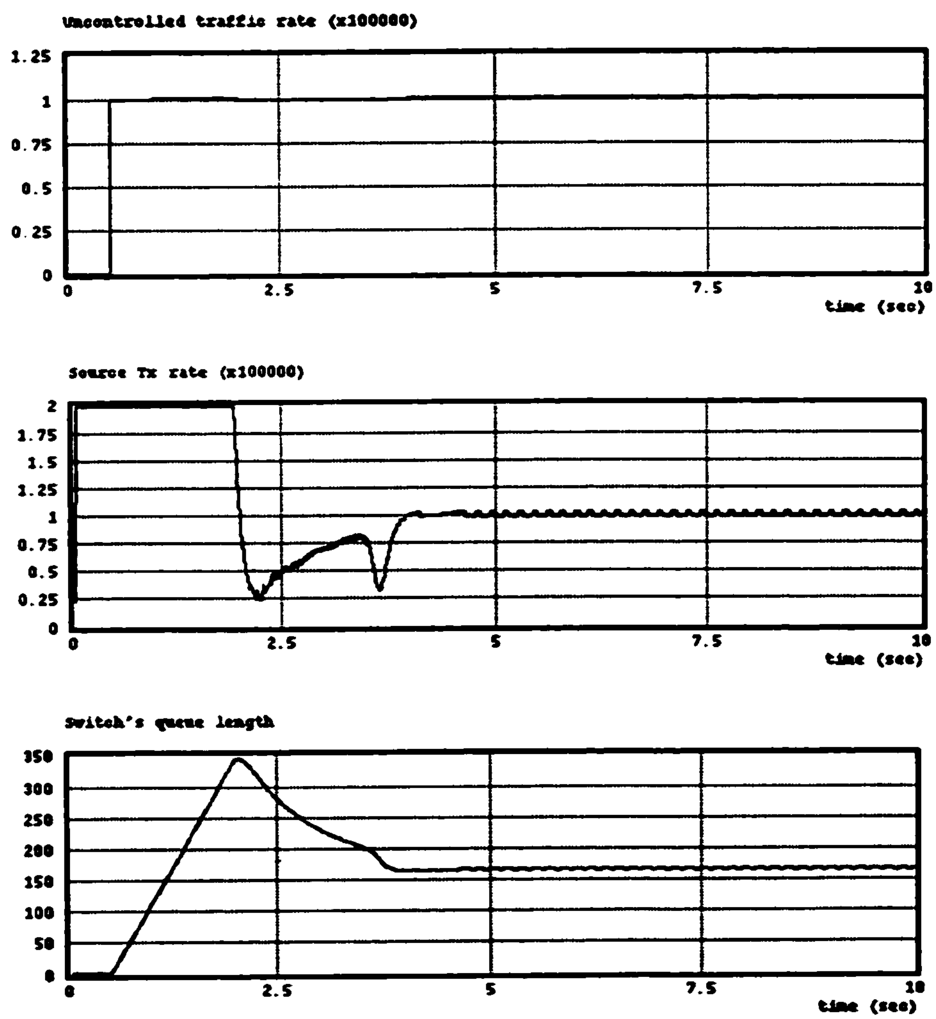

Fig. 13. Single source with τ_1', $\tau_2' = 0.01$ and $k = 10$

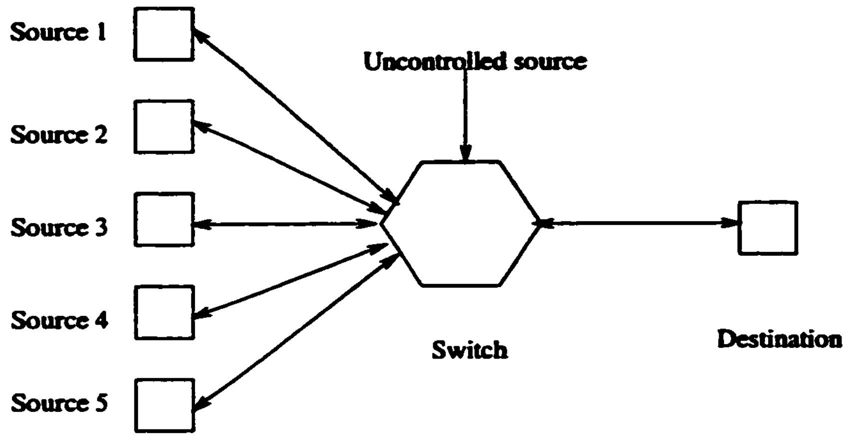

Fig. 14. A Network with Multiple Source Nodes

and the uncontrolled source generates the periodic on/off traffic with the minimum transmission rate zero and the maximum transmission rate 1 Gpbs. The threshold x_0 for the queue in the switch is 150 cells. All the other attributes of sources and links are provided in Table 1.

According to Table 1, the maximum static round-trip delay is 0.018 second. N ow we set the upper bound of round-trip delay is 0.019 second. By choosing the feedback gain $k_i = 10$, $i = 1, 2, 3, 4, 5$, we have that

$$\sum_{i=1}^{5} k_i = 50 < \frac{1}{0.019}.$$

It then follows from Theorem 3.2.1 that the network is asymptotically stable.

Figure 16 demonstrates how the sources respond to the change of the periodic uncontrolled traffic depicted in Figure 15. It can be seen from Figure 16 that each local controller can respond quickly to decrease its rate when the uncontrolled traffic rate jumps up to the maximum rate, and to increase its rate when uncontrolled traffic rate jumps down to the minimum rate. Figure 15 also confirms that the queue length is piecewise stable and tends to the threshold value $x_0 = 150$ cells.

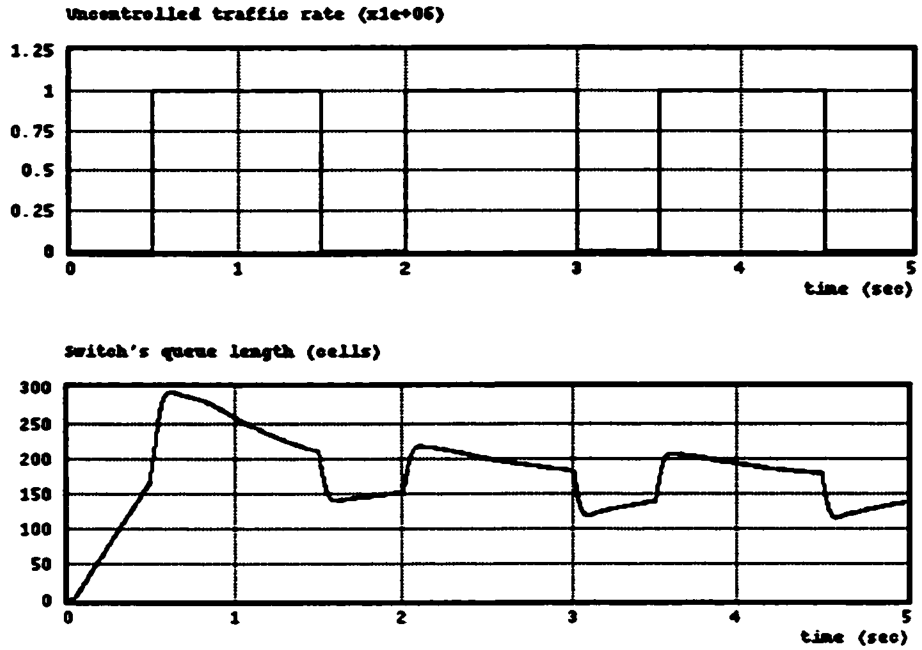

Fig. 15. Queue length in multiple sources with $k = 10$

3.4 Concluding Remarks

In this chapter, the Lyapunov approach was applied to design both the proportional traffic controller and the proportional and integral traffic controller in the continuous-time domain. Both types of controllers have a unique property that they can stablize the network with bounded round-trip delays. This property has not been seen in other existing traffic controllers so far.

The difference between the proportional traffic controller and the proportional and integral traffic controller is that the former has lower peak value in the buffer occupance while the latter has little differentiation from the buffer's threshold value x_0, i.e., zero queue deviation.

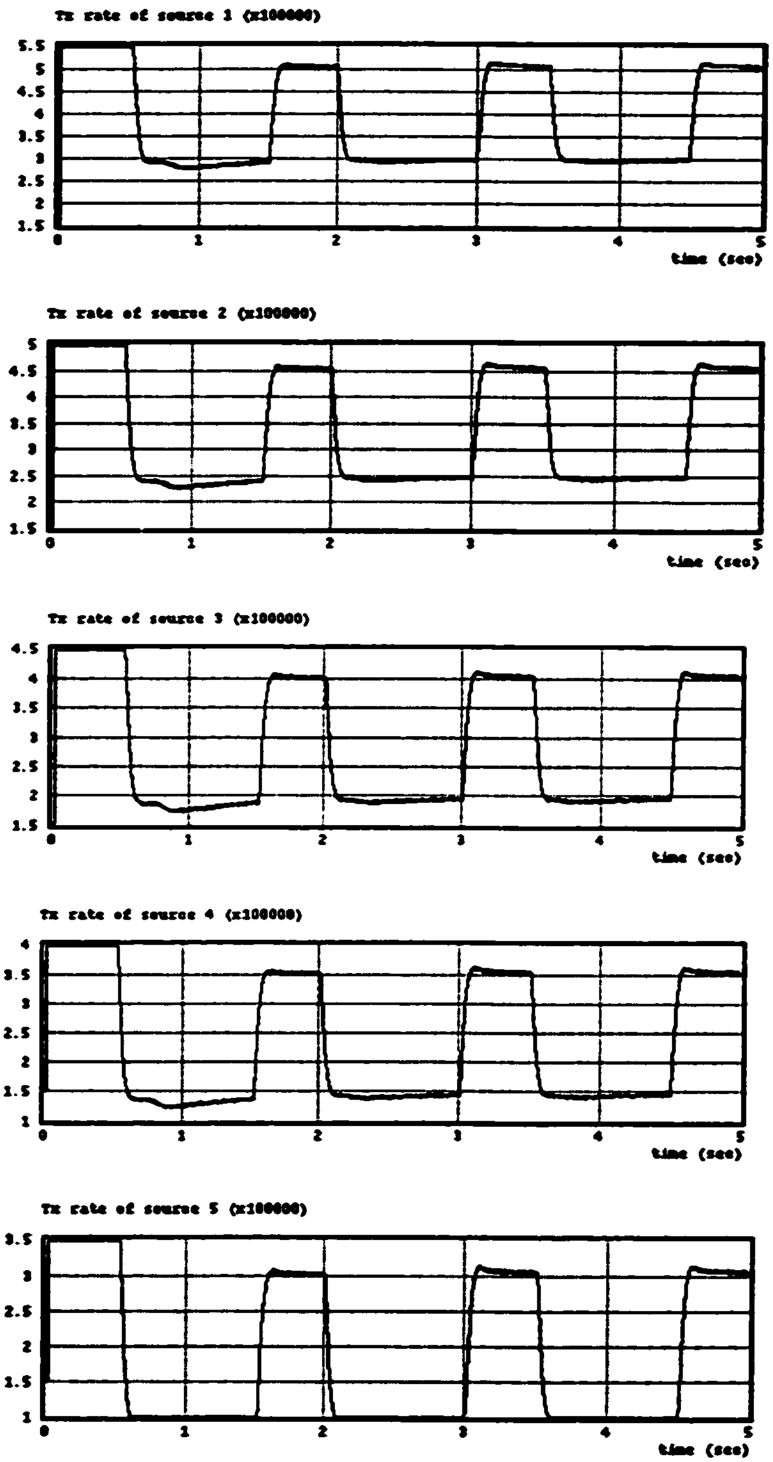

Fig. 16. Source rates in multiple sources with $k = 10$

Chapter 4

End-to-End Discrete-Time Periodic Congestion Control

In the previous section, we studied the design of traffic control in the continuous-time domain. Now we start to design the traffic control in the discrete-time domain. The discrete-time model described in (2.7) is rewritten as:

$$x(n+1) = Sat_K\{x(n) + \sum_{i=1}^{N} e_i(n-\tau_{1i})u_i(n-\tau_i) - \hat{\mu}_A(n)\} \tag{4.1}$$

Assume that μ_i/T is the maximum rate allocated for the ith VC. Let $t_l = n_l T$, $l = 1, 2, \cdots$, be the time points where the number of VCs changes (therefore the number of VCs is constant over the interval $\mathcal{T}_l := [t_l,\ t_{l+1})$). Also let the set $\mathcal{N}_{\mathcal{T}_l} := \{k,$ the kth VC is active over $\mathcal{T}_l$ $\}$.

During the interval $\mathcal{T}_l$, the local controller in the source node $i \in \mathcal{N}_{\mathcal{T}_l}$ can generally be described by a difference equation:

$$u_i(n) = -Sat_{\hat{\mu}_i}\{\sum_{j=1}^{\tau} b_{i(\tau-j)}u_i(n-j) + \sum_{j=0}^{\hat{\tau}_i} a_{i(\hat{\tau}_i-j)}x(n-j)\}\ , \tag{4.2}$$

where $\hat{\mu}_i = \mu_i^{max} - \mu_i^{min}$, b_{ij} and a_{ij} are coefficients, τ and $\hat{\tau}_i$ $(< \tau)$ are positive integers to be determined.

Then the output from the source node $i \in \mathcal{N}_{\mathcal{T}_l}$ is given by

$$\lambda_i(n) = \mu_i^{max} + u_i(n - \tau_{2i}) \; . \tag{4.3}$$

It is obvious from (4.2) and (4.3) that

$$\lambda_i(n) \geq \mu_i^{max} - \hat{\mu}_i = \mu_i^{min},$$

which implies that the minimum transmission rate μ_i^{min}/T for source i is guaranteed.

Let

$$\Delta_i^c(z) = z^{\tau} + b_{i(\tau-1)}z^{\tau-1} + \cdots + b_{i0} \; , \tag{4.4}$$

which is the characteristic equation of the local controller described in equation (4.2) when it operates in the linear region. Our primary goal now is to determine the parameters $\{a_{ij}\}$ and $\{b_{ij}\}$ to satisfy the following requirements:

1. *Piecewise stability of buffer occupancy.* Over every interval $\mathcal{T}_l$, $l = 1, 2, \cdots$, the roots of the characteristic equation $\Delta(z) = 0$ of buffer occupancy described by (4.1) with the local controllers (4.2) applied must reside inside the unit circle. The characteristic equation $\Delta(z)$ will be given in the next section.

2. *Stability of local controllers.* The local controllers are open-loop stable, i.e., all roots of characteristic equation for local controller $\Delta_i^c(z) = 0$ are inside the unit circle. This requirement is important since an open-unstable local controller may destroy the system's stability if its feedback VC link is broken.

3. *Robustness.* The parameters $\{a_{ij}\}$ and $\{b_{ij}\}$ do not depend on the number of active VCs, and variation of propagation delays, queuing delays and other processing delays.

4. *Fairness.* Under the steady state conditions, all active local controllers obtain the same feedback gain, i.e., as $n \to \infty$, $u_i(n)$ approach a constant value for all i with $e_i = 1$. Thus, it follows from (4.3) that all the VCs can fairly share the switch's bandwidth.

The above four requirements are important from practical point view. However, merely determining $\{a_{ij}\}$ and $\{b_{ij}\}$ to satisfy these requirements is not enough from a technical point of view since the computation of source rates according to the local controllers (4.2) with all nonzero $\{a_{ij}\}$ and $\{b_{ij}\}$ may still be heavy for a high speed ATM switching networks. Thus our final requirement imposed on the controller (4.2) is

5. *Simplicity.* Only a few parameters out of $\{a_{ij}\}$ and $\{b_{ij}\}$ are needed to realize the requirements 1 to 4.

In the following, we will design a congestion controller described by (4.2) to satisfy all these five requirements.

4.1 End-to-End Control: A Single VC

In this case, the change of buffer occupancy of the switch node can be discretized in the form

$$x(n+1) = Sat_K\{x(n) + u(n-\tau) + d(n) - \hat{\mu}\} \tag{4.5}$$

4.1.1 The Congestion Control Algorithm

It will be shown later that the network described by (4.5) is locally asymptotically stable if the source rate is regulated by the following algorithm:

$$\lambda(n) = Sat_{\mu_1}\{\mu_1 + \alpha[x(n-\tau_2) + \sum_{j=n-\tau}^{n-1}(\lambda(j) - \mu_1)]\} \tag{4.6}$$

where $-2 < \alpha < 0$. In particular, it will be demonstrated in our simulation results that if $\alpha = -1$, the controller in (4.6) can quickly respond to the change of the uncontrolled input $d(n)$.

It can be seen from the control structure in (4.6) that the current source rate is adjusted based on value of the feedback-delayed buffer occupancy and the sum of previous source rates from $n - \tau$ to $n - 1$. Without the consideration of the nonlinearities imposed on the systems described by (4.5) and (4.6), the last term in the control algorithm (4.6) is used to locate all poles of the closed-loop system of (4.5) and (4.6) to the unit circle.

4.1.2 Stability Analysis

To investigate the stability of the network described by (4.5) with the controller given by (4.6), it follows the assumptions in Chapter 2 that we only study the asymptotical stability properties of the linear-time network given by

$$x(n+1) = x(n) + u(n-\tau) + d(n) - (\mu - \mu_1) \tag{4.7}$$

with the linear-time congestion controller given by

$$\lambda(n) = \mu_1 + \alpha[x(n-\tau_2) + \sum_{i=n-\tau}^{n-1}(\lambda(i) - \mu_1)] \tag{4.8}$$

Let

$$y(n) = x(n) + \sum_{i=n-\tau}^{n-1} u(i) \tag{4.9}$$

where $u(n-\tau_2) := \lambda(n) - \mu_1$. Thus we have

$$\begin{aligned} y(n+1) &= x(n) + u(n-\tau) + d(n) - (\mu - \mu_1) + \sum_{i=n-\tau+1}^{n} u(i) \\ &= y(n) + u(n) + d(n) - (\mu - \mu_1) \end{aligned}$$

Choose

$$u(n) = \alpha y(n) \tag{4.10}$$

which gives that

$$y(n+1) = (1+\alpha)y(n) + d(n) - (\mu - \mu_1) \tag{4.11}$$

The characteristic equation of the system is

$$\Delta(z) = z - (1+\alpha)$$

which has one zero at $z = 1 + \alpha$. Therefore, the system is exponentially stable if and only if $-2 < \alpha < 0$.

We finally obtain that

$$\begin{aligned} \lambda(n) &= \mu_1 + u(n-\tau_2) \\ &= \mu_1 + \alpha y(n-\tau_2) \\ &= \mu_1 + \alpha[x(n-\tau_2) + \sum_{i=n-\tau-\tau_2}^{n-\tau_2-1} (\lambda(i+\tau_2) - \mu_1)] \\ &= \mu_1 + \alpha[x(n-\tau_2) + \sum_{i=n-\tau}^{n-1} (\lambda(i) - \mu_1)] \end{aligned}$$

which establishes the control algorithm (4.8).

4.1.3 Upper Bound for Buffer Occupancy

We consider the controller (4.6) with $\alpha = -1$. Since it is required that $0 \leq \lambda(n) \leq \mu_1$ for all n, it follows that $0 \leq -u(n) = \mu_1 - \lambda(n + \tau_{21}) \leq \mu_1$ for all n. Thus,

$$-u(n) = Sat_{\mu_1}\{-u(n)\}$$

Now it is assumed that the buffer size K is large enough such that there is no cell loss. Then the system (4.7) can be expressed as

$$x(n+1) = [x(n) - Sat_{\mu_1}\{-u(n-\tau_1)\} + d(n) - (\mu - \mu_1)]^+$$

where $[x]^+ = max\{x,\ 0\}$. Also the equation (4.9) becomes

$$y(n) = [x(n)]^+ - \sum_{i=n-\tau_1}^{n-1} Sat_{\mu_1}\{-u(i)\} \tag{4.12}$$

Thus we have

$$\begin{aligned} y(n+1) &= [x(n+1)]^+ - \sum_{i=n+1-\tau_1}^{n} Sat_{\mu_1}\{-u(i)\} \\ &= [x(n) - Sat_{\mu_1}\{-u(n-\tau_1)\} + d(n) - (\mu - \mu_1)]^+ - \sum_{i=n+1-\tau_1}^{n} Sat_{\mu_1}\{-u(i)\} \end{aligned}$$

If $x(n+1) < 0$, $y(n+1) = -\sum_{i=n+1-\tau_1}^{n} Sat_{\mu_1}\{-u(i)\} \leq 0$.
If $x(n+1) \geq 0$,

$$\begin{aligned} y(n+1) &\leq [x(n)]^+ - Sat_{\mu_1}\{-u(n-\tau_1)\} + [d(n) - (\mu - \mu_1)]^+ - \sum_{i=n+1-\tau_1}^{n} Sat_{\mu_1}\{-u(i)\} \\ &= y(n) - Sat_{\mu_1}\{-u(n)\} + [d(n) - (\mu - \mu_1)]^+ \end{aligned}$$

On noting from (4.10) that $-u(n) = Sat_{\mu_1}\{y(n)\}$, it follows that

$$y(n+1) \leq y(n) - Sat_{\mu_1}\{-y(n)\} + [d(n) - (\mu - \mu_1)]^+ \tag{4.13}$$

Since it is assumed that $d(n) \leq \mu$ and $y(0) = 0$, $[d(n) - (\mu - \mu_1)]^+ \leq \mu_1$. It implies from the relations (4.12) and (4.13) that $y(n) \leq \mu_1$ for all n. We then have, for all n,

$$y(n+1) \leq [d(n) - (\mu - \mu_1)]^+$$

Thus from (4.12),

$$x(n) = y(n) + \sum_{i=n-\tau_1}^{n-1} Sat_{\mu_i}\{-u(i)\} \leq \sum_{i=n-\tau_1}^{n} Sat_{\mu_1}\{y(i)\} \leq \sum_{i=n-\tau_1}^{n} [d(i-1) - (\mu - \mu_1)]^+$$

This relation shows that the buffer occupancy is the function of the rate of the uncontrolled traffic, the service rate μ/T and the maximum rate μ_1/T assigned to the source node. When the source node is too conservative, i.e., $\mu_1 < \mu$, such that $d(n) - (\mu - \mu_1) \leq 0$, the buffer is always empty, where it is assumed that $d(n)$ does not exceed μ. When the source node is too greedy, i.e., μ_1 is close to μ, a buffer of large size is then required to accumulate any burstiness in the uncontrolled traffic. Let

$$BO_1 = \max_n\{\sum_{i=n-\tau_1}^{n} [d(i-1) - (\mu - \mu_1]^+\} \tag{4.14}$$

which can be considered as the upper bound for the buffer occupancy, then the network will be lossless if the buffer size is greater than BO_1.

4.2 End-to-End Control: Multiple VCs

In this section, the control algorithm (4.6) will be generalized to a network with multiple VCs.

4.2.1 The Robust Proportional Control Algorithm

It will be shown later that the following controller can be applied to stablize a network with multiple source nodes. For the source node $i \in \mathcal{N}_{\mathcal{T}_l}$,

$$\lambda_i(n) \;=\; \mu_i^{max} + u_i(n - \tau_{2i}) \tag{4.15}$$

with

$$u_i(n) = -Sat_{\bar{\mu}_i}\{\frac{\epsilon}{N}x(n - \hat{\tau}_i)\}$$

where $\hat{\tau}_i$ is an integer to be determined.

Remark 4.2.1 *Our controller given by (4.15) has a very simple structure. The traffic output at each source node is proportional to the delayed buffer occupancy. The controller is robust in the sense that the system stability is not sensitive to the change of the number of VCs by properly choosing the number* ϵ.

4.2.2 Implementation of the Controller (4.15)

The controller given by (4.15) can be distributively implemented in the source nodes. The parameters τ_{2i}, $\hat{\tau}_i$, N and ϵ should be provided in order for the source to calculate the its data transmission rate. The following procedures give the ways to obtain these parameters.

A. Determining τ_{2i}*:*

The value of τ_{2i} is estimated by the difference between the time the RM cell arrives the source node and the time stamp recorded in the RM cell. This value is usually constant since the delay to the high priority RM cell can be ignored.

B. Determining $\hat{\tau}_i$*:*

It is assumed that source node i knows its the loop delay τ_i. Then the value of $\hat{\tau}_i$ is chosen such that $\hat{\tau}_i + \tau_i = \tau$, where τ is a uniform delay applied for all the source nodes.

C. Determining N *and* ϵ*:*

Since N is usually large and system's stability depends on the factor $\frac{\epsilon M}{N}$, we want to scale down the ratio of active number of VC and total number of allowed VCs by dividing N into a set of integers $\{N_l;\ l = 1, 2, \cdots, k\}$ with $N_1 \le N_2 \le \cdots \le N_k$. The number of active controlled VCs stored in the RM cell is used as the estimate of the current number of active controlled VCs. Then the values of (N, ϵ) can be adaptively adjusted by (N_l, ϵ_l), where N_l is chosen to be close to but larger than the estimate M, and ϵ_l is chosen such that the characteristic equation of the buffer occupancy

$$\Delta(z) = z^{\tau}(z-1) + \frac{\epsilon_l M}{N_l}$$

is a stable polynomial for all $M < N_l$.

4.2.3 Controller Design and Stability Analysis

In order to simplify the analysis of system's piecewise stability, we need the following definition.

Definition 4.2.1 *A switching network described by (2.7) is said to have a slow temporal change in load if the frequency and the change in the number of VCs are small.*

In other words, we consider the case where new VCs would not be added before the switch tends to its steady states and the number of VCs allowed to enter the switch at each time instance t_i is limited.

Our major concern in the design phase is to determine the control parameters to maintain the stability of the closed-loop system. The z-transform method is used, and the system's initial conditions are assumed to be zero because they do not affect the system's stability.

For any interval $\mathcal{T}_l$, $l = 1, 2, \cdots$, the buffer occupancy of a node with multiple controlled inputs can therefore be described by

$$x(n+1) = x(n) + \sum_{i=1}^{N} e_i(n - \tau_{1i}) u_i(n - \tau_i) + d(n) - \hat{\mu} \ , \tag{4.16}$$

and the traffic controller at source node $i \in \mathcal{N}_{\mathcal{T}_l}$ can be represented by

$$u_i(n) = -\sum_{j=1}^{\tau} b_{i(\tau-j)} u_i(n-j) - \sum_{j=0}^{\hat{\tau}_i} a_{i(\hat{\tau}_i - j)} x(n-j) \ . \tag{4.17}$$

In order to describe the characteristic equation of (4.16) and (4.17) over the interval $\mathcal{T}_l$, it is convenient and without loss of generality to assume that $t_{l+1} = \infty$ since the number of currently-active VCs is fixed during the interval $\mathcal{T}_l$, and the length of $\mathcal{T}_l$ is long enough such that the system tends to its steady states. Let $e_i' = 1$ if the ith VC is active in $\mathcal{T}_l$, otherwise $e_i' = 0$.

Then the z-transform of (4.16) gives

$$(z-1)X(z)=\sum_{i=1}^{N} e_i' z^{-\tau_i} U_i(z)+D(z)-\hat{\mu}R(z)\ , \tag{4.18}$$

where $X(z):=\sum_{n=n_l}^{\infty} x(n)z^{n-n_l}$, and $U_i(z)$, $D(z)$ and $R(z)$ are similarly defined.

Let

$$W_\tau(z):=\begin{bmatrix} z^\tau \\ \vdots \\ z \\ 1 \end{bmatrix},\quad B_{i\tau}:=\begin{bmatrix} b_{i\tau} \\ \vdots \\ b_{i1} \\ b_{i0} \end{bmatrix},\quad A_{\hat{\tau}_i}:=\begin{bmatrix} a_{i\hat{\tau}_i} \\ \vdots \\ a_{i1} \\ a_{i0} \end{bmatrix}.$$

Then the z transform of (4.17) is given by

$$U_i(z)=-z^{-\tau}B_{i\tau-1}^T W_{\tau-1}(z)U_i(z)-z^{-\hat{\tau}_i}A_{\hat{\tau}_i}^T W_{\hat{\tau}_i}(z)X(z)\ ,$$

or

$$z^{-\tau}B_{i\tau}^T W_\tau(z)U_i(z)=-z^{-\hat{\tau}_i}A_{\hat{\tau}_i}^T W_{\hat{\tau}_i}(z)X(z)\ ,$$

where $b_{i\tau}$ in $B_{i\tau}$ is 1. Then,

$$U_i(z)=-z^{\tau-\hat{\tau}_i}(B_{i\tau}^T W_\tau(z))^{-1}A_{\hat{\tau}_i}^T W_{\hat{\tau}_i}(z)X(z)\ . \tag{4.19}$$

Substituting (4.19) into (4.18), we obtain

$$(z-1)X(z)=-\sum_{i=1}^{N} z^{\tau-\hat{\tau}_i-\tau_i}e_i'(B_{i\tau}^T W_\tau(z))^{-1}A_{\hat{\tau}_i}^T W_{\hat{\tau}_i}(z)X(z)+D(z)-\hat{\mu}R(z)\ ,$$

or

$$\Delta(z)X(z)=B_{i\tau}^T W_\tau(z)[D(z)-\hat{\mu}R(z)]\ , \tag{4.20}$$

where $\hat{\mu}=\mu-\sum_{i=1}^{N} e_i'\mu_i$, and $\Delta(z)$ is the characteristic equation of the system given by

$$\Delta(z)=(z-1)B_{i\tau}^T W_\tau(z)+\sum_{i=1}^{N} z^{\tau-\hat{\tau}_i-\tau_i}e_i' A_{\hat{\tau}_i}^T W_{\hat{\tau}_i}(z)\ .$$

Let $\tau \geq max\{\tau_1, \tau_2, \cdots, \tau_N\}$ be an integer and choose $\hat{\tau}_i$ such that $\hat{\tau}_i + \tau_i = \tau$, $i \in \mathcal{N}_{T_l}$, so that $\Delta(z)$ becomes a polynomial function of z. We now obtain

$$\Delta(z) = (z-1)B_{i\tau}^T W_\tau(z) + \sum_{i=1}^{N} e_i' A_{\hat{\tau}_i}^T W_{\hat{\tau}_i}(z) \; . \tag{4.21}$$

The integer τ can be considered as a uniform delay since it is now the total delay seen by every VC. Note that the roots of $\Delta(z) = 0$ are determined by the parameters a_{ij}, $j = 0, 1, \cdots, \hat{\tau}_i$, and b_{ij}, $j = 0, 1, 2, \cdots, \tau - 1$, $i \in \mathcal{N}_{T_l}$. In order to obtain a simple control structure, we choose for $i \in \mathcal{N}_{T_l}$, $l = 1, 2, \cdots$,

$$\begin{aligned} a_{i0} &= \frac{\epsilon}{N}, \\ a_{ij} &= 0, \quad j = 1, 2, \cdots, \hat{\tau}_i \\ b_{ij} &= 0, \quad j = 0, 1, \cdots, \tau - 1 \\ b_{i\tau} &= 1, \end{aligned} \tag{4.22}$$

where ϵ is a positive number to be determined. Then the resulting characteristic equation of the buffer occupancy can be simplified as

$$\Delta(z) = z^\tau (z-1) + \frac{\epsilon M}{N} \; . \tag{4.23}$$

The following lemma will lead to our main result which also summarizes the above analysis.

Lemma 4.2.1 *Consider a polynomial equation $g_\epsilon(z) = z^\tau(z-1) + \epsilon$, where τ is an integer. There exists a positive number ϵ_0 such that for all $\epsilon \in (0, \epsilon_0)$, all the roots of $g_\epsilon(z) = 0$ are inside the unit circle.*

Proof. Let $z_i(\epsilon)$, $i = 1, 2, \cdots, \tau + 1$, be the roots of $g_\epsilon(z) = 0$. It is easy to show that $z_i(0) = 0$, $i = 1, 2, \cdots, \tau$, and $z_{\tau+1}(0) = 1$. Since $z_i(\epsilon)$ are continuous functions of ϵ, there exists a small positive number ϵ_1 such that for $\epsilon \in (0, \epsilon_1)$, $|z_i(\epsilon)| < 1/2$, $i = 1, 2, \cdots, \tau$ and $|z_{\tau+1}(\epsilon)| > 1/2$. Note that the complex roots appear in conjugate pairs. It follows that the root $z_{\tau+1}(\epsilon)$ should be a positive real number for $\epsilon \in (0, \epsilon_1)$. ¶

Now assume that there exists $\epsilon \in (0, \epsilon_1)$ such that $z_{\tau+1}(\epsilon) \geq 1$. Then we have

$$g_\epsilon(z_{\tau+1}(\epsilon)) = z_{\tau+1}^\tau(\epsilon)(z_{\tau+1}(\epsilon) - 1) + \epsilon \geq \epsilon > 0$$

which contradicts the fact that $z_{\tau+1}(\epsilon)$ is the root of equation $g_\epsilon(z) = 0$. Thus the proof is completed.

Theorem 4.2.1 *Assume that each source node only obtains feedback information on the buffer occupancy of the congestion node. Then there exists a positive number ϵ_0 such that for all $\epsilon \in (0, \epsilon_0)$, a network with a slow temporal change of load can be piecewisely stabilized by the controller (4.17) if for $i \in \mathcal{N}_{\mathcal{T}_l}$, $l = 1, 2, \cdots$,*

$$\begin{aligned}
&\hat{\tau}_i + \tau_i = \tau, \\
&\tau \geq \max\{\tau_1, \tau_2, \cdots, \tau_N\}, \\
&a_{i0} = \frac{\epsilon}{N}, \\
&a_{ij} = 0, \qquad\qquad j = 1, 2, \cdots, \hat{\tau}_i \\
&b_{ij} = 0, \qquad\qquad j = 0, 1, \cdots, \tau - 1 \\
&b_{i\tau} = 1.
\end{aligned} \tag{4.24}$$

Moreover, the local controllers defined in (4.17) are also stable.

Proof. It is obvious that $\Delta_i^c(z) = z^\tau$ for the local controllers, and therefore the roots of $\Delta_i^c(z) = 0$ are all in the origin. Thus the local controllers are stable.

Now let M be the number of VCs over the interval $\mathcal{T}_l$. By using the parameters defined in (4.24), the characteristic equation is given by (4.23). Consider the case where $M = N$. It follows from Lemma 4.2.1 that there exists a small number ϵ_0 such that for all $\epsilon \in (0, \epsilon_0)$, the system is stable over $\mathcal{T}_l$. Then for the case where $1 \leq M \leq N$, the system is still stable over $\mathcal{T}_l$ since all roots of $\Delta(z) = 0$ are also inside the unit circle for $\epsilon \in (0, \epsilon_0)$. On noting that the system's characteristic equation on any interval $\mathcal{T}_l$ can be described by (4.23), the system is thus piecewisely stable over $\{\mathcal{T}_l,\ l = 1, 2, \cdots\}$ if $\epsilon \in (0, \epsilon_0)$. ¶

Substituting the control parameters defined in (4.24) into (4.2), we obtain the control algorithm (4.15).

4.2.4 System Steady Behavior

We would like to investigate the system behavior at steady states. Its analysis would give us an idea on buffer design and fairness.

Let x_s, u_{is}, λ_{is} and d_s be the steady state values corresponding to $x(n)$, $u_i(n)$, $\lambda_i(n)$ and $d(n)$ respectively in equations (2.7) and (4.15). Then as $n \to \infty$,

$$\begin{aligned} x_s &= Sat_K\{x_s + \sum_{i=1}^{N} e_i' u_{is} + d_s - \hat{\mu}\} , \\ u_{is} &= -Sat_{\mu_i}\{\frac{\epsilon}{N} x_s\} , \\ \lambda_{is} &= \mu_i + u_{is},\ i \in \mathcal{N}_s , \end{aligned} \tag{4.25}$$

where $\mathcal{N}_s$ is the set containing all active VCs as $n \to \infty$.

The following result gives the solution to the above equations.

Theorem 4.2.2 *The steady behavior of the system described by (2.7) and (4.15) is given by*

a) if $d_s < \hat{\mu}$,

$$x_s = 0, \quad u_{is} = 0, \text{ and } \lambda_{is} = \mu_i,\ i \in \mathcal{N}_s$$

b) if $\hat{\mu} \le d_s \le \hat{\mu} + min\{M_s \mu_0,\ \frac{\epsilon K M_s}{N}\}$,

$$\begin{aligned} x_s &= \frac{N}{\epsilon M_s}(d_s - \hat{\mu}) \\ u_s &:= u_{is} = -\frac{1}{M_s}(d_s - \hat{\mu}) \\ \lambda_{is} &= \mu_i + u_s,\quad i \in \mathcal{N}_s \end{aligned} \tag{4.26}$$

where M_s *is the steady state value of* M *as* $n \to \infty$.

Proof. First, consider the case where $d_s < \hat{\mu}$. By definition, $u_i(n) \le 0$ for all n. It follows that $\sum_{i=1}^{N} e_i' u_{is} + d_s - \hat{\mu} < 0$. Then we can show that we always have that $x_s + \sum_{i=1}^{N} e_i' u_{is} + d_s - \hat{\mu} \le 0$, and hence $x_s = 0$.

By contradiction, assume that $0 < x_s + \sum_{i=1}^{N} e_i' u_{is} + d_s - \hat{\mu} \leq K$. It follows from (4.25) that $x_s = x_s + \sum_{i=1}^{N} e_i' u_{is} + d_s - \hat{\mu}$. It results in $\sum_{i=1}^{N} e_i' u_{is} + d_s - \hat{\mu} = 0$, which is not possible.

If $x_s + \sum_{i=1}^{N} e_i' u_{is} + d_s - \hat{\mu} > K$, we then have that $x_s = K$ due to saturation. From (4.26), it is required that $K + \sum_{i=1}^{N} e_i' u_{is} + d_s - \hat{\mu} > K$, which is again not possible. Thus we always have that $x_s = 0$. It then follows from the second equation in (4.26), $u_{is} = -Sat_{\mu_i}\{\frac{\epsilon}{N} x_s\} = 0$. So $\lambda_{is} = \mu_{is}$ by definition.

Now consider the case where $\hat{\mu} \leq d_s \leq \hat{\mu} + min\{M_s \mu_0, \frac{\epsilon K M_s}{N}\}$. Assume that the system operates in the linear region. Then we have

$$
\begin{aligned}
x_s &= x_s + \sum_{i=1}^{N} e_i' u_{is} + d_s - \hat{\mu} \\
u_{is} &= -\frac{\epsilon}{N} x_s
\end{aligned}
$$

which are equivalent to $x_s = \frac{N}{\epsilon M_s}(d_s - \hat{\mu})$ and $u_{is} = -\frac{1}{M_s}(d_s - \hat{\mu})$. Thus the proof is completed on noting that the conditions $0 \leq x_s \leq K$ and $-\mu_i \leq u_{is} \leq 0$, $i \in \mathcal{N}_s$, are needed to maintain the system operating in the linear region. ¶

Remark 4.2.2 *(Fairness) It is observed from Theorem 4.2.2 that the traffic rate at each source node is regulated only based on the uncontrolled traffic d_s, and that all u_{is} are equal to u_s. This shows that the source nodes are fairly treated, and they can share the switch's bandwidth without interference to each other. In particular, if all the VCs are given the same maximum allocated rate, i.e., $\mu_i = \mu_j$, where i, $j \in \mathcal{N}_s$, then they have equal share of the switch's bandwidth.*

Remark 4.2.3 *In order to design a lossless data network, it is required that the buffer size K is at least greater than $\frac{N}{\epsilon M_s}(d_s - \hat{\mu})$. Clearly, the buffer occupance x_s in (4.26) will become large if N is large, or ϵ and M_s are small.*

4.2.5 Control with Variable Delays

In the previous sections, we have shown that the controller (4.15) can stablize the network under the assumption that the input delays from the sources to bottleneck switch and feedback delays from the bottleneck switch to the sources are constant. This assumption has been widely used in most of all existing rate-based control schemes(e.g., from [1] to [28] , etc.). It is known that such an assumption is valid when queuing delays are negligible compared with the propagation delays. However, if the congestion occurs in the bottleneck switch, the queuing delays and other processing delays may no longer be negligible. Therefore, it is desirable that the congestion controller can still stablize the system in such a case.

In the following, it is assumed that significant queuing delays and other processing delays may occur in the bottleneck switching node due to congestion, and the queuing delays along the path from the sources to the bottleneck switch are small.

Let $\theta_i(n)$ be the number of cells flowing to the switching node from the ith VC in $[nT, (n+1)T)$. If the queuing delay along the path from the source to the switch is negligible, we obviously have from the assumptions in section 2 that

$$\theta_i(n) = \lambda_i(n - \tau_{1i}) \; .$$

However, a small queuing delay or other delays from the ith source to the bottleneck switch will cause the total number of cells $\theta_i(n)$ flowing into the switch during the interval $[nT, (n+1)T)$ to fluctuate around $\lambda_i(n - \tau_{i1})$. That is

$$\theta_i(n) = \lambda_i(n - \tau_{1i}) + \Delta\theta_i(n) \; ,$$

where $\Delta\theta_i(n)$ is an integer variable. The buffer equation given by (2.6) is then modified as

$$x(n+1) = Sat_K\{x(n) + \sum_{i=1}^{N} e_i\lambda_i(n - \tau_{1i}) + \sum_{i=1}^{N} e_i\Delta\theta_i(n) + d(n) - \mu\} \; . \tag{4.27}$$

Let $\tau_{2i}(n) = \tau_{2i}^1 + \tau_{2i}^2(n)$ be the feedback delay from the bottleneck to the ith source node, where $\tau_{2i}^1 T$ is the propagation delay which is constant, and $\tau_{2i}^2(n)T$ is the queuing delay along the path from the bottleneck switch back to the ith source. Note that $\tau_{2i}^2(n)T$ includes the queuing delay in the bottleneck switch. Also let $u_i(n) = \lambda_i(n + \tau_{2i}(n)) - \mu_i$. Then the buffer equation in (4.27) can be written as

$$x(n+1) = Sat_K\{x(n) + \sum_{i=1}^{N} e_i u_i(n - \tau_i(n)) + d(n) - \hat{\mu}(n)\} \ , \tag{4.28}$$

where $\hat{\mu}(n) = \mu - \sum_{i=1}^{N} e_i[\mu_i + \Delta\theta_i(n)]$ and $\tau_i(n) = \tau_{1i} + \tau_{2i}(n)$.

It can be seen from Theorem 4.2.1 that the feedback delay $\tau_{2i}(n)$, the uniform delay τ, and the value of ϵ are important factors to design a congestion controller (4.15). According to [5], the feedback delay $\tau_{2i}(n)$ and the total delay $\tau_i(n)$ of the ith VC can be measured by using time-stamped cells. Therefore, an integer τ_{2i} can be specified as the extented feedback delay for the ith VC if the delay $\tau_{2i}(n)$ is less than τ_{2i}. This implies that an extra delay is added to the delay from the bottleneck to the source node. So let $\tau_i = \tau_{1i} + \tau_{2i}$ and $u'(n) = u(n + \tau_i - \tau_i(n))$. The buffer equation in (4.28) becomes

$$x(n+1) = Sat_K\{x(n) + \sum_{i=1}^{N} e_i u_i'(n - \tau_i) + d(n) - \hat{\mu}\} \ . \tag{4.29}$$

Since the extented feedback delay τ_{2i} is constant, the congestion controller defined in (4.15) can be applied to the network described by (4.29). Figure 17 gives an implementation of this control algorithm for possible perturbations on delays. If $|\Delta\theta_i(n)|$ is small, the saturation nonlinearities in the system will not be activated. Therefore, it follows from Theorem 4.2.2 that this control algorithm can piecewisely stabilize the network described by (4.27) for the small amplitude of fluctuation $\Delta\theta_i(n)$.

4.2.6 Simulations

Since our traffic controller can regulate the source rates over time, we are particularly interested in analyzing both the transient and steady behaviors of the network. Transient behaviors such as the duration of response time and the maximum transient buffer occupancy are usually the main interests in performance analysis.

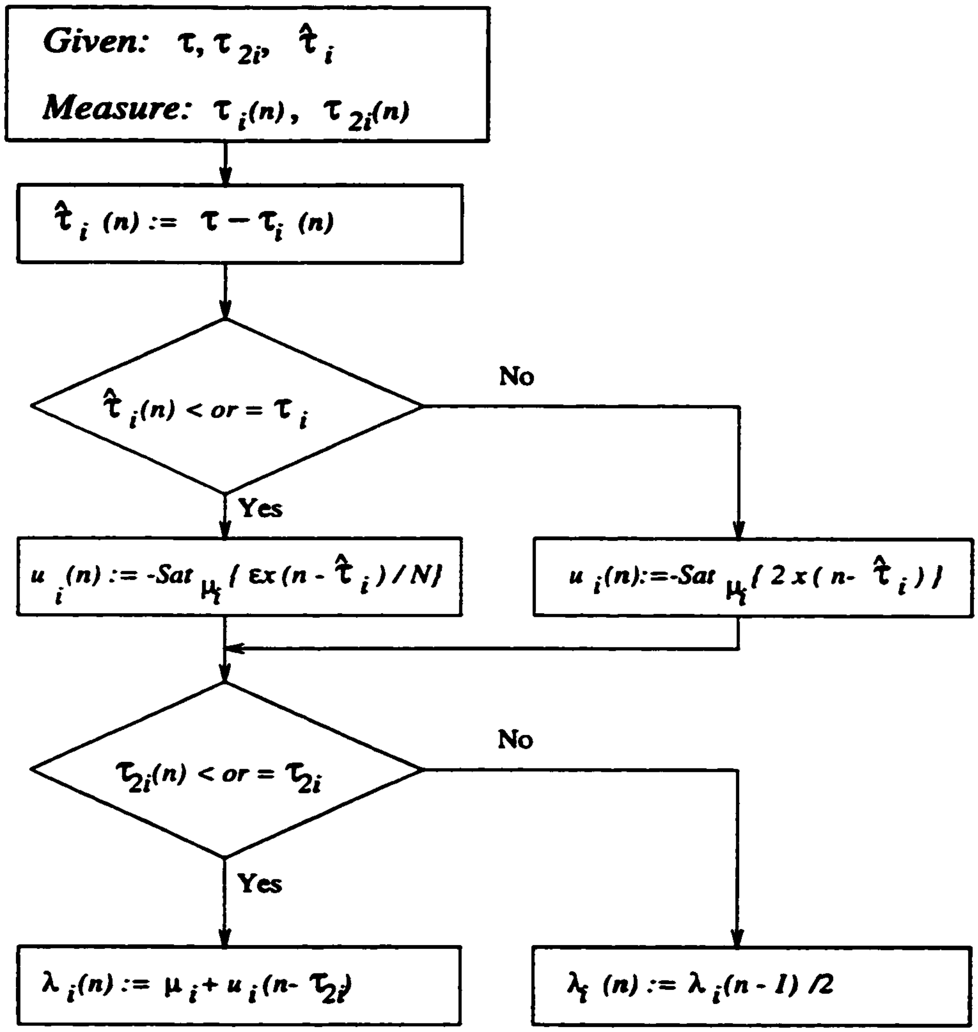

Fig. 17. Flow chart of rate calculation at the ith source with variable delays

Simulations have been performed on the model described by (2.7) with the robust proportional traffic controller given by (4.15). We have chosen a sampling time $T = 1msec$. The service capacity of the bottleneck node is 180Mbps. The maximum number of controlled VCs that are allowed to enter the switch is $N = 10$. Table 2 gives respectively the path delays from the source nodes to the bottleneck node, the path delays from the bottleneck to the source nodes, and the maximum allocated transmission rate for each VC.

VC No.	1	2	3	4	5	6	7	8	9	10
τ'_{1i} (msec)	1	1	2	3	3	4	5	6	7	8
τ'_{2i} (msec)	1	2	3	3	4	5	5	7	8	8
μ_i^{max}/T (Mbps)	50	30	40	25	30	50	30	35	45	40

Table 2. Various delays and allocated maximum transmission rates of VCs

It follows from Table 2 that the maximum total delay is $\tau_{10} = \tau'_{1,10}/T + \tau'_{2,10}/T = 16$. We choose the uniform delay $\tau = 17$. The characteristic equation of the buffer equation (4.16) is then given by

$$\Delta(z, \epsilon) = z^{17}(z-1) + \frac{\epsilon M}{10},$$

where $1 \leq M \leq 10$.

Now we study the system's behaviors related to the values of ϵ. At first, assume that the switch node is fed by three active source nodes which use virtual connections No. 3, 6, and 9 respectively. The uncontrolled traffic rate is assumed to be constant with $d(n)/T = 60Mbps$. Three cases are considered based on different values of chosen ϵ.

Case A: $\epsilon = 0.1$

Figure 18a shows the constant uncontrolled traffic rate $d(n)/T$. Figure 18b shows the controlled traffic rate $\lambda_i(n)/T$, $i = 3, 6, 9$. Figure 18c shows the total traffic rate $[\lambda_3(n) + \lambda_6(n) + \lambda_9(n) + d(n)]/T$. Figure 18d shows the buffer occupancy.

Since the total input rate to the switch exceeds the switch's capacity, the buffer occupancy increases rapidly. After the information on buffer occupancy is sent back to the source nodes, the transmission rate at each source is quickly reduced as observed in Fig. 18b. The transient time is about 35 msec. There is no overshoot in the transient period. Thus the maximum buffer occupancy is determined by its steady state:

$$x_s = \frac{N}{\epsilon M}(d_s - \hat{\mu}) = \frac{10}{0.1 \times 3}(60 - 45) = 500Kb\ .$$

The feedback gain is given by

$$u_s^{'} = -\frac{1}{M}(d_s - \hat{\mu}) = -5\ .$$

Hence, each source node obtains the same feedback gain, and the steady states of source rates are respectively given by

$$\lambda_{3s}/T = (\mu_3^{max} - u_s^{'})/T = 35Mbps,$$

$$\lambda_{6s}/T = (\mu_6^{max} - u_s^{'})/T = 45Mbps,$$

$$\lambda_{9s}/T = (\mu_9^{max} - u_s^{'})/T = 40Mbps.$$

The total input rate to the bottleneck switch at steady state can be determined to be 180Mbps, which is just equal to the switch's capacity. Thus the controller (4.15) has achieved a high utilization.

Case B: $\epsilon = 0.01$

As shown in Fig. 19, the system has a very sluggishly response behavior, which results in a large buffer occupancy. The maximum buffer occupancy can be determined to be

$$x_s = \frac{N}{\epsilon M}(d_s - \hat{\mu}) = \frac{10}{0.01 \times 3}(60 - 45) = 5000Kb\ .$$

Case C: $\epsilon = 1$

As observed from Fig. 20b and 20d, the network is unstable because of the oscillatory properties of the source rates and buffer occupancy. Although the maximum source rates can be reached at the peaks, a lot of resources are wasted due to the oscillation.

By comparing cases A, B, and C, it can be observed that ϵ has a significant effect on the system performance. If ϵ is too small, the system has a sluggish behavior. On the other hand, if ϵ is too large, the system behavior is oscillatory. A good choice of ϵ corresponds to the Case A,

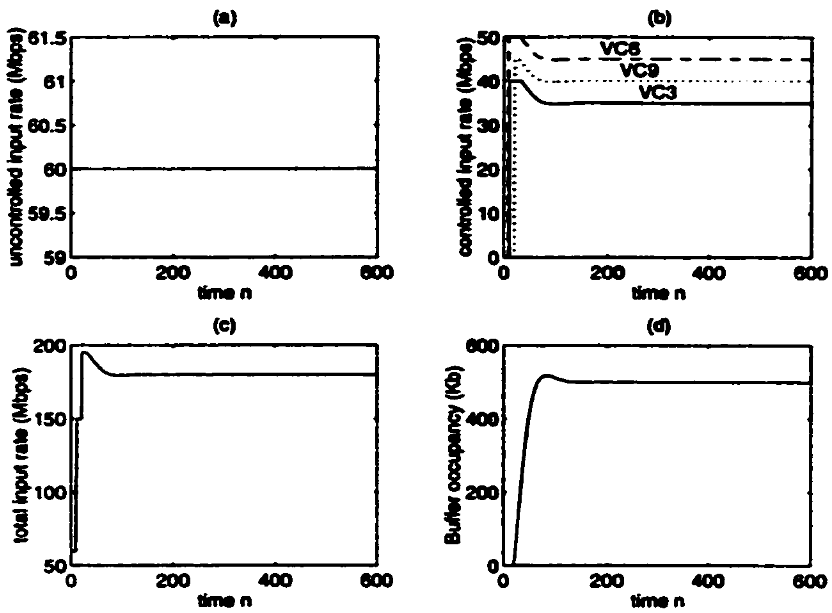

Fig. 18. Three active controlled source nodes with $\epsilon = 0.1$

where the system has a short response time and the small maximum buffer occupancy compared with the Case A.

Finally, let us observe how the system responses to the change of M and the change of $d(n)/T$ for $\epsilon = 0.06$. Figure 21a shows that the number of VCs is increasing from zero to six. Figure 21b shows the change of the input rate from the uncontrolled traffic steam. It can be seen from Figure 21c that the local controller responses quickly to the combined changes of both M and $d(n)/T$. Note that the source rate is decreased if either M or $d(n)/T$ increases, and the source rate is increased if $d(n)/T$ decreases. Figure 21d shows the buffer occupancy corresponding to the changes of M and $d(n)/T$. From the above discussion, it can be seen that the buffer occupancy is piecewise stable.

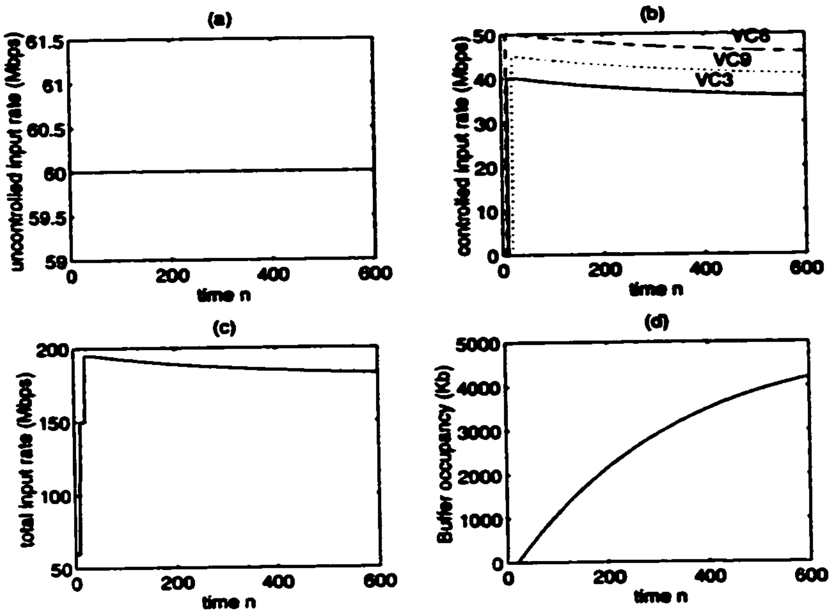

Fig. 19. Three active controlled source nodes with $\epsilon = 0.01$

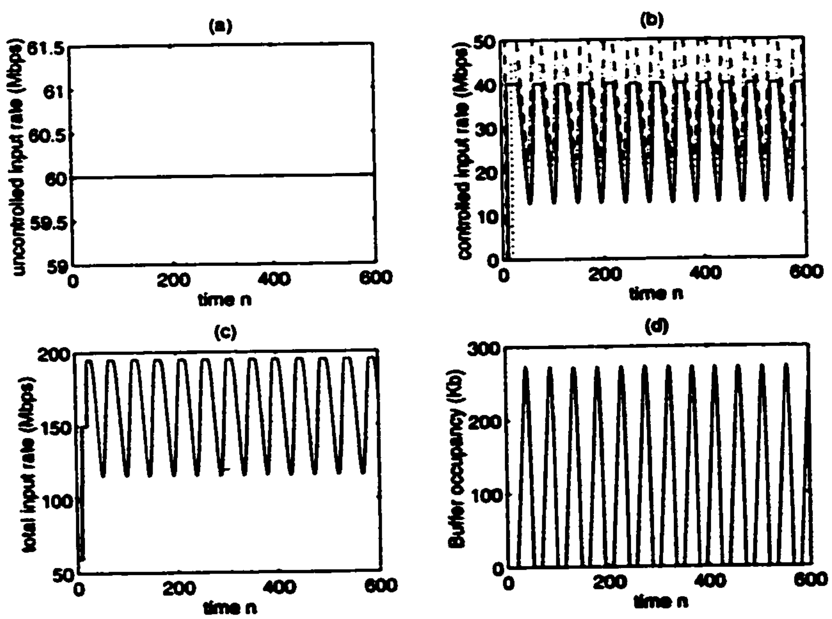

Fig. 20. Three active controlled source nodes with $\epsilon = 1$

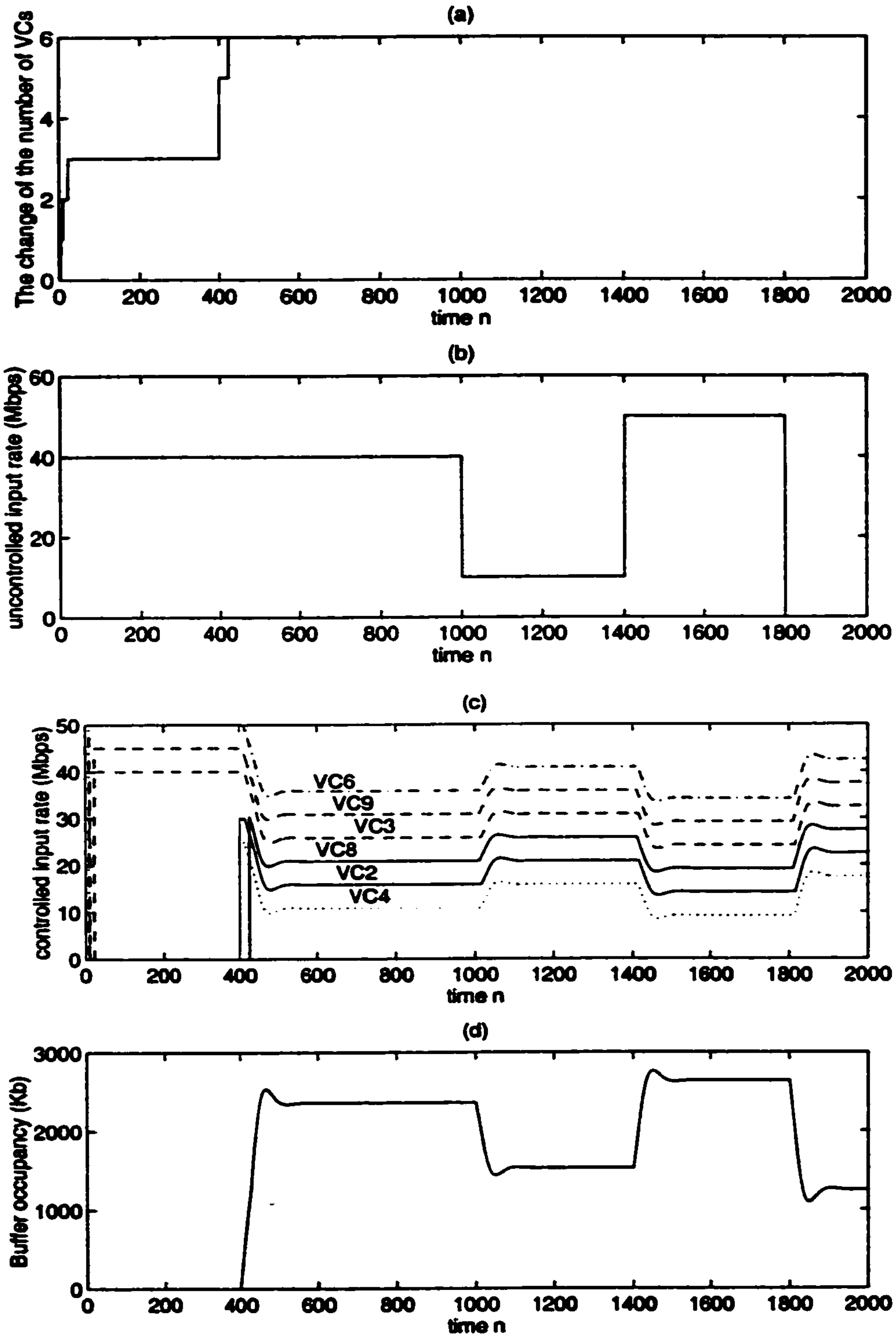

Fig. 21. System's responses to the changes of M and $d(n)/T$ with $\epsilon = 0.06$

4.3 Concluding Remarks

In this chapter, a discrete-time fluid model was used to design a traffic control algorithm for the high-speed network which can accumulate both guaranteed service traffic and best-effort service traffic. The traffic controller is geographically distributed over the source nodes with a simple structure. Each local controller can determine the maximum allowed rate at which the source can transmit data to the network.

We have analyzed a robust congestion controller in the sense that the controller is insensitive to the change of number of VCs during the network operation. With this controller applied, we demonstrate that the network is piecewisely asymptotically stable and exhibits a good transient behavior. We have also extended our proposed controller to the network with bounded queuing delays.

Chapter 5

Hop-by-Hop Congestion Control

The reasons why most of these end-to-end flow control mechanisms in [4] - [30] cause oscillation in the network are that the sources have a slow response to react to the changes of traffic overloads in the network, and feedback information sent to the sources may be outdated due to relatively long propagation delays in high speed networks. Consequently, the switch also needs a large size buffer to prevent congestion.

In this chapter, the fluid-flow modeling technique is still used to study the dynamic and steady behaviors among the source nodes, the intermediate switching nodes and the destination node. Figure 5 in chapter 2 is repeated here to represent the model our hop-by-hop controller is applied to. This model only describes an intermediate switch with incoming traffic from multiple sources in the upstream switches and outgoing traffic destinated to the downstream switches. We first propose a hop-by-hop control along a single virtual connection. Then we extend our results to the hop-by-hop control along a virtual path.

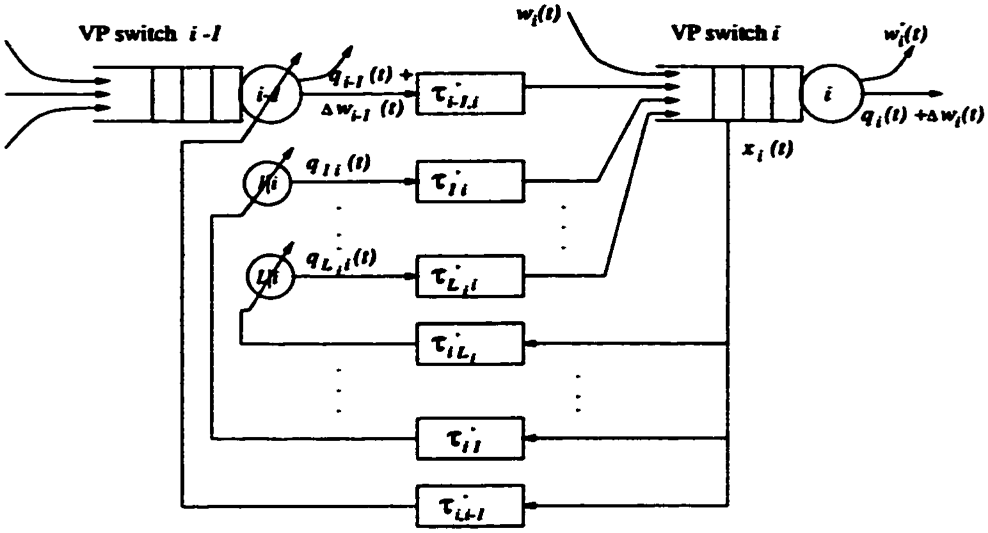

Fig. 5. System model

5.1 Hop-by-Hop Control: a single VC

In this case, the discrete-time fluid flow model 2.12 for a hop-by-hop controlled network can be written as

$$\begin{aligned} x_i(n+1) &= Sat_{K_i}\{x_i(n) + u_{i-1}(n-\tau_i) + d_i(n) - \hat{\mu}_i(n)\}, \\ \mu_{i-1}(n) &= Sat_{\mu_{i-1}}\{Sat_{\mu^*_{i-1}}\{\lambda_{i-1}(n)\} + d'_{i-1}(n)\}, \quad i = 1, 2, \cdots, k. \end{aligned} \tag{5.1}$$

5.1.1 The Congestion Flow Control Algorithm

It will be shown later that the network described by Equ. (5.1) is locally asymptotically stable if the transmission rate at each node is regulated by the following algorithm:

$$\lambda_{i-1}(n) = Sat_{\mu^*_{i-1}}\{\mu^*_{i-1} + \alpha_i[x_i(n-\tau_{i,i-1}) + \sum_{j=n-\tau_i}^{n-1}(\lambda_{i-1}(j) - \mu^*_{i-1})]\}, \quad i = 1, 2, \cdots, k, \tag{5.2}$$

where $-2 < \alpha_i < 0$. In particular, it will be demonstrated in our simulation results that if $\alpha_i = -1$, the controller in (5.2) can quickly respond to the change of the external input $d_i(n)$

It can be seen from the control structure in (5.2) that the current transmission rate at node $(i-1)$ is adjusted based on the buffer occupancy, delayed by τ_i at node i and on the sum of previous transmission rates from $n-\tau_i$ to $n-1$. Without the consideration of the nonlinearities imposed on the systems described by (5.1) and (5.2), the last term in the control algorithm (5.2) is used to locate all poles of the closed-loop system of (5.1) and (5.2) inside the unit circle.

5.1.2 Stability Analysis

To investigate the stability of the network described by (5.1) with the controller given by (5.2), it has been shown in [10] and [13] that it suffices to study the locally asymptotical stability properties of the system by removing the saturation nonlinearities posed on the network (5.1) and the controller (5.2). The reasons are 1) although a rigorous proof of stability of the system using Liapunov's second approach [10] may be possible, the gain from the analysis is slight, and 2) these nonlinearities will not be activated for small deviations around network's operating points. Thus in the following, we only study the asymptotical stability properties of the network given by

$$\begin{aligned} x_i(n+1) &= x_i(n) + u_{i-1}(n-\tau_i) + d_i(n) - (\mu_i(n) - \mu^*_{i-1}), \\ \mu_{i-1}(n) &= \lambda_{i-1}(n) + d'_{i-1}(n), \quad i = 1, 2, \cdots, k, \end{aligned} \tag{5.3}$$

with the flow controller given by

$$\lambda_{i-1}(n) = \mu^*_{i-1} + \alpha_i[x_i(n-\tau_{i,i-1}) + \sum_{j=n-\tau_i}^{n-1} (\lambda_{i-1}(j) - \mu^*_{i-1})] \,. \tag{5.4}$$

Let

$$y_i(n) = x_i(n) + \sum_{j=n-\tau_i}^{n-1} u_{i-1}(j), \quad i = 1, 2, \cdots, k, \tag{5.5}$$

where $u_{i-1}(n) := \lambda_{i-1}(n+\tau_{i,i-1}) - \mu^*_{i-1}$. Thus we have

$$\begin{aligned} y_i(n+1) &= x_i(n) + u_{i-1}(n-\tau_i) + d_i(n) - (\mu_i(n) - \mu^*_{i-1}) + \sum_{j=n-\tau_i+1}^{n} u_i(j) \\ &= y_i(n) + u_{i-1}(n) + d_i(n) - (\mu_i(n) - \mu^*_{i-1}) \end{aligned}$$

Choose

$$u_{i-1}(n) = \alpha_i y_i(n), \quad i = 1, 2, \cdots, k, \tag{5.6}$$

which gives that

$$y_i(n+1) = (1+\alpha_i)y_i(n) + d_i(n) - (\mu_i(n) - \mu_{i-1}^*) \ . \qquad (5.7)$$

On noting from (5.6) that $\lambda_i(n) = \alpha_{i+1}y_{i+1}(n-\tau_{i+1,i}) + \mu_i^*$, we obtain from (5.3) and (5.7) that *A)* for $i = 1, 2, \cdots, k-1$,

$$\begin{aligned} y_i(n+1) &= (1+\alpha_i)y_i(n) + d_i(n) - (\lambda_i(n) + d_i'(n) - \mu_{i-1}^*) \\ &= (1+\alpha_i)y_i(n) - \alpha_{i+1}y_{i+1}(n-\tau_{i+1,i}) + (d_i(n) - d_i'(n)) + (\mu_{i-1}^* - \mu_i^*) \end{aligned}$$

B) for $i = k$,

$$y_k(n+1) = (1+\alpha_k)y_k(n) + d_k(n) - (\mu_k - \mu_{k-1}^*)$$

It can be shown easily, from the equations in cases *A)* and *B)*, that the characteristic equation describing the traffic flow from node $(i-1)$ to node i is given by $z - (1+\alpha_i)$, where $i = 1, 2, \cdots, k$. On noting that all nodes are connected in tandem, the characteristic equation describing the traffic flow from node 0 to node k is given by

$$\Delta(z) = \prod_{i=1}^{k} [z - (1+\alpha_i)] \ ,$$

which has k zeros at $z_i = 1 + \alpha_i$, where $i = 1, 2, \cdots, k$. Therefore, the system is exponentially stable if and only if $-2 < \alpha_i < 0$, $i = 1, 2, \cdots, k$.

We finally obtain that for $i = 1, 2, \cdots, k$,

$$\begin{aligned} \lambda_{i-1}(n) &= \mu_{i-1}^* + u_{i-1}(n - \tau_{i,i-1}) \\ &= \mu_{i-1}^* + \alpha_i y_i(n - \tau_{i,i-1}) \\ &= \mu_{i-1}^* + \alpha_i[x_i(n-\tau_{i,i-1}) + \sum_{j=n-\tau_i-\tau_{i,i-1}}^{n-\tau_{i,i-1}-1} (\lambda_{i-1}(j+\tau_{i,i-1}) - \mu_{i-1}^*)] \\ &= \mu_{i-1}^* + \alpha_i[x_i(n-\tau_{i,i-1}) + \sum_{j=n-\tau_i}^{n-1} (\lambda_{i-1}(j) - \mu_{i-1}^*)] \end{aligned}$$

which establishes the control algorithm (5.2).

5.1.3 Upper Bound for Buffer Occupancy

We now consider the controller (5.6) with $\alpha = -1$ and assume that the external traffic rate is always less than the node's service rate. Since it is required that $0 \le \lambda_{i-1}(n) \le \mu^*_{i-1}$ for all n, it follows that $0 \le -u_{i-1}(n) = \mu^*_{i-1} - \lambda_{i-1}(n+\tau_{i,i-1}) \le \mu^*_{i-1}$ for all n. Thus,

$$-u_{i-1}(n) = Sat_{\mu^*_{i-1}}\{-u_{i-1}(n)\}, \quad i = 1, 2, \cdots, k.$$

Now if the buffer size K_i is assumed to be large enough so that there is no packet loss, then the system (5.1) can be expressed as

$$x_i(n+1) = [x_i(n) - Sat_{\mu^*_i}\{-u_{i-1}(n-\tau_i)\} + d_i(n) - (\mu_i(n) - \mu^*_{i-1})]^+ \ ,$$

where $[x]^+ = max\{x,\ 0\}$. Also equation (5.5) becomes

$$y_i(n) = [x_i(n)]^+ - \sum_{j=n-\tau_i}^{n-1} Sat_{\mu^*_{i-1}}\{-u_{i-1}(j)\} \ . \tag{5.8}$$

Thus we have

$$\begin{aligned} y_i(n+1) &= [x_i(n+1)]^+ - \sum_{j=n+1-\tau_i}^{n} Sat_{\mu^*_{i-1}}\{-u_{i-1}(j)\} \\ &= [x_i(n) - Sat_{\mu^*_{i-1}}\{-u_{i-1}(n-\tau_i)\} + d_i(n) - (\mu_i(n) - \mu^*_{i-1})]^+ \\ &\quad - \sum_{j=n+1-\tau_i}^{n} Sat_{\mu^*_{i-1}}\{-u_{i-1}(j)\} \end{aligned}$$

If $x_i(n+1) < 0$, $y_i(n+1) = -\sum_{j=n+1-\tau_i}^{n} Sat_{\mu^*_{i-1}}\{-u_{i-1}(j)\} \le 0$.
If $x_i(n+1) \ge 0$,

$$\begin{aligned} y_i(n+1) &\le [x_i(n)]^+ - Sat_{\mu^*_{i-1}}\{-u_{i-1}(n-\tau_i)\} + [d_i(n) - (\mu_i(n) - \mu^*_{i-1})]^+ \\ &\quad - \sum_{j=n+1-\tau_i}^{n} Sat_{\mu^*_{i-1}}\{-u_{i-1}(j)\} \\ &= y_i(n) - Sat_{\mu^*_{i-1}}\{-u_{i-1}(n)\} + [d_i(n) - (\mu_i(n) - \mu^*_{i-1})]^+ \ . \end{aligned}$$

On noting from (5.6) that $-u_{i-1}(n) = Sat_{\mu^*_{i-1}}\{y_i(n)\}$, it follows that

$$y_i(n+1) \le y_i(n) - Sat_{\mu^*_{i-1}}\{y_i(n)\} + [d_i(n) - (\mu_i(n) - \mu^*_{i-1})]^+ \ . \tag{5.9}$$

Since it is assumed that $d_i(n) \leq \mu_i(n)$ and $y_i(0) = 0$, $[d_i(n) - (\mu_i(n) - \mu^*_{i-1})]^+ \leq \mu^*_{i-1}$. By mathematical induction, It can be shown from relations (5.8) and (5.9) that $y_i(n) \leq \mu^*_{i-1}$ for all n. We then have, for all n,

$$y_i(n+1) \leq [d_i(n) - (\mu_i(n) - \mu^*_{i-1})]^+$$

Thus from (5.8),

$$x_i(n) = y_i(n) + \sum_{j=n-\tau_i}^{n-1} Sat_{\mu_i}\{-u_i(j)\} \leq \sum_{j=n-\tau_i}^{n} Sat_{\mu^*_{i-1}}\{y_i(j)\} \leq \sum_{j=n-\tau_i}^{n} [d_i(j-1) - \mu_i(j-1) + \mu^*_{i-1}]^+$$

This relation shows that the buffer occupancy is the function of the rate of the external traffic, the service rate $\mu_i(n)/T$ and the maximum rate μ^*_i/T assigned to the node i, and the loop delay τ_i. When the node i is too conservative, i.e., $\mu^*_i < \mu_i$, such that $d_i(n) - (\mu_i(n) - \mu^*_i) \leq 0$, the buffer is always empty, where it is assumed that $d_i(n)$ does not exceed μ_i. When the node i is too greedy, i.e., μ^*_i is close to μ_i, a buffer of large size is then required to accumulate any burstiness in the external traffic.

5.1.4 Simulation

Simulation is performed on the model described by (5.1) with $k = 3$ hops and the hop-by-hop flow controller given in (5.2). We choose a sampling time $T = 1msec$. Table 3 gives respectively the maximum service data of node i, the maximum link transmission rate assigned to the ith node, the link delay from node $i-1$ to node i, and the link delay from node i to node $i-1$.

Node i	$i=0$	$i=1$	$i=2$	$i=3$
μ_i/T (Mbps)	80	155	155	155
μ^*_i/T (Mbps)	80	80	80	80
$\tau'_{i-1,i}$ (msec)		1	5	8
$\tau'_{i,i-1}$ (msec)		2	6	10

Table 3. Network's parameters

It follows from Table 3 that the loop delays are respectively given by

$$\tau_1 = \tau_{01} + \tau_{10} = 3, \quad \tau_2 = \tau_{12} + \tau_{21} = 11, \quad \tau_3 = \tau_{23} + \tau_{32} = 18 .$$

Now we study the system's behaviors related to the values of α given in (5.2), where $\alpha = \alpha_i$, $i = 1, 2, 3$. Assume that the external traffic and crossing traffic are periodical signals with $d_i(n) = d_i'(n)$, where $i = 1, 2$, i.e., the sum of uncontrolled and controlled traffic rates. By choosing different values of α, three cases are considered.

Case A: $\alpha = -1$

Figure 22a shows uncontrolled traffic (or external input) rates going to Node 1, 2 and 3, which are represented by the solid, dashed and dotted lines respectively. These rates are periodic along the sampling point n.

Figure 22b shows the controlled traffic rate $\lambda_i(n)/T$, $i = 0, 1, 2$, in response to the uncontrolled rate, which are represented by the solid, dashed and dotted lines respectively. Figure 22c shows the total traffic rate $[\lambda_{i-1}(n) + d_i(n)]/T$, $i = 1, 2, 3$, which are represented by the solid, dashed and dotted lines respectively. Figure 22d shows the buffer occupancies $x_i(n)$, $i = 1, 2, 3$, which are also represented by the solid, dashed and dotted lines respectively..

Since at the beginning total input rate to each node is less than the node's capacity μ_i/T, the buffer at each node is empty. The VC obtains its maximum service rate 80Mbps at the source node. Thus, the nodes 1,2 and 3 also provide the service rate 80Mbps for this VC. When $n \geq 50$, the external input rate to the receiver jumps to 80Mbps, which makes the total input rate to the receiver greater than the receiver's capacity. The buffer occupancy at the receiving node increases rapidly. After the information on buffer occupancy is sent back to node 2, the transmission rate $\lambda_2(n)/T$ is quickly reduced (Fig. 22b). Similarly, the transmission rates $\lambda_1(n)/T$ and $\lambda_0(n)/T$ are reduced correspondingly. It is observed from Fig. 22b or Fig. 22c that the transient time of the controlled input rate $\lambda_2(n)/T$ at node 2 is the loop delay τ_3. Similarly, the transient time of $\lambda_1(n)/T$ at node 1 is the sum of the loop delays $\tau_2 + \tau_3$, and the transient time of $\lambda_0(n)/T$ at the source node is the round trip delay $\tau_1 + \tau_2 + \tau_3$. There is no overshoot in the transient period.

Case B: $\alpha = -0.1$

In this case, we can see the phenomenon is similar to the case of $\alpha = -1$, but the system has much longer transient times than the case of $\alpha = -1$. This sluggishly response behavior results in a larger size of buffer occupancy as observed in Fig. 23d.

Case C: $\alpha = -1.8$

In this case, the system has an oscillatory response behavior as observed in Fig. 24b, because the parameter $\alpha = -1.8$ is close to the stability boundary of $\alpha = -2$.

By comparing cases A, B, and C, it can be observed that α has a significant effect on the system's performance. If $|\alpha|$ is too small, the system has a sluggish behavior. On the other hand, if $|\alpha|$ is too large, the system behavior is oscillatory. A good choice of α corresponds to the Case A, where the system has a short response time and the small maximum buffer occupancy compared with the Case B.

As can be seen, all nodes upstream to the bottleneck node maintain their buffer occupancies respectively. This allows for a faster alleviation of congestion in the bottleneck node since its neighboring node can respond tp the congestion information quickly after a loop delay, compared with a round-trip delay and a larger buffer occupancy as observed from Fig. 25 for an end-to-end controller with $\alpha = -1$.

5.2 Hop-by-Hop Control: a single VP

Another problem in the end-to-end rate-based control is that the destination end needs to send network information to every sources. This implies that a lot of traffic along the feedback virtual connections will be generated since the number of sources are large in general. As it is known that many virtual connections are grouped into a virtual path to carry traffic between two switches, it is possible for one switch to send feedback information back to the other switch along the virtual path instead of the virtual connections.

This section therefore proposes a new hop-by-hop rate-based flow control scheme which controls the allocation of the bandwidth of a VP switching node to its VC connections. Under

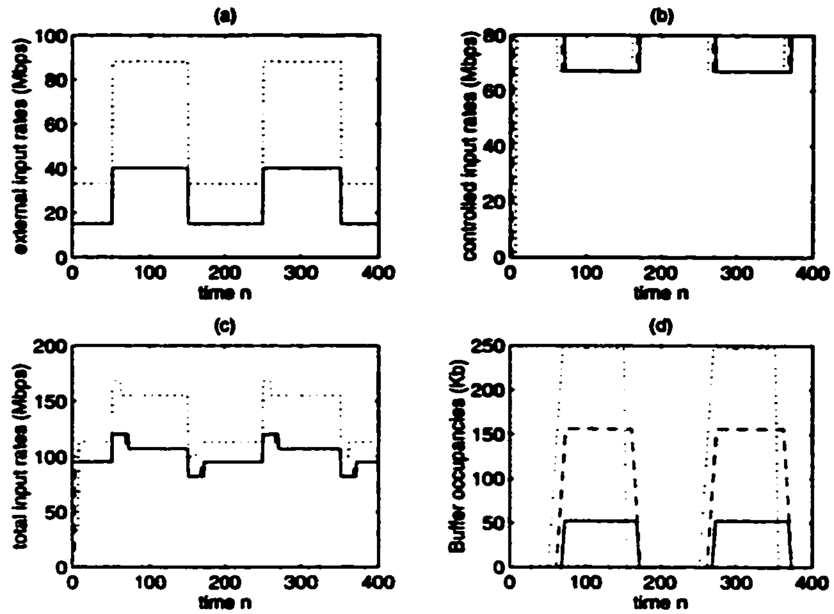

Fig. 22: Single controlled VC with three hops and $\alpha = -1$

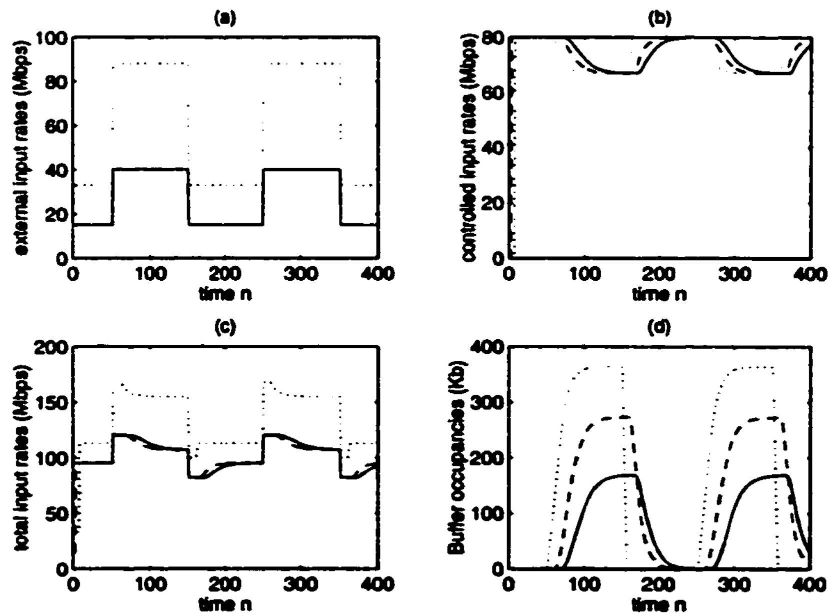

Fig. 23: Single controlled VC with three hops and $\alpha = -0.1$

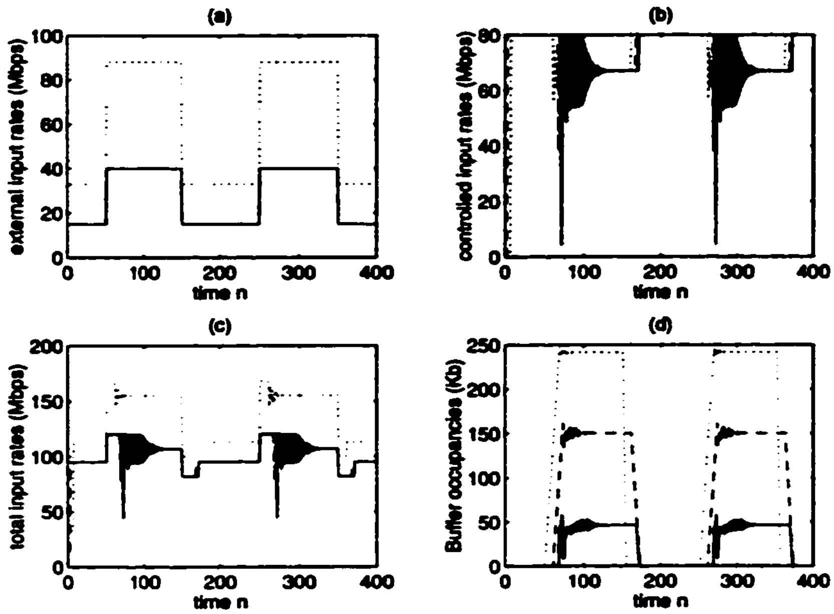

Fig. 24: Single controlled VC with three hops and $\alpha = -1.8$

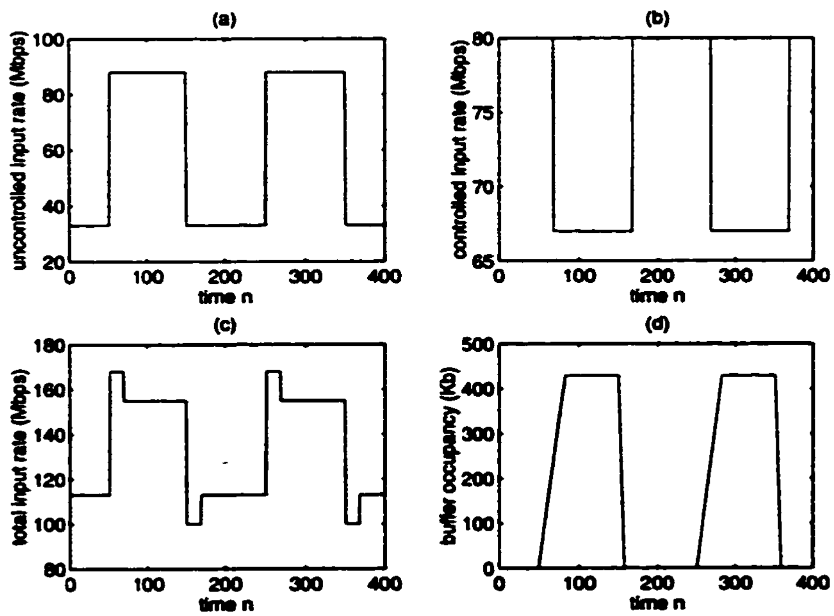

Fig. 25: Single end-to-end controlled VC with $\alpha = -1$

this scheme, each VP switching node plays an active role in regulating aggregated traffic. The sending rate in each node is periodically computed based on local information on the server capacity and the link capacity, and based on feedback information on buffer occupancy sent by the downstream VP switching node along the virtual path. Thus the overhead generated along the feedback path is greatly reduced in comparison with the overhead generated along the virtual connections.

5.2.1 The Hop-by-Hop Robust Proportional Flow Control Algorithm

It will be shown later that the network described by (2.7) is locally asymptotically stable if the transmission rate at each node is regulated by the following algorithm:
For VP switch $(i-1)$,

$$\lambda_{i-1}(n) = \mu_{i-1} + u_{i-1}(n - \tau_{i,i-1}), \quad i = 2, 3, \cdots, I, \tag{5.10}$$

where

$$u_{i-1}(n) = -Sat_{\Gamma_{i-1}}\{\frac{\epsilon_i M_i}{N_i} x_i(n - \hat{\tau}_i)\}$$

The value of M_i is known to VP switch $(i-1)$ since M_i represents the number of active VCs along a VP connection between VP switch $(i-1)$ and VP switch i. The values of N_i and ϵ_i are constant to be determined.
For the external node $j|i$ to VP switch i,

$$\lambda_{ji}(n) = \mu_{ji} + u_{ji}(n - \tau_{ij}), \quad i = 1, 2, \cdots, I, \; j = 1, 2, \cdots L_i, \tag{5.11}$$

where

$$u_{ji}(n) = -Sat_{\mu_{ji}}\{\frac{\epsilon_i}{N_i} x_i(n - \hat{\tau}_{ji})\} .$$

It can be seen from the control structure in (5.10) and (5.11) that the current transmission rates $\lambda_{i-1}(n)/T$ and $\lambda_{ji}(n)/T$ are adjusted only based on the buffer occupancy x_i at their downstream VP switch. Without the consideration of the nonlinearities imposed on the systems described by (2.7) and (5.10), the number ϵ_i in the control algorithm (5.10) and (5.11) is used to locate all poles of the closed-loop system of (2.7), (5.10) and (5.11) inside the unit circle.

Remark 5.2.1 *It is obvious that our controller given by (5.10) and (5.11) has a very simple structure. The traffic output at each VP switch is proportional to the delayed buffer occupancy from the down-stream VP switch. The controller is robust in the sense that the system's stability is not sensitive to the change of number of active VCs by properly choosing the number* ϵ_i.

5.2.2 Design and Analysis

Our major concern in design phase is to determine the control parameters to maintain the stability of the closed-loop system. Thus in the following, we would only consider the locally asymptotical stability properties of the network (2.12).

Assume that VP switch I is a link-congested node. The buffer occupancy of VP switch $i(\leq I)$ with multiple controlled inputs can therefore be described by

$$\begin{aligned} x_i(n+1) &= x_i(n) + u_{i-1}(n-\tau_i) + \sum_{j=1}^{L_i} u_{ji}(n-\tau_j^i) + d_i(n) + \Delta d_{i-1}(n-\tau_i) - \hat{\mu}_i(n) \\ \mu_i(n) &= \begin{cases} \lambda_i(n) + \Delta d_i(n) + d_i'(n) = u_i(n-\tau_{i+1,i}) - \mu_i + \Delta d_i(n) + d_i'(n), & i \leq I-1 \\ \\ \Gamma_I^* + d_I'(n), & i = I \end{cases} \end{aligned} \tag{5.12}$$

where $u_0(n) = 0$.

On noting that $\hat{\mu}_i(n) = \mu_i(n) - \mu_{i-1} - \sum_{j=1}^{L_i} \mu_{ji}$, we have that

$$x_i(n+1) = x_i(n) + u_{i-1}(n-\tau_i) + \sum_{j=1}^{L_i} u_{ji}(n-\tau_j^i) - u_i(n-\tau_{i+1,i}) + v_i(n)$$

where

$$v_i(n) = \begin{cases} \mu_i - \mu_{i-1} - \sum_{j=1}^{L_i} \mu_{ji}, & i = 1, 2, \cdots I-1 \\ d_I(n) + \Delta d_{I-1}(n) - d_I'(n) + \Gamma_I^* - \mu_{I-1} - \sum_{j=1}^{L_I} \mu_{jI}, & i = I\ . \end{cases}$$

The traffic controller at VP switch $(i-1)$ is defined by

$$u_{i-1}(n) = -\sum_{j=1}^{\tau^i_{max}} a_{i(\tau^i_{max}-j)} u_{i-1}(n-j) - \sum_{j=0}^{\hat{\tau}_i} M_i b_{i(\hat{\tau}_i-j)} x_i(n-j) \ , \tag{5.13}$$

and the traffic controller at the external node $j|i$ is defined as

$$u_{ji}(n) = -\sum_{j=1}^{\tau^i_{max}} a_{i(\tau^i_{max}-j)} u_i(n-j) - \sum_{j=0}^{\hat{\tau}^i_j} c_{i(\hat{\tau}^i_j-j)} x(n-j) \ . \tag{5.14}$$

where a_{ij}, b_{ij} and c_{ij} are coefficients, and $\hat{\tau}_i$, $\hat{\tau}^i_j$ and τ^i_{max} are integers to be determined.

In order to describe the characteristic equation of (5.12) with (5.13) and (5.14), the z-transform method is used, where the system's initial conditions are assumed to be zero because they do not affect the system's stability. Then the z-transform of (5.12) is

$$(z-1)X_i(z) = z^{-\tau_i} U_{i-1}(z) + \sum_{j=1}^{L_i} z^{-\tau^i_j} U_{ji}(z) - z^{-\tau_{i+1,i}} U_i(z) + V_i(z) \ , \tag{5.15}$$

where $X_i(z) := \sum_{n=0}^{\infty} x_i(n) z^n$, and $U_{i-1}(z)$, $U_{ji}(z)$, and $V_i(z)$ are similarly defined.

Let

$$W_{i\tau}(z) := \begin{bmatrix} z^\tau \\ \vdots \\ z \\ 1 \end{bmatrix}, \quad A_{i\tau} := \begin{bmatrix} a_{i\tau} \\ \vdots \\ a_{i1} \\ a_{i0} \end{bmatrix}, \quad B_{i\tau} := \begin{bmatrix} b_{i\tau} \\ \vdots \\ b_{i1} \\ b_{i0} \end{bmatrix}, \quad C_{i\tau} := \begin{bmatrix} c_{i\tau} \\ \vdots \\ c_{i1} \\ c_{i0} \end{bmatrix},$$

Then the z transform of (5.14) is given by

$$U_{i-1}(z) = -z^{-\tau^i_{max}} A^T_{i(\tau^i_{max}-1)} W_{\tau^i_{max}-1}(z) U_{i-1}(z) - z^{-\hat{\tau}_i} M_i B^T_{\hat{\tau}_i} W_{\hat{\tau}_i}(z) X_i(z) \ ,$$

$$U_{ji}(z) = -z^{-\tau^i_{max}} A^T_{i(\tau^i_{max}-1)} W_{\tau^i_{max}-1}(z) U_{ji}(z) - z^{-\hat{\tau}^i_j} C^T_{\hat{\tau}^i_j} W_{\hat{\tau}^i_j}(z) X_i(z) \ ,$$

or

$$z^{-\tau^i_{max}} A^T_{i\tau^i_{max}} W_{\tau^i_{max}}(z) U_{i-1}(z) = -z^{-\hat{\tau}_i} M_i B^T_{\hat{\tau}_i} W_{\hat{\tau}_i}(z) X_i(z) \ ,$$

$$z^{-\tau^i_{max}} A^T_{i\tau^i_{max}} W_{\tau^i_{max}}(z) U_{ji}(z) = -z^{-\hat{\tau}^i_j} C^T_{\hat{\tau}^i_j} W_{\hat{\tau}^i_j}(z) X_i(z) \ ,$$

where $a_{i\tau^i_{max}}$ in $A_{i\tau^i_{max}}$ is 1. Then,

$$U_{i-1}(z) = -z^{\tau^i_{max}-\hat{\tau}_i}(A^T_{i\tau^i_{max}} W_{\tau^i_{max}}(z))^{-1} M_i B^T_{\hat{\tau}_i} W_{\hat{\tau}_i}(z) X_i(z) \ . \tag{5.16}$$

$$U_{ji}(z) = -z^{\tau^i_{max}-\hat{\tau}^i_j}(A^T_{i\tau^i_{max}} W_{\tau^i_{max}}(z))^{-1} C^T_{\hat{\tau}^i_j} W_{\hat{\tau}^i_j}(z) X_i(z) \ . \tag{5.17}$$

Substituting (5.16) into (5.15), we obtain

$$\begin{aligned}(z-1)X_i(z) \ &= \ -z^{\tau^i_{max}-\hat{\tau}_i-\tau_i}(A^T_{i\tau^i_{max}} W_{\tau^i_{max}}(z))^{-1} M_i B^T_{\hat{\tau}_i} W_{\hat{\tau}_i}(z) X_i(z) \\ &\quad -\sum_{j=1}^{L_i} z^{\tau^i_{max}-\hat{\tau}_i-\tau^i_j}(A^T_{i\tau^i_{max}} W_{\tau^i_{max}}(z))^{-1} C^T_{\hat{\tau}^i_j} W_{\hat{\tau}^i_j}(z) X_i(z) \\ &\quad -X_{i+1}(z) + V_i(z) \ .\end{aligned} \tag{5.18}$$

Let

$$\Delta_i(z) = (z-1)A^T_{i\tau^i_{max}} W_{\tau^i_{max}}(z) + z^{\tau^i_{max}-\hat{\tau}_i-\tau_i} M_i B^T_{\hat{\tau}_i} W_{\hat{\tau}_i}(z) + \sum_{j=1}^{L_i} z^{\tau^i_{max}-\hat{\tau}_i-\tau^i_j} C^T_{\hat{\tau}^i_j} W_{\hat{\tau}^i_j}(z) \ ,$$

where

$$R_i(z) = A^T_{i\tau^i_{max}} W_{\tau^i_{max}}(z).$$

It is clear that $\Delta_i(z)$ is the characteristic equation of the sub-system of VP switch i. Then equation (5.18) can be rewritten as

$$\Delta_i(z) X_i(z) + R_i(z) X_{i+1}(z) = R_i(z) V_i(z) \ . \tag{5.19}$$

By grouping the equations (5.19) for $i = 1, 2, \cdots, I$, we obtain

$$\begin{bmatrix} \Delta_1(z) & R_1(z) & & & 0 \\ & \Delta_2(z) & R_2(z) & & \\ & & \ddots & \ddots & \\ & & & \Delta_{I-1}(z) & R_{I-1}(z) \\ 0 & & & & \Delta_I(z) \end{bmatrix} \begin{bmatrix} X_1(z) \\ X_2(z) \\ \vdots \\ X_{I-1}(z) \\ X_I(z) \end{bmatrix} = \begin{bmatrix} R_1(z)V_1(z) \\ R_2(z)V_2(z) \\ \vdots \\ R_{I-1}(z)V_{I-1}(z) \\ R_I(z)V_I(z) \end{bmatrix}$$

Thus the characteristic equation of the network (5.12) with the controllers (5.13) and (5.14) is given by

$$\Delta(z) = \prod_{i=1}^{I} \Delta_i(z) \ . \tag{5.20}$$

This implies that the network is stable if and only if the subsystem of VP switch i is stable, $i = 1, 2, \cdots, I$. For the subsystem i, choose $\hat{\tau}_i$ and $\hat{\tau}_i$ such that

$$\hat{\tau}_i + \tau_i = \tau^i_{max} ,$$

$$\hat{\tau}^i_j + \tau^i_j = \tau^i_{max} ,$$

where $\tau^i_{max} \geq \{\tau_i, \tau^i_j, \ j = 1, 2, \cdots, L_i\}$. This results in that $\Delta_i(z)$ is a polynomial function of z. We now obtain

$$\Delta_i(z) = (z-1)A^T_{i\tau^i_{max}} W_{\tau^i_{max}}(z) + M_i B^T_{\hat{\tau}_i} W_{\hat{\tau}_i}(z) + \sum_{j=1}^{L_i} C^T_{\hat{\tau}^i_j} W_{\hat{\tau}^i_j}(z) \ . \tag{5.21}$$

Note that the roots of $\Delta_i(z) = 0$ are determined by the coefficients a_{ij}, b_{ij} and c_{ij}. In order to obtain a simple control structure, we choose for $i = 1, 2, \cdots, I$:

$$\begin{aligned}
a_{ij} &= 0, \qquad j = 0, 1, \cdots, \tau^i_{max} - 1 , \\
b_{i0} &= \frac{\epsilon_i M_i}{N} , \\
b_{ij} &= 0, \qquad j = 1, 2, \cdots, \hat{\tau}_i , \\
c_{i0} &= \frac{\epsilon_i}{N} . \\
c_{ij} &= 0, \qquad j = 1, 2, \cdots, \hat{\tau}^i_j .
\end{aligned} \tag{5.22}$$

Then the resulting characteristic equation of the buffer occupancy can be simplified as

$$\Delta_i(z) = z^{\tau^i_{max}}(z-1) + \frac{M_i + L_i}{N}\epsilon_i \ . \tag{5.23}$$

The following result can be established by using Lemma 4.2.1.

Theorem 5.2.1 *Consider a network defined in (2.12). There exist positive numbers* ϵ^0_i, $i = 1, 2, \cdots, I$, *such that for all* $\epsilon_i \in (0, \epsilon^0_i)$, *the network (2.12) can be stabilized by the local controllers*

(5.13) and (5.14) if for $i = 1, 2, \cdots, I$,

$$
\begin{aligned}
&\tau^i_{max} \geq \max\{\tau_i, \tau^i_j,\ j = 1, 2, \cdots, L_i\}\ , && \\
&\hat{\tau}_i + \tau_i = \tau^i_{max}\ , && \\
&\hat{\tau}^i_j + \tau^i_j = \tau^i_{max}\ , && \\
&a_{ij} = 0, && j = 0, 1, \cdots, \tau^i_{max} - 1\ , \\
&b_{i0} = \frac{\epsilon_i M_i}{N}\ , && \\
&b_{ij} = 0, && j = 1, 2, \cdots, \hat{\tau}_i\ , \\
&c_{i0} = \frac{\epsilon_i}{N}\ , && \\
&c_{ij} = 0, && j = 1, 2, \cdots, \hat{\tau}^i_j\ .
\end{aligned}
\tag{5.24}
$$

Moreover, the local controllers defined in (5.14) are also open-loop stable.

Proof. It follows from the equation (4.23) and lemma 4.2.1 that for the subsystem of VP switch i, there exists a positive number ϵ^0_i such that for all $\epsilon_i \in (0,\ \epsilon^0_i)$, all the roots of $\Delta_i(z) = 0$ are inside the unit circle. So are all the roots of $\Delta(z) = \prod_{i=1}^{I} \Delta_i(z) = 0$. Therefore the network (2.7) can be stabilized by the controllers (5.13) and (4.17).

It is obvious that the characteristic equation of the local controller (5.13) is $\Delta^c_i(z) = z^{\tau^i_{max}}$ by using the parameters (4.24). Similarly the characteristic equation of the local controller (4.17) is $\Delta^c_{ji}(z) = z^{\tau^i_{max}}$. Therefore the roots of both $\Delta^c_i(z) = 0$ and $\Delta^c_{ji}(z) = 0$ are all in the origin. Hence the local controllers are open-loop stable. ¶

Substituting the control parameters defined in (4.24) into (5.13) and (4.17), we obtain the control algorithms (5.10) and (5.11) where the saturation is considered.

Remark 5.2.2 *From practical point view, it is important for the local controller at the intermediate VP switches to be open-loop stable since an open-loop unstable local controller may destroy the system's stability if its feedback link is broken.*

5.2.3 System Steady Behavior

We would like to investigate the system behavior at steady states. Its analysis would give us an idea on buffer design and fairness.

For VP switch i, let x_i^s, u_i^s, u_{ji}^s, λ_i^s λ_{ji}^s, d_i^s and $d_i'^s$ be the steady state values corresponding to $x(n)$, $u_i(n)$, $u_{ji}(n)$, $\lambda_i(n)$, $\lambda_{ji}(n)$, $d_i(n)$ and $d_i'^s(n)$ respectively in equations (2.12), (5.13), (5.14) and (5.24). For simplicity, we consider that the virtual path has one single persistently link-congested VP switch I. This implies that the traffic between VP switch i and VP switch $(i+1)$ does not exceed the link capacity Γ_i^* for $i = 1, 2, \cdots, I-1$, while the traffic may exceed the link capacity between VP switch I and VP switch $(I+1)$. Thus we have

$$\lambda_i^s + \Delta d_i^s < \Gamma_i^*, \quad i = 1, 2, \cdots, I-1$$

$$\lambda_I^s + \Delta d_I^s \geq \Gamma_I^* .$$

Then as $n \to \infty$, the steady state equations for VP i $(i = 1, 2, \cdots, I)$ are described by

$$
\begin{aligned}
x_i^s &= Sat_{K_i}\{x_i^s + u_{i-1}^s + \sum_{j=1}^{L_i^s} u_{ji}^s + d_i^s + \Delta d_{i-1}^s - \hat{\mu}_i^s\}, \\
\mu_i^s &= \begin{cases} Sat_{\Gamma_i}\{\lambda_i^s + \Delta d_i^s + d_i'^s\}, & i \leq I-1 \\ \\ Sat_{\Gamma_I}\{\Gamma_I^* + d_I'^s\} \end{cases} \\
u_{i-1}^s &= -Sat_{\Gamma_{i-1}}\{\frac{\epsilon_i M_i^s}{N} x_i^s\}, \quad \lambda_{i-1}^s = \mu_{i-1} + u_{i-1}^s \\
u_{ji}^s &= -Sat_{\mu_{ji}}\{\frac{\epsilon_i}{N} x_i^s\}, \quad \lambda_{ji}^s = \mu_{ji} + u_{ji}^s, \quad j = 1, 2, \cdots, L_i^s
\end{aligned}
\tag{5.25}
$$

where $u_0^s = \lambda_0^s = 0$, and M_i^s and L_i^s are the steady values of M_i and L_i respectively as $n \to \infty$.

The following result gives the solution to the above equations.

Theorem 5.2.2 *Assume that switch I is persistently link-congested, and that switch i is not persistently link-congested, $i = 1, 2, \cdots, I-1$. Let $\hat{d}_i^s := d_i^s + \Delta d_{i-1}^s$ be the total input of uncontrolled traffic to VP switch i ($i = 1, 2, \cdots, I$), and let $\mu_i^s := \sum_{j=1}^{M_i^s} \mu_j^i$. Then the steady behavior of VP switch i described by (5.25) is given by*

a) if $\hat{d}_i^s < \hat{\mu}_i^s$,

$$x_i^s = 0, \quad u_{i-1}^s = 0, \quad \lambda_{i-1}^s = \mu_{i-1}^s, \quad u_{ji}^s = 0, \text{ and } \lambda_{ji}^s = \mu_{ji}, \quad j = 1, 2, \cdots, L_i^s$$

b) if $\hat{\mu}_i^s \leq \hat{d}_i^s \leq \hat{\mu}_i^s + min\{(M_i^s + L_i^s)\mu_i^0, \ \frac{\epsilon_i K_i (M_i^s + L_i^s)}{N}\}$,

$$\begin{aligned}
x_i^s &= \frac{N}{\epsilon_i (M_i^s + L_i^s)}(\hat{d}_i^s - \hat{\mu}_i^s) \\
u_{i-1}^s &= -\frac{M_i^s}{(M_i^s + L_i^s)}(\hat{d}_i^s - \hat{\mu}_i^s) \\
\lambda_{i-1}^s &= \mu_{i-1} + u_{i-1}^s \\
u_{ji}^s &= -\frac{1}{(M_i^s + L_i^s)}(\hat{d}_i^s - \hat{\mu}_i^s) \\
\lambda_{ji} &= \mu_{ji} + u_{ji}^s, \quad j = 1, 2, \cdots, L_i^s
\end{aligned} \tag{5.26}$$

where $\mu_i^0 := min\{\mu_{i-1}^s / M_i^s, \mu_{ji}; \ \ j = 1, 2, \cdots, L_i^s\}$.

Proof. First, consider the case where $\hat{d}_i^s < \hat{\mu}_i^s$. By definition, $u_{i-1}(n) \leq 0$ and $u_{ji}(n) \leq 0$, for all n. It follows that $u_{i-1}^s + \sum_{j=1}^{L_i^s} u_{ji}^s + \hat{d}_i^s - \hat{\mu}_i^s < 0$. Then we can show that we always have that $x_i^s + u_{i-1}^s + \sum_{j=1}^{L_i^s} u_{ji}^s + \hat{d}_i^s - \hat{\mu}_i^s \leq 0$, and hence $x_i^s = 0$ by definition.

By contradiction, assume that $0 < x_i^s + u_{i-1}^s + \sum_{j=1}^{L_i^s} u_{ji}^s + \hat{d}_i^s - \hat{\mu}_i^s \leq K_i$. It follows from (5.25) that $x_i^s = x_i^s + u_{i-1}^s + \sum_{j=1}^{L_i^s} u_{ji}^s + \hat{d}_i^s - \hat{\mu}_i^s$. It results in $u_{i-1}^s + \sum_{j=1}^{L_i^s} u_{ji}^s + \hat{d}_i^s - \hat{\mu}_i^s = 0$, which is not possible.

If $x_i^s + u_{i-1}^s + \sum_{j=1}^{L_i^s} u_{ji}^s + \hat{d}_i^s - \hat{\mu}_i^s > K_i$, we then have that $x_i^s = K_i$ due to saturation. From (5.25), it is required that $K_i + u_{i-1}^s + \sum_{j=1}^{L_i^s} u_{ji}^s + \hat{d}_i^s - \hat{\mu}_i^s > K_i$, which is again not possible. Thus we always have that $x_i^s = 0$. It then follows from the fourth and sixth equations in (5.25), $u_{i-1}^s = -Sat_{\Gamma_{i-1}}\{\frac{\epsilon_i M_i^s}{N_i} x_i^s\} = 0$, and $u_{ji}^s = -Sat_{\mu_{ji}}\{\frac{\epsilon_i}{N_i} x_i^s\} = 0$. Thus by definition, $\lambda_{i-1}^s = \mu_{i-1}^s = \sum_{j=1}^{M_i^s} \mu_j^i$ and $\lambda_{ji} = \mu_{ji}$, $j = 1, 2, \cdots, L_i^s$.

Now consider the case b). Assume that the system operates in the linear region except the equation for μ_i^s. Then we have

$$\begin{aligned}
x_i^s &= x_i^s + u_{i-1}^s + \sum_{j=1}^{N_i} u_{ji}^s + \hat{d}_i^s - \hat{\mu}_i^s \\
u_{i-1}^s &= -\frac{\epsilon_i M_i^s}{N_i} x_i^s \\
u_{ji}^s &= -\frac{\epsilon_i}{N_i} x_i^s, \quad j = 1, 2, \cdots, L_i^s
\end{aligned}$$

which give that $x_i^s = \frac{N_i}{\epsilon_i (M_i^s + L_i^s)}(\hat{d}_i^s - \hat{\mu}_i^s)$. It turns out that $u_{i-1}^s = -\frac{M_i^s}{(M_i^s + L_i^s)}(\hat{d}_i^s - \hat{\mu}_i^s)$, and $u_{ji}^s = -\frac{1}{(M_i^s + L_i^s)}(\hat{d}_i^s - \hat{\mu}_i^s)$. Thus the proof is completed on noting that the conditions $0 \le x_i^s \le K_i$, $-\mu_{i-1} \le u_{i-1}^s \le 0$, and $-\mu_{ji} \le u_{ji}^s \le 0$, $j = 1, 2, \cdots, L_i^s$, are needed to maintain the system operating in the linear region, and these conditions can be guaranteed by $\hat{\mu}_i^s \le \hat{d}_i^s \le \hat{\mu}_i^s + min\{(M_i^s + L_i^s)\mu_i^0, \frac{\epsilon K_i (M_i^s + L_i^s)}{N_i}\}$. ¶

Remark 5.2.3 *In order to design a lossless data network, it is required that the buffer size K_i is at least greater than $\frac{N}{\epsilon_i (M_i^s + L_i^s)}(\hat{d}_i^s - \hat{\mu}_i^s)$. Clearly, the buffer occupance x_i^s in (5.26) will become large if N is large, or ϵ_i, M_i^s and L_i^s are small.*

Now we assume that VP switch i ($i = 1, 2, \cdots, I-1$) is persistently congestion free. This implies that both link capacity and node capacity are not exceeded. So we have that

$$\lambda_i^s + \Delta d_i^s + d_i'^s \le \mu_i \ .$$

Then we have from (5.25) that

$$\mu_i^s = \lambda_i^s + \Delta d_i^s + d_i'^s \ .$$

Let $\hat{\mu}_i^c = -(\lambda_i^s - \mu_{i-1}^s - \sum_{j=1}^{L_i^s} \mu_{ji})$. On noting that the total input of uncontrolled traffic to VP switch i is equal to the total output of uncontrolled traffic from VP switch i, we obtain

$$d_i^s + \Delta d_{i-1}^s = d_i'^s + \Delta d_i^s \ .$$

It then follows from (5.25) that

$$x_i^s = Sat_{K_i}\{x_i^s + u_{i-1}^s + \sum_{j=1}^{L_i^s} u_{ji}^s + \hat{\mu}_i^c\} \ .$$

This implies that the buffer occupancy of a congestion free VP switch is independent of the uncontrolled traffic.

Corollary 5.2.1 *Assume that switch I is persistently link-congested, and that switch i is persistently congestion free, $i = 1, 2, \cdots, I-1$. Also assume that $\lambda_i^s + \Delta d_i^s + d_i'^s \le \mu_i$. Then the steady behavior of congestion-free VP switch i ($i \le I-1$) can be given by*

a) if $\hat{\mu}_i^c < 0$,

$$x_i^s = 0, \quad u_{i-1}^s = 0, \quad \lambda_{i-1}^s = \mu_{i-1}^s, \quad u_{ji}^s = 0, \ and \ \lambda_{ji}^s = \mu_{ji}, \quad j = 1, 2, \cdots, L_i^s$$

b) if $0 \le \hat{\mu}_i^c \le min\{(M_i^s + L_i^s)\mu_i^0, \ \frac{\epsilon_i K_i (M_i^s + L_i^s)}{N}\}$,

$$\begin{aligned}
x_i^s &= \frac{N}{\epsilon_i (M_i^s + L_i^s)} \hat{\mu}_i^c \\
u_{i-1}^s &= -\frac{M_i^s}{(M_i^s + L_i^s)} \hat{\mu}_i^c \\
\lambda_{i-1}^s &= \mu_{i-1}^s + u_{i-1}^s \\
u_{ji}^s &= -\frac{1}{(M_i^s + L_i^s)} \hat{\mu}_i^c \\
\lambda_{ji} &= \mu_{ji} + u_{ji}^s, \quad j = 1, 2, \cdots, L_i^s \ .
\end{aligned} \tag{5.27}$$

Proof. This result can be established by replacing the item $(\hat{d}_i^s - \hat{\mu}_i^s)$ in (4.26) with $\hat{\mu}_i^c$.

Since VP switch $(i-1)$ has M_i^s VCs going to VP switch i, it is desirable that each of VCs can obtain the same amplitude of feedback to adjust its transmission rate. Let ${}_j u_{i-1}^s$ be the feedback gain to the jth VC in the VP switch $(i-1)$. We then define

$$
\begin{aligned}
{}_ju_{i-1}^s &:= \tfrac{1}{M_i^s}u_{i-1}^s, \quad j = 1,2,\cdots,M_i^s, \\
p_i &:= -\frac{1}{M_i^s + L_i^s}(\hat{d}_i^s - \hat{\mu}_i^s), \quad i = 1,2,\cdots,I.
\end{aligned}
\tag{5.28}
$$

It thus follows from (5.26) that

$$
{}_ju_i^s = u_{ki}^s = p_i, \quad j = 1,2,\cdots,M_i^s, \quad k = 1,2,\cdots,L_i^s\ . \tag{5.29}
$$

This shows that each VC of $(M_i^s + L_i^s)$ VCs flowing into VP switch i obtains the same feedback gain p_i from VP switch i. Additionally, let

$$
\mu_i^j = \theta_j, \quad j = 1,2,\cdots,M_i^s
$$

$$
\mu_{ji} = \theta_{j+M_i^s}, \quad j = 1,2,\cdots,L_i^s.
$$

This implies that each VC keeps the same maximum transmission rate from its source to its destination. Then for VP switch i, it follows from (5.27) and (5.29) that

$$
\begin{aligned}
{}_j\lambda_{i-1}^s &= \theta_j + p_i, \quad j = 1,2,\cdots,M_i^s \\
\lambda_{ji}^s &= \theta_{j+M_i^s} + p_i, \quad j = 1,2,\cdots,L_i^s\ .
\end{aligned}
$$

If VP switch i $(i = 1,2,\cdots,I-1)$ is not persistently link-congested, but has no loss of controlled packets, i.e., $K_i \geq \dfrac{N}{\epsilon_i(M_i^s + L_i^s)}(\hat{d}_i^s - \hat{\mu}_i^s)$, it then follows from the flow balance principle that

$$
\lambda_i^s = \lambda_{i-1}^s + \sum_{j=1}^{L_i^s}\lambda_{ji}^s, \quad i = 1,2,\cdots,I-1,
$$

where $\lambda_0^s = 0$.

On noting that

$$
\begin{aligned}
\lambda_i^s &= \sum_{j=1}^{M_{i+1}^s} {}_j\lambda_i^s \\
&= \sum_{j=1}^{M_{i+1}^s}\theta_j + M_{i+1}^s p_{i+1}
\end{aligned}
$$

and that

$$
\begin{aligned}
\lambda_{i-1}^s + \sum_{j=1}^{M_i^s}\lambda_{ji}^s &= \sum_{j=1}^{M_i^s}\theta_j + M_i^s p_i + \sum_{j=1}^{L_i^s}\theta_{j+M_i^s} + L_i^s p_i \\
&= \sum_{j=1}^{M_{i+1}^s}\theta_j + M_{i+1}^s p_i
\end{aligned}
$$

where $M_{i+1}^s = M_i^s + L_i^s$, we then obtain that

$$p := p_i = p_{i+1}, \quad i = 1, 2, \cdots, I-1$$

which yields the following theorem:

Theorem 5.2.3 *(Fairness) Assume that VP switch I is persistently link-congested, and that VP switch i is not persistently link-congested, $i = 1, 2, \cdots, I-1$. Also assume that VP switch i has no loss of controlled packets, $i = 1, 2, \cdots, I-1$. Then the fairness property is achieved in the sense that every VC obtains the same feedback gain p along the virtual path.*

Remark 5.2.4 *It is observed from Theorems 5.2.2 and 5.2.3 that the traffic rate at each source node is regulated based on the same feedback gain p which is only dependent on the uncontrolled traffic $\hat{d}_i^s$. This shows that the source nodes are fairly treated, and they can share the switch's bandwidth without interference to each other. In particular, if all the VCs are given the same maximum allocated rate along the virtual path, i.e.,*

$$\mu_i^j = \mu_{ki} = \theta, \quad i = 1, 2, \cdots, H, \quad j = 1, 2, \cdots, M_i^s, \quad k = 1, 2, \cdots, L_i^s,$$

then they have equal share of the bandwidth of the virtual path:

$$\lambda_{ij} = \theta + p, \quad i = 1, 2, \cdots, H, \quad j = 1, 2, \cdots, L_i^s.$$

5.3 Implementation of the Proportional Controller

The controller (5.10) and (5.11) can be distributively implemented in the source nodeso, the switching nodes and the destination node. The normalized one-hop feedback propagation delays $\tau_{i,i-1}$ and τ_{ij} need to be estimated. The other parameters $\hat{\tau}_i$, $\hat{\tau}_j^i$, and N_i and ϵ_i should also be provided in order for the intermediate switching nodes and the external sources to calculate the their data transmission rates respectively.

The resource management (RM) cells are used to carry the values of four components: (1) the transmission time of a RM cell in the hop source node, (2) the transmission time of a RM cell in the hop destination node, (3) the number of active controlled VCs and (4) the buffer occupancy in the hop destination node. The transmission time of a RM cell in the hop source node is used to measure the one-hop loop delay τ_i or τ_j^i, and the transmission time of a RM cell in the hop destination node is used to calculate the one-hop feedback delay $\tau_{i,i-1}$ or τ_{ij}.

When VP switch i receives the RM cells generated from VP switch $(i-1)$ or its external source nodes at every sampling interval T, it writes its buffer occupancy and the time before the RM cell is send back to its source into the RM cell and then sends the RM cell back to VP switch i or the external source node. The following procedures are used to obtain the parameters required in the controller (5.10) and (5.11).

A. Determining $\tau_{i,i-1}$ and τ_{ij}:

The value of $\tau_{i,i-1}$ is estimated by the difference between the time the RM cell arrives VP switch $(i-1)$ and the time stamp recorded in the RM cell by VP switch i. The value of τ_{ij} is estimated by the difference between the time the RM cell arrives the external source node j and the time stamp recorded in the RM cell by VP switch i. These one-hop feedback delays are usually constant since the RM cells have high priority for processing and transmission.

B. Determining $\hat{\tau}_i$ and $\hat{\tau}_j^i$:

Using the time stamp recorded in the RM cell by the one-hop source node, the one-hop loop delay τ_i between two VP switches and τ_j^i between VP switch i and its external node j are determined by the difference between the time the RM cell returns to its source and the time stamp recorded in the RM cell. Then the value of $\hat{\tau}_i$ is chosen such that $\hat{\tau}_i + \tau_i = \tau_{max}^i$, and the value of $\hat{\tau}_j^i$ is chosen such that $\hat{\tau}_j^i + \tau_j^i = \tau_{max}^i$, where τ_{max}^i is a uniform delay applied for all VCs going to VP switch i.

C. Determining N_i and ϵ_i:

Since $N_i > M_i + L_i$ is usually large, it is divided into a set of integers $\{N_{i,l};\ l = 1, 2, \cdots, k_i\}$ with $N_{i,1} \leq N_{i,2} \leq \cdots \leq N_{i,k_i}$. The number of active controlled VCs stored in the RM cell is used as the estimate of the current number of active controlled VCs. Then the values of $(N_i,\ \epsilon_i)$

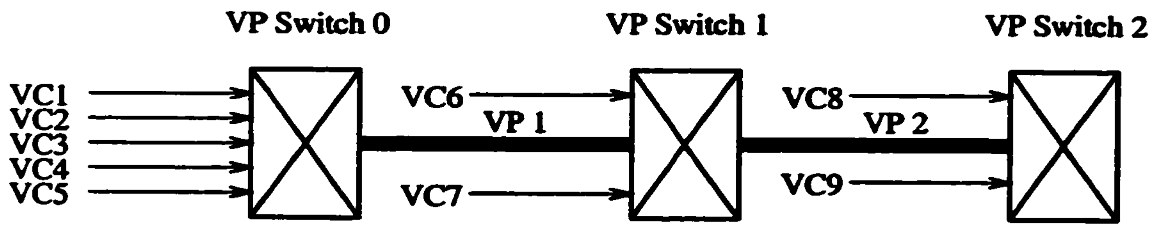

Fig. 26. Simulation model

can be adaptively adjusted by $(N_{i,l},\ \epsilon_{i,l})$, where $N_{i,l}$ is chosen to be close to but larger than the estimated $M_i + L_i$, and $\epsilon_{i,l}$ is chosen such that the characteristic equation of the buffer occupancy

$$\Delta(z) = z^{\tau}(z-1) + \frac{\epsilon_{i,l}(M_i + L_i)}{N_{i,l}}$$

is a stable polynomial for all $M_i + L_i < N_{i,l}$. These values of $(N_{i,l},\ \epsilon_{i,l})$ can be obtained by running the MATLAB tool [54].

5.4 Simulation

The simulation results on the controller (5.13), (5.14) and (5.24) would be presented here.

Since our hop-by-hop flow controller regulates the VP switch's service rate over time, we are particularly interested in analyzing both the transient and steady behaviors of the network. Transient behaviors such as the duration of response time and the maximum transient buffer occupancy at each VP switch are the main concerns in performance analysis.

The example is based on the model described in Figure 26 with three VP switches. Table 4 gives respectively the link delay from VP switch $i-1$ to VP switch i, the link delay from VP switch i to VP switch $i-1$, and the maximum link transmission rate assigned to each VC. It is also assumed that the node capacity $\Gamma_i/T = 180Mbps$, the link capacity $\Gamma_i/T = 180Mbps$, uncontrolled traffic $d_i^s = 0$, where $i = 1, 2, 3$, and the sampling time $T = 1msec$.

VP Switch i	$i=1$					$i=2$			$i=3$		
	VC1	VC2	VC3	VC4	VC5	VC6	VC7	VP1	VC8	VC9	VP2
τ'_{ji} (msecs)	1	2	2	3	3	1	3		5	5	
τ'_{ij} (msecs)	2	3	3	3	4	3	3		5	6	
$\tau'_{i,i-1}$ (msecs)								3			4
$\tau'_{i-1,i}$ (msecs)								3			3
μ_{ji}/T (Mbps)	40	24	32	20	24	40	24		28	36	

Table 4. Network's parameters along the single VP

It can be seen from Figures 27a, 28a and 29a that the numbers of VCs in switch 1, 2 and 3 are increased from 0 to 5, to 7 and to 9 respectively. We have that

$$M_1^s = 0, \quad M_2^s = 5, \quad M_3^s = 7,$$

$$L_1^s = 5, \quad L_2^s = 2, \quad L_3^s = 2.$$

So the total number of VCs in the virtual path is $\sum_{i=1}^{3} L_i^s = 9$. From Table 4, We then have that

$$\mu_1^s/T = \sum_{j=1}^{L_1^s} \mu_{j1}/T = 140(Mbps) \ ,$$

$$\mu_2^s/T = \mu_1^s/T + \sum_{j=1}^{L_2^s} \mu_{j2}/T = 204(Mbps) \ ,$$

$$\mu_3^s/T = \mu_2^s/T + \sum_{j=1}^{L_3^s} \mu_{j3}/T = 268(Mbps) \ .$$

It is known from [10], [17] and [26] that in order to obtain high utilization, all VCs in Table 4 would be allowed to transmit data at their maximum assigned rate μ_{ji} if the VP switches are not congested. But if no control is applied on these VCs, it is obvious that VP switch 2 and VP switch 3 may be congested since $\mu_2^s > \Gamma_2$ and $\mu_3^s > \Gamma_3$.

Now we apply the controller given in (5.10) and (5.11) to prevent the virtual path from congestion with the parameters:

$$\hat{\tau}_1^1 = 4, \quad \hat{\tau}_2^1 = 2, \quad \hat{\tau}_3^1 = 2, \quad \hat{\tau}_4^1 = 1, \quad \hat{\tau}_5^1 = 0,$$

$$\hat{\tau}_2^1 = 1, \quad \hat{\tau}_2^2 = 0,$$

$$\hat{\tau}_3^1 = 5, \quad \hat{\tau}_3^2 = 4,$$

$$\epsilon = \epsilon_i = 0.08, \quad i = 1, 2, 3,$$

$$N = 10.$$

It can be observed from Figure 29 that the congestion occurs just after two VCs (VC8 and VC9) are added into VP switch 3. The buffer occupancy x_3 is increased very quickly. Then it can be seen from Figure 28b that VP switch 3 enforces VP switch 2, VC8 and VC 9 to reduce their transmission rates, which in turn increase the buffer occupancy x_2 since at this moment VP switch 1 and other external nodes do not obtain the congestion information. Similarly the congestion information in VP switch 3 is propagated through buffer occupancy x_2 in VP switch 2 to VP switch 1, VC5 and VC6 with the effect of reducing their transmission rates. Finally the congestion information in VP switch 3 is propagated through buffer occupancy x_1 in VP switch 1 to VCi, $i = 1, 2, 3, 4, 5$ so that their transmission rates are reduced. The whole process takes about 0.02 second.

It follows from Theorem 5.2.3 and (5.28) that the proposed controller has the fairness property. The feedback gain is given by

$$p := p_i = -9.7778, \quad i = 1, 2, 3.$$

We then have the following results:

$$\lambda_1^s/T = 91.11(Mbps), \quad \lambda_2^s/T = 135.55(Mbps), \quad \lambda_3^s/T = 180(Mbps),$$

$$x_1^s = x_2^s = x_3^s = 1.2222(Mb).$$

All above values can be verified by the simulation results (b) and (d) in Figure 27, 28 and 29 respectively.

5.5 Concluding Remarks

In this chapter, a discrete-time fluid model was used to model a virtual connection and a virtual path which go through a number of intermediate switching nodes. Each node can aggregate both guaranteed service traffic and best-effort service traffic. We started to design a traffic controller for a simple case of one virtual connection. Then such a controller was extended to the case of a virtual path along the VP switching network.

The traffic controller is geographically distributed over the intermediate VP switches and source nodes. Each local controller can determine the maximum allowed rate at which the source can transmit data to a VP switch and a VP switch can transmit data to its down-stream VP switch. We have analyzed a robust congestion controller in the sense that the controller is not sensitive to the change of number of VCs during the network operation. With this controller applied, we demonstrate that the virtual path is asymptotically stable and exhibits a good transient behavior. We also demonstrate that the controller provides high utilization of network and is fair to each VC.

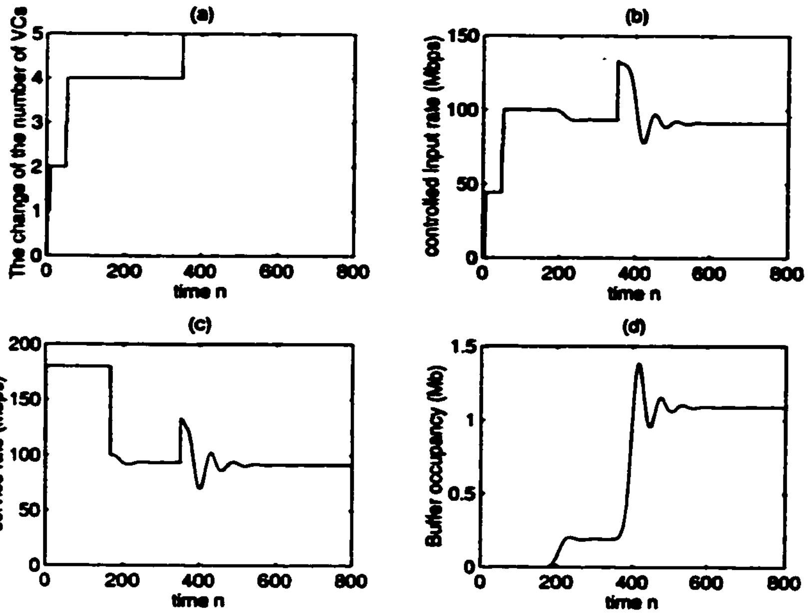

Fig. 27 Performance in VP switch 1

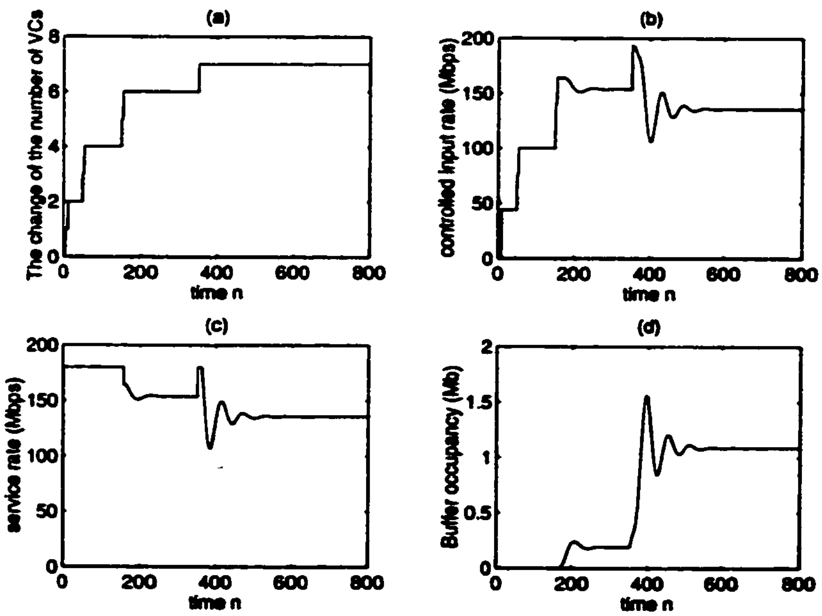

Fig. 28 Performance in VP switch 2

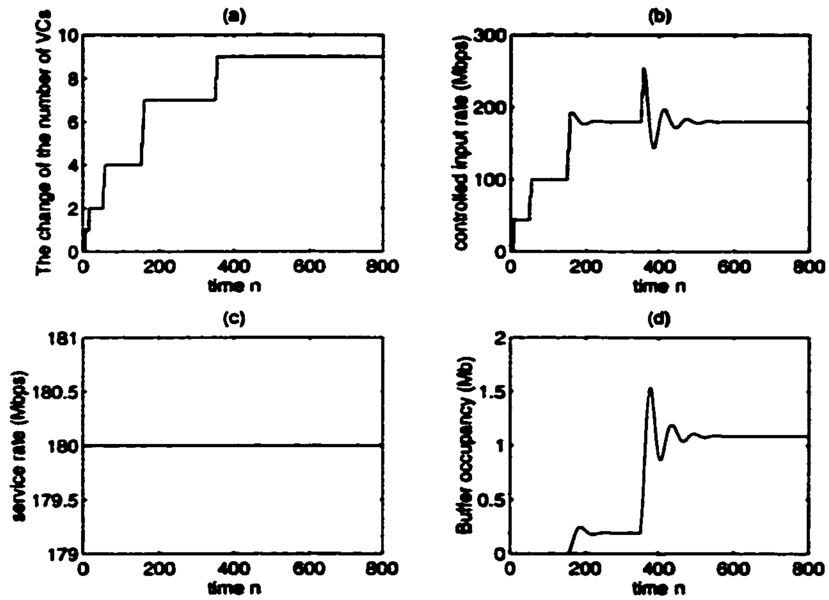

Fig. 29 Performance in VP switch 3

Chapter 6

Conclusions

In this thesis, we have obtained some fundamental results on the continuous-time and discrete-time traffic controllers for the high speed networks that can accommodate both guaranteed service and best-effort service traffic based on the continuous and discrete time models respectively. These traffic controllers are geographically distributed over the source nodes, and each local controller at a source node need only to determine the maximum rate at which the source is allowed to transmit data to the network.

Through an analysis using the Lyapunov approach in the continuous-time fluid model, we have designed an end-to-end controller that can stabilize the network with a bounded queuing delay in each node. Two types of controllers are designed. One is the proportional controller which has a very simple control structure. The other one is the proportional and integral (PI) controller which can greatly reduce the deviation of mean buffer occupancy to the specified buffer threshold. It also has faster response to the change of traffic load in the network than the simple proportional controller. The major advantage of these two controllers is that they are not sensitive to the variance of propagation delays, queuing delays and processing delays in the network. Therefore they can be used a long haul end-to-end traffic control.

Through an analysis by using the z-transform approach in the discrete-time fluid model, we have proposed a class of end-to-end and hop-by-hop controllers that are robust in the sense that the controllers are insensitive to the change of number of VCs during the network operation, and to the variation of propagation delays, queuing delays and other processing delays. With this controller applied to an end-to-end controlled network, we demonstrate that the network is piecewise asymptotically stable and exhibits a good transient behavior. With this controller applied to a hop-by-hop controlled network, we demonstrate that the response time to the load change and size of buffer occupancy are reduced greatly, and also overhead traffic along the feedback path is reduced greatly. Therefore, these types of control algorithms can be applied to a high-speed network requiring fast response to the load change while allowing small perturbation on delays.

6.1 Future Works

In this thesis, we solved some fundamental problem existed in the current congestion control approaches such as stability and variable delays. However, there are still many problems left for continuous development on our new proposed congestion controllers. For future work, we can extend our study of the traffic control to the following items:

- fairness for multiple congestion nodes; if there exist two congested nodes and upstream congested node is worse than the downstream node, then our fairness property applied to the virtual channels going through the upstream congested node is not applied to virtual channels which only go through the downstream congested node.

- saturation problem; all of our results in this thesis are based on the assumption that network is operating on the linear region. Thus, it is desirable to have an engineering guidance to avoid saturation problem. For example, a guidance to choose the upper bound of buffers, threshold for the congestion level, and a slow-start mechanism. It is also desirable to have a systematic analysis on what impact would be on the network when the saturation occurs.

- a PID type of controller which can achieve both good dynamic performance and good steady performance, i.e., to increase both gain margin and phase margin of the system.

- the optimization of all parameters involved in the proposed control algorithms.
- a hybrid approach to integrate the congestion control and routing technique.
- a practical protocol which can describe and implement all proposed algorithms according to the ATM forum and other industrial standards.

Bibliography

[1] "Traffic Management Specification", Version 4.0, The ATM Forum, April 1996.

[2] C. Q. Yang and A.A.S. Reddy, "A taxonomy for congestion control algorithms in packet switching networks," IEEE Network, pp. 34-45, 1995.

[3] C.G. Omidyar and G. Pujolle, "Introduction to flow and congestion control," IEEE Communication Magazine, pp. 30-32, November, 1996.

[4] R. Jain, S. Kalyanaraman, S. Fahmy, and R. Goyal, "Source behavior for ATM ABR traffic management: an explanation," IEEE Communication Magazine, pp. 50-57, November, 1996.

[5] K.Y. Siu and H.Y. Tzeng, "Intelligent congestion control for ABR service in ATM networks," ACM Comp. Commun. Rev., vol. 35, pp. 81-106, 1995.

[6] H. Chen and A. Mandelbaum, "Discrete flow networks: bottleneck analysis and fluid approximation," Mathematics of Operations Research, vol. 16, no.2, pp. 408-447, 1991.

[7] K. Fendick, M. Rodrigues, and A. Weiss, "Analysis of a rate-based control strategy with delayed feedback," Proc. ACM SIGCOMM'92, pp. 136-148, 1992.

[8] K. Fendick and M. Rodrigues,"Asymptotic analysis of adaptive rate control for diverse sources with delayed feedback," IEEE Trans. Information Theory, vol. 40, no. 6, pp. 2008-2025, 1994.

[9] W.P. Wang, D. Tipper, and S. Banerjee, "A simple approximation for modeling nonstationary queues," IEEE INFOCOM, vol.1, pp. 255-262, 1996. Also to appear in *Int. J. Commun. Syst.*, 2001.

[10] S. Keshav, "A control-theoretic approach to flow control," Proc. ACM SIGCOMM'91, pp. 3-15, 1991.

[11] J.C. Bolot and A.U. Shankar, "Dynamic behavior of rate-based flow control mechanism," Proc. ACM SIGCOMM, pp. 35-49, 1990.

[12] J.C. Bolot and A.U. Shankar, "Analysis of a fluid approximation to flow control dynamics," Proc. IEEE INFOCOM, pp. 2398-2407, 1992.

[13] L. Benmohamed and S.M. Meekov, "Feedback control of congestion in packet switching networks: The case of a single congested node," IEEE/ACM Trans. Networking, vol. 1, pp. 693-707, 1993.

[14] R. Izmailov, "Delayed feedback control algorithms in high-speed networks," Proc. IEEE GLOBECOM, pp. 1040-1044, 1996.

[15] H. Kanakia, P. Mishra and A. Reibman, "An adaptive congestion control scheme for real-time packet video transport," Proc. ACM SIGCOMM'93, 1993.

[16] K. Park, "Warp control: a dynamically stable congestion protocol and its analysis," Proc. ACM SIGCOMM'93, pp. 137-147, 1993.

[17] H. Ohsaki et al., "Rate-based congestion control for ATM Networks," ACM Comp. Commun. Rev., vol. 35, pp. 60-72, 1995.

[18] S. Mascolo, D. Cavendish, and M. Gerla, "ATM rate based congestion control using a Smith pridictor: an EPRCA implementation," Proc. IEEE INFOCOM, vol.2, pp. 569-576, 1996.

[19] R. Krishnan "Rate-based control schemes for ABR traffic - design priciples and performance comparison," Computer Networks and ISDN Systems, vol. 29, pp. 583-593, 1997.

[20] A. Arulambalam and X. Chen, "Allocating fair rates for available bit rate service in ATM networks," IEEE Communication Magazine, pp. 92-100, November, 1996.

[21] D. Cavendish et al., "Proportional rate-based congestion control under long propagation delay," Int. J. Communication Systems, vol. 8, pp. 79-89, 1995.

[22] Y. Zhao and S.Q. Li, "Feedback control of multiloop ABR traffic in presence of CBR/VBR traffic transmission," Proc. ICC'96 conference, pp. 1717-1782, 1996.

[23] Y. Zhao, S.Q. Li and S. Sigarto, "A linear dynamic model for design of stable Explicit-Rate ABR control schemes", Proc. IEEE INFOCOM, 1997.

[24] F. Bonomi, D. Mitra and J.B. Seery, "Adaptive algorithms for feedback-based flow control in high-speed, wide-area ATM networks," IEEE J. Select. Areas Comm., vol.13, pp. 1267-1283, 1995.

[25] M. Hluchyj and N. Yin, "On closed-loop rate control for ATM networks," Proc. IEEE INFOCOM, pp. 99-108, 1994.

[26] Y. Gong and K. Lee, "Dynamic traffic control using feedback and traffic prediction in ATM networks," Proc. IEEE INFOCOM, pp. 91-98, 1994.

[27] I. Iliadis, "A new feedback congestion control policy for long propagation delays," IEEE J. Select. Aeras Commun., vol. 13, pp. 1284-1295, 1995.

[28] F. Bonomi and K. Fendick, "The rate-based flow framework for the available bit rate ATM service," IEEE Network Mag., vol. 9, pp. 25-39, 1995.

[29] H. Kung, T. Blackwell and A. Chapman, "Credit-based flow control for ATM networks: Credit update protocol, adaptive credit allocation, and statistical multiplexing," Proc. SIGCOMM'94, pp. 101-114, 1994.

[30] D. Mitra and J. Seery, "Dynamic adaptive windows for high speed data networks: theory and simulations," Proc. ACM SIGCOMM'90, pp. 30-37, 1990.

[31] B. Xu and Y. Liu, "An improved Razumikhin-type theorem and its applications," IEEE Trans. AC, vol. 39, no. 4, pp. 839-841, 1994.

[32] P.P. Mishra and H. Kanakia, "A hop by hop rate based congestion control scheme," in *Proc. ACM SIGCOMM'92*, pp. 112-123, 1992.

[33] P.P. Mishra, H. Kanakia, and S.K. Tripathi, "On hop-by-hop rate-based congestion control," IEEE/ACM Trans. Networking, vol. 4, pp. 224-239, 1996.

[34] K.T. Ko, P.P. Mishra and S.K. Tripathi, "Interaction among virtual circuits using predictive congestion control," Computer Networks and ISDN Systems, vol. 25, pp. 681-699, 1993.

[35] G. Ramamurthy and B. Sengupta, "A predictive hop-by-hop congestion control policy for high speed networks," in Proc. IEEE INFOCOM'93, vol. 4, pp. 1033-1041, 1993.

[36] Shivkumar Kalyanaraman, Raj Jain, Jianping Jiang, Rohit Goyal, and Sonia Fahmy, "Virtual source/virtual destination (VS/VD): design consideration," ATM Forum/96-1759, December, 1996.

[37] B. Vandalore, S. Jain, R. Goyal, and M. Goyal, "A definition of general weighted fairness and its support in explicit rate switch algorithms," *Proceedings of ICNP'98*, pp.22-30, Oct. 1998.

[38] T. Sudo, M. Okuda, K. Nakamichi and T. Ishihara, "Analysis of ABR behavior over ATM-based broadband access networks," *IEEE Trans. in Communications*, vol. E81-B, No.2, pp.402-408, 1998.

[39] S. Floyd, M. Handley etc. "Equation-based congestion control for unicast applications," in *ACM SIGCOMM'2000*, Aug. 2000.

[40] N. Golmie, M. Corner, J. Liebeherr, and D. Su, "ATM traffic control in hybrid fiber-coax networks - Problems and solutions," Computer Communications, Vol. 22, No. 1 (1999), pp 30-39.

[41] E. Baydal, P. Lopez, and J. Duato, "A simple and efficient mechanism to prevent saturation in wormhole networks. In Proceedings of *14th International Parallel and Distributed Processing Symposium*, pages 617–622, 2000

[42] M. Thottethodi, A. R. Lebeck, and S. S. Mukherjee. *SelfTuned congestion control for multiprocessor networks*. Technical Report CS-2000-15, Duke University, November 2000.

[43] Morabito G., Akyildiz, I.F., Palazzo, S., "ABR t raffic control for satellite ATM networks", *IEEE Globecom'99 Conference*, Rio De Janeiro, December 1999.

[44] L. Kleinrock, *Queueing Systems. Volume II: Computer Application*, Wiley, 1976.

[45] J. Filipiak, *Modeling and control of dynamic flows in communication networks*, Springer-Verlag, 1988.

[46] K. Ogata, "Discrete time control system," Prentice Hall, 1987.

[47] J.K. Hale, *Theory of Functional Differential Equations*. New York, Springer-Verlag, 1997.

[48] H. Kevin and O. Yang, "ABR controllability under sharp bandwidth changes and long propogation delays," OPNETworks 99, 1999.

[49] H. Zhang, O. Yang and H. Mouftah, "Adaptive rate-based congestion control in ATM switching networks," *Computer Syst. Sci. & Eng.*, vol 6, pp. 361-367, 1996.

[50] H. Zhang, O. Yang and H. Mouftah, "A control policy for the stabilization of ene-to-end congestion: Multiple sources case," in *Proc. of the 34th Annual Allerton Conf. on Communication, control, and computing*, pp. 1-9, 1996.

[51] H. Zhang, O. Yang and H. Mouftah, "Design of robust congestion controllers for ATM networks," in *Proc. IEEE INFOCOM'97*, pp. 302-309, 1997, also in the CCG Report, 1997.

[52] H. Zhang, O. Yang and H. Mouftah, "Discrete-time model of a hop-by-hop controller," presented in *Annual Conf. OR and Info. Tech. Management*, May 27, 1997, also in the CCG Report, 1997.

[53] H. Zhang, O. Yang and H. Mouftah, "A hop-by-hop flow controller for a virtual path," *Computer Networks and ISDN Systems*, vol. 32, pp. 99-119, 2000.

[54] "MATLAB 5.3 User Guide," ISBN 0-13-272550-9, Prentice-Hall, Inc.

[55] "OPNET Modeler Manuals," OPNET Version 3.5, MIL 3 Inc., 1997.